Exclusive Processes in Quantum Chromodynamics and the Light-Cone Fock Representation[*]

Stanley J. Brodsky
Stanford Linear Accelerator Center
Stanford, California 94309
e-mail: sjbth@slac.stanford.edu

ABSTRACT

Exclusive processes provide a window into the bound state structure of hadrons in QCD as well as the fundamental processes which control hadron dynamics at the amplitude level. The natural calculus for describing bound state structure of relativistic composite systems needed for describing exclusive amplitudes is the light-cone Fock expansion which encodes the multi-quark, gluonic, and color correlations of a hadron in terms of frame-independent wavefunctions. In hard exclusive processes in which hadrons receive a large momentum transfer, perturbative QCD leads to factorization theorems which separate the physics of bound state structure from that of the relevant quark and gluonic hard-scattering reactions which underlie these reactions. At leading twist, the bound state physics is encoded in terms of universal "distribution amplitudes," the fundamental theoretical quantities which describe the valence quark substructure of hadrons as well as nuclei. The combination of discretized light-cone quantization and transverse lattice methods are now providing nonperturbative predictions for the pion distribution amplitude. A basic feature of the gauge theory formalism is "color transparency," the absence of initial and final state interactions of rapidly-moving compact color-singlet states. Other applications of the factorization formalism are briefly discussed, including semileptonic B decays, deeply virtual Compton scattering, and dynamical higher twist effects in inclusive reactions. A new type of jet production reaction, "self-resolving diffractive interactions" provide empirical constraints on the light-cone wavefunctions of hadrons in terms of their quark and gluon degrees of freedom as well as the composition of nuclei in terms of their nucleon and mesonic degrees of freedom.

1   Introduction and Overview

Exclusive processes, as defined by Feynman,[1] are scattering reactions in which the kinematics of all initial and final state particles are specified. Hadronic exclusive processes present an extraordinary challenge to theoretical analysis in quantum chromodynamics. Virtually all the complexities of perturbative and non-perturbative QCD are relevant to exclusive reactions, from confinement and chiral symmetry breaking at low momentum transfers, to the dynamics of quarks and gluons at high momentum transfers. A complete description of exclusive amplitudes must deal with all of the complexities of the non-perturbative structure of hadrons—not just the single-particle flavor, momentum, and helicity distributions of the quark constituents familiar from inclusive reactions—but also multi-quark, gluonic, hidden-color correlations, and the phase structure intrinsic to hadronic and nuclear wavefunctions.

Exclusive hadronic reactions range from the space-like and time-like form factors measured in electron-hadron scattering and electron-positron annihilation, to hadronic scattering reactions such as proton-proton scattering, pion photoproduction,

and diffractive vector meson electroproduction. Exclusive amplitudes also govern the decay of heavy hadrons and quarkonia into a specific final states. One of the most pressing goals is to understand the QCD physics of exclusive B-meson decays at the amplitude level, since the interpretation of the basic parameters of electroweak theory and CP violation depend on hadronic dynamics and phase structure.

Exclusive processes are particularly challenging to compute in QCD because of their sensitivity to the unknown non-perturbative bound state dynamics of the hadrons. However, in some important cases, the leading power-law behavior of an exclusive amplitude at large momentum transfer can be computed rigorously via a factorization theorem which separates the soft and hard dynamics. The key ingredient is the factorization of the hadronic amplitude at leading twist. As in the case of inclusive reactions, factorization theorems for exclusive processes allow the analytic separation of the perturbatively-calculable short-distance contributions from the long-distance non-perturbative dynamics associated with hadronic binding.

Other important examples of exclusive processes which are particularly relevant to QCD analyses are the transition form factor $F_{\gamma \pi^0}$ measured in $e\gamma \to e\pi^0 e$ in which only a single hadron appears, two-photon reactions such as $\gamma\gamma \to \pi^+\pi^-$, virtual Compton scattering $\gamma^* p \to \gamma p$, elastic scattering reactions such as $K^+ p \to K^+ p$, photoproduction reactions such as $\gamma p \to \pi^- \Delta^{++}$, quarkonium decay, hard diffractive reactions such as $\gamma^* p \to \rho^0 p$ and nuclear reactions such as deuteron photodisintegration $\gamma d \to pn$.

The main focus of this introductory review will be on the fundamental quark and gluon processes and hadron wavefunctions which control hadron dynamics at the amplitude level. Despite much progress, the subject is still in its infancy, and many important problems, controversies, and puzzles remain unresolved. A number of excellent specialized reviews of exclusive processes in QCD are available which can provide further technical details and additional references.[2, 3, 4, 5, 6, 7]

Compton scattering on a proton, $\gamma p \to \gamma p$, the elastic scattering of a real photon on a proton is a primary example of an exclusive amplitude. Covariance and discrete symmetries reduce the number of helicity amplitudes $M_{\lambda_\gamma, \lambda_p, \lambda_{\gamma'}, \lambda_{p'}}(\gamma p \to \gamma' p')$ to 6 analytic functions $F_I(s,t), (I = 1, \ldots 6)$ of the invariants $s = (k+p)^2$ and $t = (p-p')^2$. These amplitudes, by $s \to t$ crossing, also describe pair production in photon-photon collisions $\gamma\gamma \to p\overline{p}$ as well as pair annihilation $p\overline{p} \to \gamma\gamma$. The challenge is to compute the scattering of the proton by photons starting from a basis where the fundamental carriers of the electromagnetic current are confined quarks. Furthermore, in a relativistic quantum field theory, a bound state has fluctuations of arbitrary number or quanta. A comprehensive review of real and virtual Compton scattering has recently been given by Vanderhaeghen.[7] The analytic behavior of the Compton amplitude is constrained by general considerations: see Fig. 1.

(1) The low energy theorem[8, 9] for forward Compton scattering normalizes the proton and photon helicity-conserving amplitude at threshold $s = M^2$ and $t = 0$ to
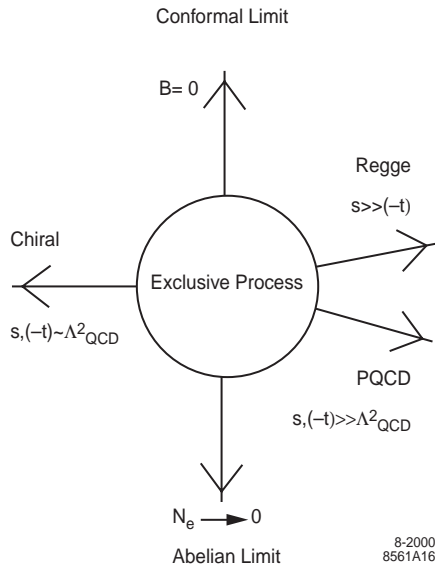
Figure 1: Domains of exclusive amplitudes in QCD.

the total charged squared of the target proton. Similarly, the helicity-flip amplitude at threshold is normalized to the square of the proton's anomalous magnetic moment. The explicit demonstration of these facts for the case of a composite target is highly non-trivial: there is a remarkable cancelation of the terms proportional to the sum of quark charges squared from photons scattering on the constituents with contributions involving the proton intermediate state.[10]

(2) The optical theorem relates the imaginary (absorptive) part of the forward photon and proton helicity-conserving Compton amplitude to the total photoabsorption cross section. Given the total cross section, one can use dispersion relations to derive the s dependence of the entire forward Compton amplitude. Thus all of the complexities of photoabsorption cross section are implicitly contained in the exclusive amplitude. These include multiple scattering Glauber/Gribov processes, which in the case of a nuclear target, lead to shadowing and anti-shadowing on a nuclear target.

(3) The Regge limit: At fixed t with $s \gg -t$, the analytic form of any $2 \to 2$ exclusive scattering amplitude is characterized by a sum of Regge terms,

$$M(s,t) = \sum_R \beta_R(t) s^{\alpha_R(t)} S[\alpha(t)] \tag{1}$$

where

$$S(\alpha) = \frac{1 \pm e^{-i\pi\alpha(t)}}{\sin \pi\alpha(t)}$$

is the signature factor determined by $s \to u$ crossing and unitarity. The Compton amplitude is described in Regge theory by even signature $C = +$ Regge poles and cuts including the Pomeron. At small t, the exchange of a virtual π^0 through its

4

anomalous $\pi^0 \to \gamma\gamma$ coupling can also enter. At large t the Pomeron can be calculated in the BFKL formalism [11] which sums multi-gluon exchange. In addition, both photons can interact locally on the same quark line leading to a fixed Regge contribution at $\alpha_R = 0$, the "$J = 0$ fixed pole" contribution,[12, 13] thus distinguishing proton processes from the corresponding processes involving vector mesons. Crossing and Regge theory at $t > -s$ from the cross-channel baryonic Reggeon exchange trajectories provide further constraints.

(4) The Chiral Correspondence Principle: At long wavelengths where hadron substructure cannot be resolved, QCD must reduce to a dual effective theory of hadrons, such as the chiral Lagrangian.[14] This duality between the quark and gluon degrees of freedom in the propagators of local color-singlet operators is the basis of the QCD sum rules. [15, 16] In addition, soft exclusive amplitudes must match to the amplitudes calculated in the chiral theories. Since baryons enter as solitons, as described in the Skyrme model, the annihilation process $p\overline{p} \to \gamma\gamma$ at small relative velocities should can be described in terms of Skyrmion – anti-Skyrmion annihilation.[17] Conversely, the production process $\gamma\gamma \to p\overline{p}$ amplitude corresponds to Skyrmion – anti-Skyrmion formation. This duality constraint has profound consequences for the analytic behavior of the proton Compton amplitude since the soliton picture of $p\overline{p}$ annihilation implies the existence of an important scale in the proton Compton amplitude at $t \approx 4M_p^2$. [18]

(5) Asymptotic High Momentum Transfer Constraints: Although the physics of the Compton amplitude for general kinematics is extraordinarily complicated, perturbative QCD provides a simple guide to the physics of the Compton process at large momentum transfer. The physical picture is as follows: the valence quarks in a hadron wavefunction are dominated by kinematic configurations in which its constituent quark have small relative momenta $\langle k_\perp^2 \rangle \simeq 300$ MeV^2. Thus at high momentum transfer $-t, u \gg \langle k_\perp^2 \rangle$ with fixed t/s or center-of-mass angle, one expects that proton Compton scattering should be driven by the perturbative process $\gamma(qqq) \to \gamma'(qqq)'$ where the valence quarks scatter from a direction roughly collinear with the initial proton to that of the final proton. Since the coupling is dimensionless, such a tree amplitude falls nominally as $1/t^2$. Furthermore since quark helicity is conserved at high energy in QCD, and the dominant valence quark wavefunctions have $L_z = 0$, proton helicity $\lambda_p = \lambda_{p'}$ should be conserved.

Since the coupling is dimensionless, simple power-law scaling [19, 20, 21] implies that the proton helicity-conserving Compton amplitude will have the nominal falloff $f(t/s)/t^2$. Wavefunction configurations with more than the minimum number of constituents are power-law suppressed since more hard interactions are required. The corresponding fixed-cm-angle cross section is thus predicted to fall as

$$ d\sigma/dt(\gamma p \to \gamma p) \propto \frac{|f(t/s)|^2}{s^2 t^4}. $$

This prediction is consistent with the scaling of the large angle Compton scattering data [22]: $s^6 d\sigma/dt(\gamma p \to \gamma p) \sim$ const at $4 < s < 12$ GeV^2. As seen in Fig. 2, the

experimental data for Compton scattering indicates consistency with $s^6 d\sigma/dt$ scaling at momentum transfers as small as a few GeV. In fact, the angular dependence of the data appears to have universal angular function when the differential cross section is scaled by the nominal s^6 power.
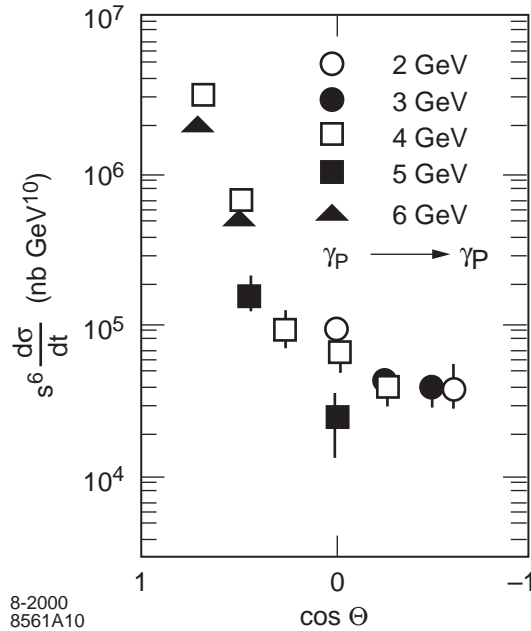

Figure 2: Scaling of proton Compton scattering at fixed θ_{cm}. The data and from Shupe *et al.*[22]

Asymptotic freedom implies that the magnitude of the effective coupling $\alpha_s(q^2)$ of the exchanged gluons which carry the large momentum transfer is sufficiently small that a perturbative analysis of the underlying hard scattering amplitude $T_H(\gamma(qqq) \to \gamma'(qqq)')$ is meaningful. The nominal power-law fall off given by dimensional counting will then be modified by the dependence in the running coupling associated with the two hard gluon exchanges as well as additional logarithms arising from the evolution of the proton wavefunction. The crossed channel processes can be obtained by simple $s \to t$ crossing.

The asymptotic predictions obtained from perturbative QCD also imply important analytic constraints on the form of the Compton amplitude.[23] For example, if Regge theory is to be consistent with the power fall-off predictions of perturbative QCD, then the Reggeon powers $\alpha_R(t)$ must asymptote at large $-t$ to negative integers: $\lim_{-t\to\infty} \alpha_R(t) = 0, -1$. Similarly, the Regge coefficient functions $\beta_R(t)$ must have power-law fall-off.

The hard scattering physical picture outlined above for the proton Compton amplitude is the basis for a general formalism for analyzing the behavior of hard exclusive

6

processes in which some or all of the interacting particles receive a high momentum transfer. In fact in many cases, factorization theorems can be derived which at leading power in the momentum transfer Q allow one to write the full hadron amplitude as the convolution of the amplitude T_H for the hard scattering of the valence quarks, collinear up to the scale $\tilde{Q}$, with the hadron distribution amplitudes $\phi(x_i, \tilde{Q})$ representing each of the hadron receiving a hard momentum. [24]

In this introductory review, I will outline many of the developments in the application of QCD to exclusive processes. Many technical details will not be given here, but are available in the original papers. An essential tool will be light-front (light-cone) quantization which provides a frame-independent representation of relativistic bound state wavefunctions in quantum field theory. The quantization procedure and rules of calculation in light-cone time-ordered perturbation theory are outlined in the Appendix. The general framework for the applications to QCD are illustrated schematically in Figs. 3 and 4. In each of the illustrated processes, one sees a factorization of the hadronic physics in terms of the light-cone Fock wavefunctions convoluted with perturbatively-calculable hard scattering amplitudes.

The natural calculus for describing bound state structure of relativistic composite systems in quantum field theory is the light-cone Fock expansion. The light-cone Fock wavefunctions $\psi_{n/H}(x_i, \vec{k}_{\perp i}, \lambda_i)$ thus interpolate between the hadron H and its quark and gluon degrees of freedom. The light-cone momentum fractions of the constituents, $x_i = k_i^+/P^+$ with $\sum_{i=1}^{n} x_i = 1$, and the transverse momenta $\vec{k}_{\perp i}$ with $\sum_{i=1}^{n} \vec{k}_{\perp i} = \vec{0}_{\perp}$ appear as the momentum coordinates of the light-cone Fock wavefunctions. A crucial feature is the frame-independence of the light-cone wavefunctions. The x_i and $\vec{k}_{\perp i}$ are relative coordinates independent of the hadron's momentum P^{μ}. The actual physical transverse momenta are $\vec{p}_{\perp i} = x_i \vec{P}_{\perp} + \vec{k}_{\perp i}$. The light-cone Fock representation is an extraordinarily useful tool for representing hadrons in terms of their quark and gluon degrees of freedom. It also provides exact representation of the electromagnetic form factors and other local matrix elements at all momentum transfer. I will also review this formalism in the following sections.

The principles of factorization of soft and hard dynamics have been recently extended in a number of other directions:

(1) The deeply virtual Compton amplitude $\gamma^* p \to \gamma p$ has emerged as one of the most important exclusive QCD reactions.[25, 26, 27, 28] The process factorizes into a hard amplitude representing Compton scattering on the quark times skewed parton distributions. The resulting skewed parton form factors can be represented as diagonal and off-diagonal convolutions of light-cone wavefunctions, as in semileptonic B decay.[29] New sum rules can be constructed which correspond to gravitons coupling to the quarks of the proton. [25]

(2) The hard diffraction of vector mesons $\gamma^* p \to V^0 p$ at high Q^2 and high energies for longitudinally polarized vector mesons factorizes into a skewed parton distribution times the hard scale $\gamma^* g \to g V^0$ amplitude, where the physics of the vector meson is

(a)   Light Cone Fock Expansion

$|p\rangle = \quad$ u u u d $|uud\rangle + \quad$ u u g d $|uudg\rangle + ...$

Ψ_{uud} $\quad\quad$ Ψ_{uudg}

$\langle p | qqq \rangle : \quad$ $x_1, \vec{k}_{\perp 1}, \lambda_1$
$\quad\quad$ $x_2, \vec{k}_{\perp 2}, \lambda_2$
Ψ_{uud} $\quad$ $x_3, \vec{k}_{\perp 3}, \lambda_3$

$\Psi_n (x_i, \vec{k}_{\perp i}, \lambda_i) : \sum_{i=1}^{n} x_i = 1, \sum_{i=1}^{n} \vec{k}_{\perp i} = 0$

(b)   Distribution Amplitude

$\phi_M^{(x,Q)} = \int d^2 k_\perp \quad$ $x, \vec{k}_\perp$
$\quad\quad$ $1-x, -\vec{k}_\perp$
Ψ_2

$M_n^2 < Q^2$

(c) Deep Inelastic $\ell p \rightarrow \ell' X \quad \langle p | J^+(z) J^+(0) | p \rangle$

γ^* q $\quad$ γ^* q
$p \quad p$ $\quad = \sum_n \quad$ q $\quad$ q
$\quad$ x $\quad$ x
$p \quad p$
$\Psi_n \quad \Psi_n$

$q(x_{B_J}, Q) = \sum_n \int \Pi \, d^2 k_\perp dx \, \left| \begin{array}{c} x_q, \vec{k}_\perp \\ \Psi_n \end{array} \right|^2$

$M_n^2 < Q^2, \quad x_q = x_{B_J}$

(d)   Form Factors $\quad \ell p \rightarrow \ell' \, p' \quad \langle p' \, \lambda' | \, J^+(0) \, | p \lambda \rangle$

q
$F_{\lambda\lambda'}(Q^2) = \sum_n \quad x, \vec{k}_\perp \quad x, \vec{k}_\perp + \vec{q}_\perp$

$p, \lambda \quad\quad p+q, \lambda'$
$\Psi_n \quad\quad \Psi_n$

$\Downarrow$
Large Q^2

T_H
$\phi \quad\quad \phi$
$p, \lambda \quad\quad p+q, \lambda'=\lambda$

$x_1 \quad \gamma^* \quad y_1$
$T_H = \sum \quad x_2 \quad\quad y_2 \quad + \quad ...$
$x_3 \quad\quad y_3$

$= \dfrac{\alpha_s^2}{Q^4} \, f(x_i, y_i,)$

(e)   Compton $\quad \gamma \, p \rightarrow \gamma' \, p' \quad \langle p' | J^\mu(z) J^\nu(0) | p \rangle$

Large s, t $\quad k \quad\quad k'$

T_H
$\phi \quad\quad \phi$
$p, \lambda \quad\quad p+q, \lambda'=\lambda$

$k \quad\quad k'$
$x_1 \quad\quad y_1$
$T_H^{Compton} = \sum \quad x_2 \quad\quad y_2 \quad + \quad ...$
$x_3 \quad\quad y_3$

$= \dfrac{\alpha_s^2}{P_T^4} \, f(x_i, y_i, \theta_{cm})$
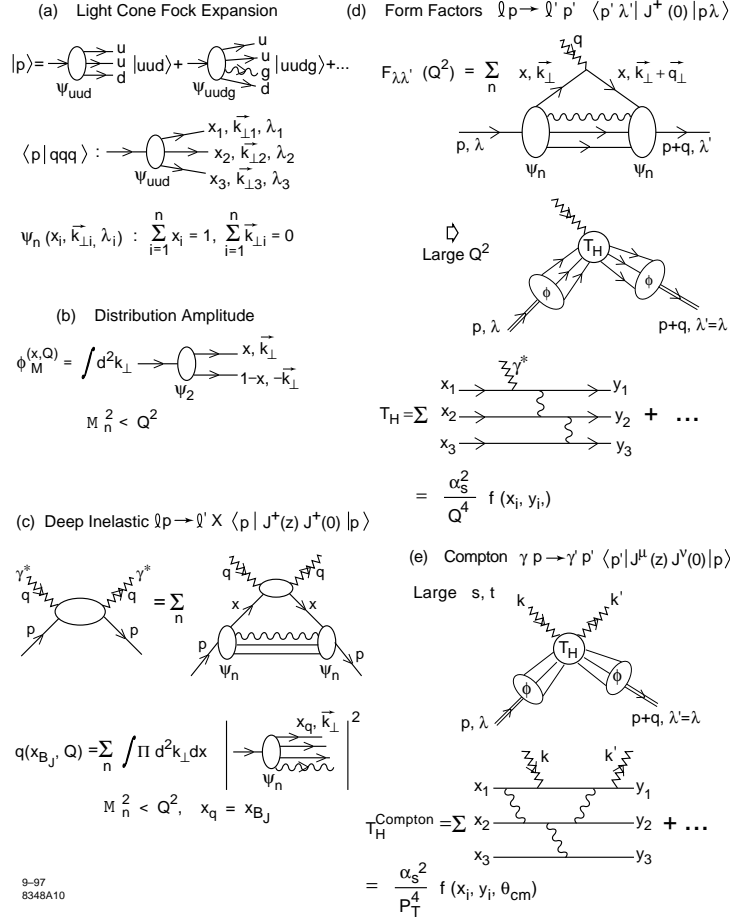
9–97
8348A10

Figure 3: Representation of QCD hadronic processes in the light-cone Fock expansion. (a) The valence uud and $uudg$ contributions to the light-cone Fock expansion for the proton. (b) The distribution amplitude $\phi(x,Q)$ of a meson expressed as an integral over its valence light-cone wavefunction restricted to $q\bar{q}$ invariant mass less than Q. (c) Representation of deep inelastic scattering and the quark distributions $q(x,Q)$ as probabilistic measures of the light-cone Fock wavefunctions. The sum is over the Fock states with invariant mass less than Q. (d) Exact representation of spacelike form factors of the proton in the light-cone Fock basis. The sum is over all Fock components. At large momentum transfer the leading twist contribution factorizes as the product of the hard scattering amplitude T_H for the scattering of the valence quarks collinear with the initial to final direction convoluted with the proton distribution amplitude. (e) Leading-twist factorization of the Compton amplitude at large momentum transfer.
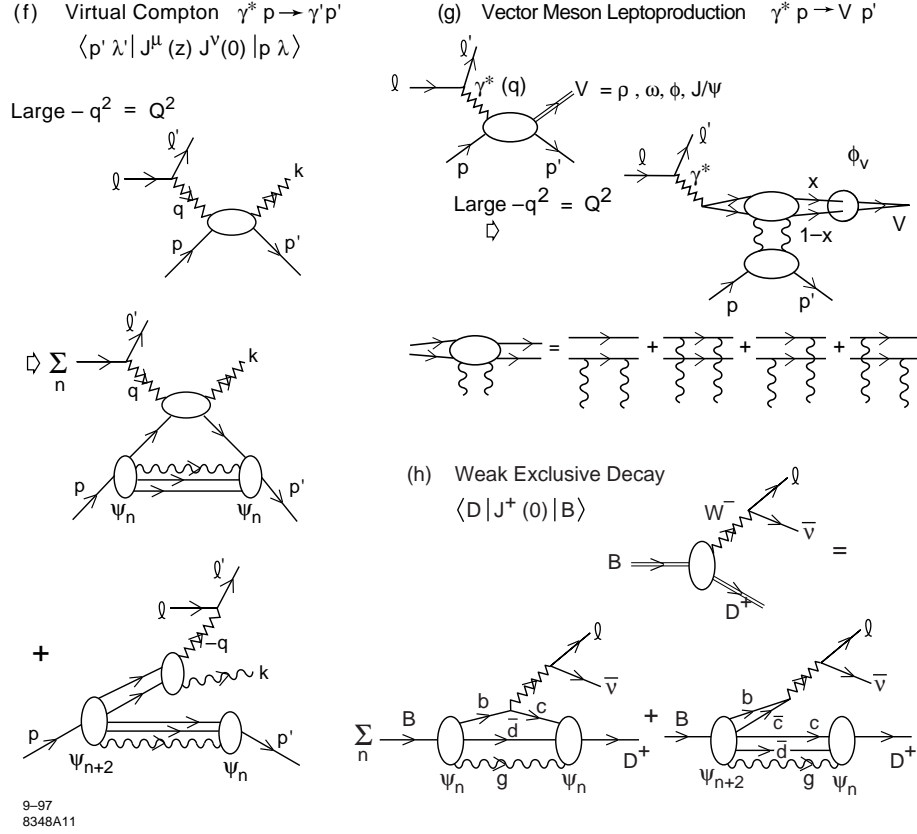
Figure 4: (f) Representation of deeply virtual Compton scattering in the light-cone Fock expansion at leading twist. Both diagonal $n \to n$ and off-diagonal $n + 2 \to n$ contributions are required. (g) Diffractive vector meson production at large photon virtuality Q^2 and longitudinal polarization. The high energy behavior involves two gluons in the t channel coupling to the compact color dipole structure of the upper vertex. The bound-state structure of the vector meson enters through its distribution amplitude. h Exact representation of the weak semileptonic decays of heavy hadrons in the light-cone Fock expansion. Both diagonal $n \to n$ and off-diagonal pair annihilation $n + 2 \to n$ contributions are required.

contained in its distribution amplitude.[30, 31, 32] The data appears consistent with the s, t and Q^2 dependence predicted by theory. Ratios of these processes for different mesons are sensitive to the ratio of $1/x$ moments of the V^0 distribution amplitudes.

(3) The two-photon annihilation process $\gamma^* \gamma \to$ hadrons, which is measurable in single-tagged $e^+ e^- \to e^+ e^-$ hadrons events provides a semi-local probe of even charge conjugation $C =^+$ hadron systems $\pi^0, \eta^0, \eta', \eta_c, \pi^+ \pi^-$, etc. The perturbative QCD calculation of the simplest channel, $\gamma^* \gamma \to \pi^0$, will be discussed in the next section. The $\gamma^* \gamma \to \pi^+ \pi^-$ hadron pair process is related to virtual Compton scattering on a pion target by crossing. Hadron pair production is of particular interest since the leading twist amplitude is sensitive to the $1/x - 1/(1 - x)$ moment of the two-pion distribution amplitude coupled to two valence quarks. [31, 33]

2 Calculations of Exclusive Processes in QCD

2.1 The Photon-to-Pion Transition Form Factor

The simplest illustration of an exclusive reaction in QCD is the evaluation of the photon-to-pion transition form factor $F_{\gamma \to \pi}(Q^2)$ since only one hadron is involved. The transition form factor is measurable in single-tagged two-photon $ee \to ee\pi^0$ reactions. The form factor is defined via the invariant amplitude

$$\Gamma^\mu = -ie^2 F_{\pi\gamma}(Q^2)\epsilon^{\mu\nu\rho\sigma}p_\nu^\pi \epsilon_\rho q_\sigma \; . \tag{2}$$

The lowest order contribution is shown in Fig. 5. It is convenient to choose a frame where the virtual photon has zero q^+: $q = (q^+, q^-, q_\perp) = (0, 2p \cdot q/p^+), p = (p^+, p^-, p_\perp) = (p^+, M^2/p^+, 0_\perp)$ with $q_\perp^2 = Q^2 = -q^2$.

We can readily compute the $\gamma^* \gamma \to \pi^0$ amplitude in light-cone time-ordered perturbation theory using the rules given in the Appendix. The central input will be the two-particle irreducible light-wave Fock state amplitude:

$$\psi(x, k_\perp) = F.T. \left\langle 0|T\overline{\psi}(z/2)\psi(-z/2)|\pi \right\rangle |_{z^+=0} \; . \tag{3}$$

which sums all of the nonperturbative physics associated with the pion. The denominator in Fig. 5(b) associated with the fermion propagator between the two photons is proportional to $(k_\perp + x_1 q_\perp)^2$. As in inclusive reactions, one must specify a factorization scheme which divides the integration regions of the loop integrals into hard and soft momenta, less or more than the resolution scale $\tilde{Q}$. At large Q^2 one then finds [34, 35, 24] $(x_1 + x_2 = 1)$

$$F_{\pi\gamma}(Q^2) = \frac{2\sqrt{(N_c)(e_u^2 - e_d^2)}}{Q^2} \int_0^1 \frac{dx}{x_1 x_2} \int^{k_\perp^2 < \tilde{Q}^2} \frac{d^2 k_\perp}{16\pi^2} \psi(x, k_\perp) \tag{4}$$

where the factorization scale separating the soft and hard domains of integration in the wavefunction is $\tilde{Q} = (\min_{i=1,2} x_i)Q$.
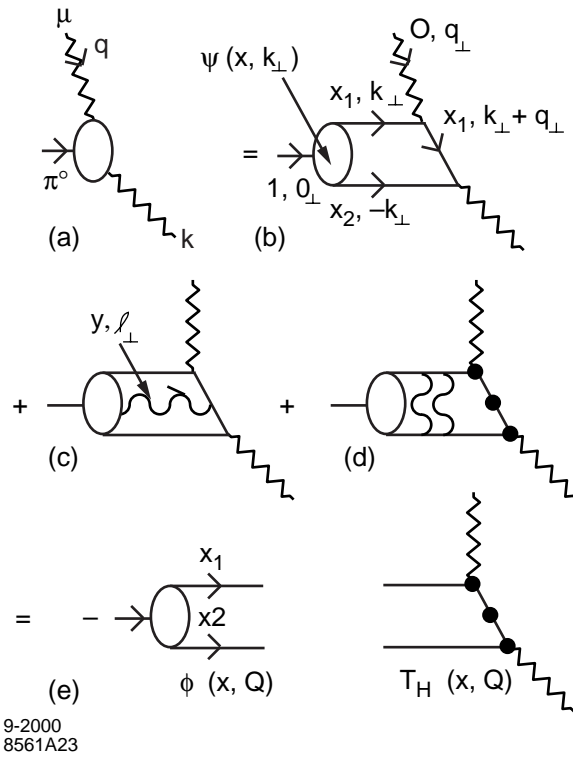
10

Figure 5: Perturbative QCD analysis of the $\gamma\gamma^* \to \pi^0$ amplitude. The contribution of (c) for finite $\ell_\perp$ is power law suppressed in light-cone gauge. The factorization of $F_{\pi^0\gamma}(Q^2)$ is shown in (d).

11

The crucial non-perturbative input is the pion distribution amplitude, $\phi(x, \tilde{Q})$, the integral over transverse momenta of the renormalized hadron valence wavefunction in the light-cone gauge at fixed light-cone time:[34, 35, 24]

$$\phi(x, \tilde{Q}) = \int d^2\vec{k}_\perp \, \theta \left(\tilde{Q}^2 - \frac{\vec{k}_\perp^2}{x(1-x)} \right) \psi^{(\tilde{Q})}(x, \vec{k}_\perp). \tag{5}$$

The fact that a meson has a finite non-zero probability to contain exactly two quark constituents is possible because it is a color singlet. In contrast, the probability for an electron to exist as a single bare fermion in QED is exponentially suppressed by the infrared divergence of the virtual radiative corrections.

The pion distribution amplitude can be defined formally as the gauge invariant Bethe-Salpeter wavefunction evaluated at equal light-cone time:

$$\phi_\pi(x, Q) =$$
$$P_\pi^+ \int \frac{dz^-}{4\pi} \exp(ixP_\pi^+ z^-/2) \left\langle 0|\overline{\psi}(0)\mathcal{P}\frac{\gamma^+\gamma_5}{2\sqrt{2}N_C}\psi(z)\pi \right\rangle^{(Q)} |_{z^+=z_\perp=0},$$

where

$$\mathcal{P} = P \exp \left[\int_0^1 ds \, ig \, A(sz) \cdot z \right] \tag{6}$$

is the "string operator" which becomes unity in light-cone gauge $A \cdot z = A^+ z^-/2 = 0$. The physical pion form factor must be independent of the separation scale $\tilde{Q}$. In the light-cone Fock representation, a natural variable in which to make this separation is the light-cone energy, or equivalently the invariant mass $\mathcal{M}^2 = \vec{k}_\perp^2/x(1-x)$, of the off-shell partonic system.[36, 34, 35, 24] Any residual dependence on the choice of $\tilde{Q}$ for the distribution amplitude will be compensated by a corresponding dependence of the NLO correction in T_H.

The higher-order QCD radiative corrections entering the transition form factor can be organized in the following way: First consider the loop integration $\ell_\perp, y$ associated with gluons which attach to the exchanged fermion. For the ultraviolet region $\ell_\perp > \tilde{Q}$, the vertex and self-energy insertions lead to a fermion line renormalization factor. For $\ell_\perp < \tilde{Q}$, one obtains either higher corrections in $\alpha_s(\tilde{Q}^2)$ to the $q\overline{q} + \gamma^* \to \gamma$ amplitude or in the case where the gluon interrupts the hot line, power-law suppressed contributions. It is crucial to use $A^+ = 0$ gauge to obtain this simplification. The gluons which are exchanged between the quark legs are included in the definition of the wavefunction $\psi(x, k_\perp)$ and lead to a power-law tail $\psi(x, k_\perp) \sim k_\perp^{-2}$. This implies a logarithmic Q^2 dependence for the gauge-independent distribution amplitude. We thus obtain

$$F_{\pi\gamma}(Q^2) = \frac{2}{\sqrt{3}Q^2} \int \frac{dx_0^1}{x_1 x_2} \phi(x, \tilde{Q}) = \frac{2\sqrt{N}_C(e_u^2 - e_d^2)}{Q^2} \sum_{n=0,2} a_n \ln^{-\gamma_n} \frac{Q^2}{\Lambda^2} \tag{7}$$

corresponding to the evolution of the pion distribution amplitude:

$$\phi(x, Q) = x_1 x_2 \sum_{n=0}^{\infty} a_n \ln^{-\gamma_n} \frac{Q^2}{\Lambda^2} \, C_n^{3/2}(x_1 - x_2). \tag{8}$$

The corrections are of order in $\alpha_s(\tilde{Q}^2)$ and m^2/Q^2. The decay $\pi \to \mu\nu$ determines the wave function at the origin:

$$\frac{a_0}{6} = \int_0^1 dx \phi(x, Q) = \frac{f_\pi}{2\sqrt{3}}. \tag{9}$$

The distribution amplitude $\phi(x, Q)$ is boost and gauge invariant and evolves in $\ln Q$ through an evolution equation.[34, 35, 24] The evolution equation for mesons will be discussed in more detail in Section 3.6. Since it is formed from the same product of operators as the non-singlet structure function, the anomalous dimensions controlling $\phi(x, Q)$ dependence in the ultraviolet $\log Q$ scale must be the same as those which appear in the DGLAP evolution of structure functions. [37] The Bethe-Salpeter form also allows contact with both QCD sum rules [15] and lattice gauge theory; for example, moments of the pion distribution amplitudes have been computed in lattice gauge theory. [38, 39, 40]

The PQCD predictions for the photon-to-pion transition form factor have been tested in recent measurements of $e\gamma \to e\pi^0$ by the CLEO collaboration [41] See Fig. 6. The data confirms a key prediction of QCD at leading twist: 7 $Q^2 F_{\gamma\pi^0}(Q^2)$ is essentially constant for 1 GeV$^2 < Q^2 < 8$ GeV^2.

Unlike the electromagnetic form factor $F_\pi(Q^2)$, the $F_{\pi\gamma}(Q^2)$ form factor in leading order has no explicit dependence on $\alpha_s(Q^2)$. Consequently an accurate measurement of $F_{\pi\gamma}(Q^2)$ will determine $\int \frac{dx}{x_1 x_2} \phi(x, \tilde{Q})$. This can be combined with the normalizing sum rule to constrain the x-dependence of $\phi(x, \tilde{Q})$. In fact, as discussed in Section 4, the normalization is consistent with QCD at NLO if one assumes that the pion distribution amplitude takes on the form $\phi_\pi^{\mathrm{asympt}}(x) = \sqrt{3} f_\pi x(1 - x)$ which is the asymptotic solution [34, 35, 24] to the evolution equation for the pion distribution amplitude. [42, 43, 44, 45]

2.2   Meson Form Factors

Let us now consider hadronic form factors in general. As we shall discuss in Sections 16, the matrix element of a spacelike current at any momentum transfer can be expressed as the diagonal particle-conserving sum of overlap integrals of the hadron light-cone wavefunctions. At large momentum transfer, when the arguments of the wavefunctions exceed the factorization scale $\tilde{Q}$ the equations of motion for the wavefunctions can be iterated so as to isolate the hard momentum transfer processes into the hard scattering amplitude T_H for the constituents scattering collinear from the
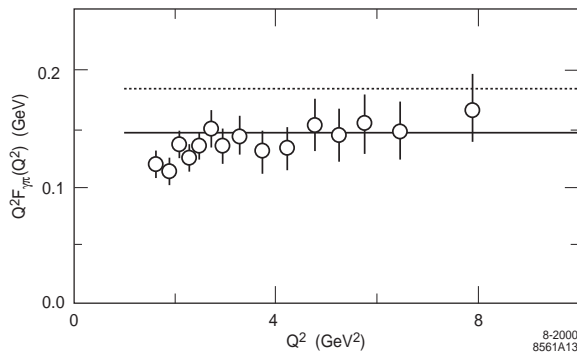
Figure 6: Scaling of the transition photon to pion transition form factor $Q^2 F_{\gamma\pi^0}(Q^2)$. The data are from the CLEO collaboration. [41]

initial to final hadrons. For example, the leading $1/Q^2$ fall-off of pseudoscalar meson form factors can be computed as a convolution:

$$F_M(Q^2) = \int_0^1 dx \int_0^1 dy \phi_M(x, \tilde{Q}) T_H(x, y, Q^2) \phi_M(y, \tilde{Q}), \tag{10}$$

where $\phi_M(x, \tilde{Q})$ is the process-independent meson distribution amplitude, which encodes the non-perturbative dynamics of the bound valence quarks at the resolution scale $\tilde{Q}$, and

$$T_H(x, y, Q^2) = \frac{16\pi C_F \alpha_s(\mu)}{(1-x)(1-y)Q^2} \left(1 + \mathcal{O}(\alpha_s)\right) \tag{11}$$

is the leading-twist perturbatively-calculable subprocess amplitude $\gamma^* q(x)\overline{q}(1-x) \rightarrow q(y)\overline{q}(1-y)$, obtained by replacing the incident and final mesons by nearly collinear valence quarks. Thus [46, 34, 35, 24, 47, 48, 49, 50]

$$F_\pi(Q^2) = \frac{16\pi\alpha_s(Q^2)}{3Q^2} \int_0^1 \frac{dx \phi(x, \tilde{Q}_x)}{x(1-x)} \int_0^1 \frac{dy \phi(y, \tilde{Q}_y)}{y(1-y)}, \tag{12}$$

to leading order in $\alpha_s(Q^2)$ and m^2/Q^2. The factorization is illustrated in Fig. 7.

The non-perturbative physics of the hadron enters the pion form factor at leading twist solely through its distribution amplitude $\phi_{H_I}(x_j, Q)$. The distribution amplitude is the fundamental gauge-invariant valence wavefunction of the hadron, describing the distribution of the longitudinal momentum fractions x_i of the valence quarks, at the resolution scale Q. The distribution amplitude is a specific attribute of the hadron itself, so that if it is known for one exclusive process, it is known for all others. The distribution amplitudes thus contain the soft physics intrinsic to the nonperturbative structure of the hadrons. They are process independent, fundamental theoretical quantities which describe the valence quark substructure of hadrons as well as nuclei.

14

$q^2 = -Q^2$

x   y

ϕ T_H ϕ

1 - x   1 - y

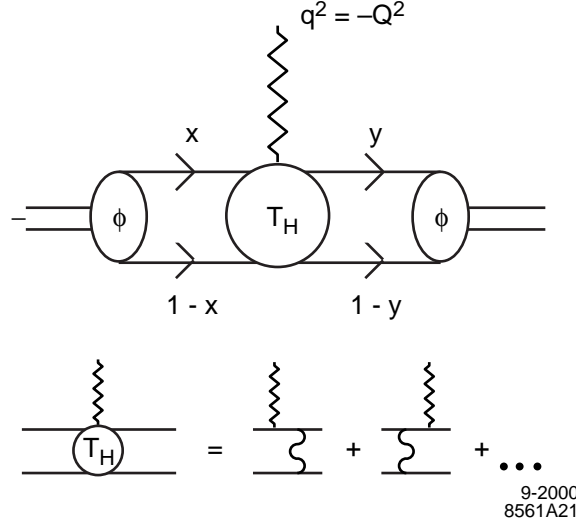T_H = $\{$ + $\{$ + ...

9-2000
8561A21

Figure 7: Factorized structure and leading order contributions to meson form factors in QCD.

The contributions from non-valence Fock states and corrections from fixed transverse momentum entering the hard subprocess amplitude are higher twist, *i.e.*, power-law suppressed. The integration over transverse momenta up to the scale $\tilde{Q}$ lead to the evolution of the distribution amplitude. Loop corrections involving hard momenta give next-to-leading-order (NLO) corrections in α_s. In the case of the pion form factor, the contribution from the endpoint regions of integration, $x \sim 1$ and $y \sim 1$, are power-law and Sudakov suppressed and thus contribute corrections at higher order in $1/Q$.[34, 35, 24]

The x-dependence of the integrand of $F_{\pi\gamma}(Q^2)$ form factor is identical to that of the pion elastic form factor. Consequently all dependence on $\phi(x, \tilde{Q})$ can be removed by comparing the two processes. In fact, a measurement of each provides a direct determination of the QCD coupling:

$$\alpha_s(Q^2) = \frac{1}{4\pi} \frac{F_\pi(Q^2)}{Q^2 |F_{\pi\gamma}(Q^2)|^2} + \mathcal{O}[\alpha_s^2(Q^2)]. \tag{13}$$

Since the $\mathcal{O}(\alpha_s^2)$ corrections have been computed, this could be used to measure $\alpha_s(Q^2)$ in a given renormalization prescription such as minimal subtraction. Conversely the ratio can be used to define a renormalization scheme for QCD directly from exclusive processes. Of course all of these formulae are valid only at large Q^2; the $\mathcal{O}(m^2/Q^2)$ corrections become important at lower Q^2. However the $Q^2 \to 0$ behavior of $F_{\pi\gamma}$ is fixed by the decay $\pi^0 \to \gamma\gamma$ which implies

$$F_{\pi\gamma} \to \frac{1}{4\pi^2 f_\pi} \tag{14}$$

15

for $Q^2 \to 0$. To estimate the effects due to $\mathcal{O}(m^2/Q^2)$ corrections, one can write $F_{\pi\gamma}$ as a monopole

$$F_{\pi\gamma} \simeq \frac{1}{4\pi^2 f_\pi} \frac{1}{1 + (Q^2/8\pi^2 f_\pi^2)} \sim \frac{0.27\text{GeV}^{-1}}{(1 + Q^2/M^2)} \tag{15}$$

where $M^2 \sim 0.68$ GeV^2 which interpolates between the $Q^2 = 0$ and $Q^2 \to \infty$ limits.

These meson form factor results can also be derived using renormalization group methods, as has been shown by Duncan and Mueller [51] The essence of their method is to prove Callan-Symansik equations for moments of the reducible quark scattering amplitudes. The evolution equation method and the renormalization group methods are equivalent, differing only in the organization of the calculation. The light-cone perturbation theory Fock-state methods, however, have a number of advantages: (a) direct calculation in the physical momentum-space $k_\perp$ and x variables; (b) simple connections between the Bethe-Salpeter wave functions, distribution amplitudes, and Fock state amplitudes; and (c) straightforward analyses of higher Fock states. Finally, it should be emphasized that the distribution amplitudes are physical, gauge-invariant measures of the hadron wave functions at short distances.

2.3   Exclusive Two-Photon Processes

Exclusive two-photon processes provide highly valuable probes of coherent effects in quantum chromodynamics. For example, in the case of exclusive final states at high momentum transfer and fixed θ_{cm} such as $\gamma\gamma \to p\overline{p}$ or meson pairs, photon-photon collisions provide a timelike microscope for testing fundamental scaling laws of PQCD and for measuring distribution amplitudes.

Traditionally, $\gamma\gamma$ data has come from the annihilation of Weisäcker–Williams effective photons emitted in $e^-e^\pm$ collisions. Data for $\gamma\gamma \to$ hadrons from $ep \to e'p'R^0$ events at HERA has also now become available. The HERA diffractive events will allow studies of photon and pomeron interference effects in hadron-induced amplitudes. As emphasized by Klein, [52] nuclear-coherent $\gamma\gamma \to$ hadrons reactions can be observed in heavy-ion collisions at RHIC or the LHC, e.g. $Z_1 Z_2 \to Z_1 Z_2 \pi^+ \pi^-$. Eventually $\gamma\gamma$ collisions will be studied at TeV energies with back-scattered laser beams, allowing critical probes of Standard Model and supersymmetric processes with polarized photons in exclusive channels such as Higgs production $\gamma\gamma \to W^+ W^-$, and $\gamma\gamma \to W^+ W^- W^+ W^-$. [53]

Two-photon reactions, $\gamma\gamma \to H\overline{H}$ at large s $= (k_1 + k_2)^2$ and fixed θ_{cm}, provide a particularly important laboratory for testing QCD since these cross-channel "Compton" processes are, by far, the simplest calculable large-angle exclusive hadronic scattering reactions. The main features of these reactions were calculated by Brodsky and Lepage.[54] The helicity structure, and often even the absolute normalization can be rigorously computed for each two-photon channel. In the case of meson pairs, dimensional counting predicts that for large s, $s^4 d\sigma/dt(\gamma\gamma \to M\overline{M}$ scales at fixed t/s or $\theta_{\text{c.m.}}$ up to factors of $\ln s/\Lambda^2$.

16

The angular dependence of the $\gamma\gamma \to H\overline{H}$ amplitudes can be used to determine the shape of the process-independent distribution amplitudes, $\phi_H(x, Q)$, the basic short-distance wavefunctions which control the valence quark distributions in high momentum transfer exclusive reactions. An important feature of the $\gamma\gamma \to M\overline{M}$ amplitude for meson pairs is that the contributions of Landshoff pitch singularities are power-law suppressed at the Born level – even before taking into account Sudakov form factor suppression. There are also no anomalous contributions from the $x \to 1$ endpoint integration region. Thus, as in the calculation of the meson form factors, each fixed-angle helicity amplitude can be written to leading order in l/Q in the factorized form $Q^2 = p_T^2 = tu/s; \tilde{Q}_x = \min(xQ, (l-x)Q)$:

$$\mathcal{M}_{\gamma\gamma \to M\overline{M}} = \int_0^1 dx \int_0^1 dy \phi_{\overline{M}}(y, \tilde{Q}_y) T_H(x, y, s, \theta_{\text{c.m.}} \phi_M(x, \tilde{Q}_x), \tag{16}$$

where T_H is the hard-scattering amplitude $\gamma\gamma \to (q\overline{q})(q\overline{q})$ for the production of the valence quarks collinear with each meson, and $\phi_M(x, Q)$ is the (process-independent) distribution amplitude for finding the valence q and $\overline{q}$ with light-cone fractions of the meson's momentum, integrated over transverse momenta $k_\perp < \tilde{Q}$. The contribution of non-valence Fock states are power-law suppressed. Furthermore, the spin-selection rule of QCD predicts that vector mesons are produced with opposite helicities to leading order in $1/Q$ and all orders in $1/Q$. Here T_H is the quark/gluon hard scattering amplitude for $\gamma\gamma \to (q\overline{q})(q\overline{q})$ where the outgoing quarks are taken collinear with their respective pion parent. To lowest order in α_s, the hard scattering amplitude is linear in α_s. As will be discussed in Section 4, the most convenient definition of the coupling is the effective charge $\alpha_V(Q^2)$, defined from the potential for the scattering of two infinitely heavy test charges, in analogy to the definition of the QED running coupling.

Some forty Feynman diagrams contribute to the hard-scattering amplitudes for $\gamma\gamma \to M\overline{M}$ (for nonsinglet mesons). These can be derived from the four independent diagrams by particle interchange. The resulting amplitudes for helicity-zero mesons are

$$
\begin{aligned}
T_{++} = T_{--} &= \frac{16\pi\alpha_s}{3s} \frac{32\pi\alpha}{x(1-x)y(1-y)} \frac{(e_1 - e_2)^2 a}{1 - \cos^2\theta_{\text{c.m.}}} \\
T_{+-} = T_{-+} &= \frac{16\pi\alpha_s}{3s} \frac{32\pi\alpha}{x(1-x)y(1-y)} \left[\frac{(e_1 - e_2)^2(1-a)}{1 - \cos^2\theta_{\text{c.m.}}} \right. \\
&\left. + \frac{a(e_1 e_2)[y(1-y) + x(1-x)]}{a^2 - b^2 \cos^2\theta_{\text{c.m.}}} \right].
\end{aligned}
\tag{17}
$$

Here $a, b = (l - x)(1 - y) \pm xy$, the subscripts $++-, --, \dots$ refer to incident photon helicities, and e_1, e_2 are the quark charges (i.e., the mesons have charges $\pm(e_1 - e_2)$). The essential input for the $\gamma\gamma \to M\overline{M}$ amplitude $\mathcal{M}_{\lambda,\lambda'}$ are thus the meson distribution amplitudes. Notice that the dependence in x and y of several terms in $T_{\lambda,\lambda'}$ is quite similar to that appearing in the meson's electromagnetic form factor.

Thus much of the dependence on $\phi_M(x, Q)$ can be eliminated by expressing it in terms of the meson form factor, *e.g.*,

$$\mathcal{M}_{++} = \mathcal{M}_{--} = 16\pi\alpha F_M(s)\frac{\langle(e_1 - e_2)^2\rangle}{1 - \cos^2\theta_{\text{c.m.}}}. \tag{18}$$

In fact, the ratio of the $\gamma\gamma \to \pi^+\pi^-$ and $e^+e^- \to \mu^+\mu^-$ amplitudes at large s and fixed θ_{CM} can be predicted since the ratio is nearly insensitive to the running coupling and the shape of the pion distribution amplitude:

$$\frac{\frac{d\sigma}{dt}(\gamma\gamma \to \pi^+\pi^-)}{\frac{d\sigma}{dt}(\gamma\gamma \to \mu^+\mu^-)} \sim \frac{4|F_\pi(s)|^2}{1 - \cos^2\theta_{\text{c.m.}}}. \tag{19}$$

The comparison of the PQCD prediction for the sum of $\pi^+\pi^-$ plus K^+K^- channels with recent CLEO data[55] is shown in Fig. 8. Results for separate pion and kaon channels have been given by the TPC/2γ collaboration.[56]
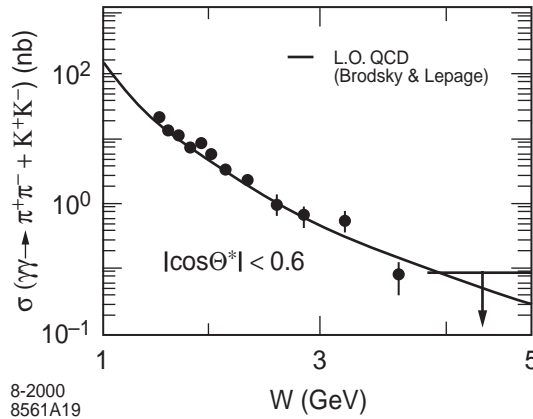
Figure 8: Comparison of the sum of $\gamma\gamma \to \pi^+\pi^-$ and $\gamma\gamma \to K^+K^-$ meson pair production cross sections with the parameter-free perturbative QCD prediction of Brodsky and Lepage.[54] The data are from the CLEO collaboration.[55]

The angular distribution of meson pairs is also predicted by PQCD at large momentum transfer. [54] This is illustrated in Fig. 9 for charged and neutral pions for and transversely polarized (opposite helicity) ρ mesons in Fig. 10.

The PQCD prediction for charged pions and kaons is insensitive to the shape of the meson distribution amplitudes as seen in Fig. 9. The CLEO data for charged pion and kaon pairs show a clear transition to the angular distribution predicted by PQCD for $W = \sqrt{s_{\gamma\gamma}} > 2$ GeV. See Fig. 11. It is clearly important to measure the two-photon production of neutral pions and $\rho^+\rho^-$ cross sections in view of their strong sensitivity to the shape of meson distribution amplitudes. Furthermore, the ratio of $\pi^+\pi^-$ to $\pi^0\pi^0$ cross sections is highly sensitive to the production dynamics.
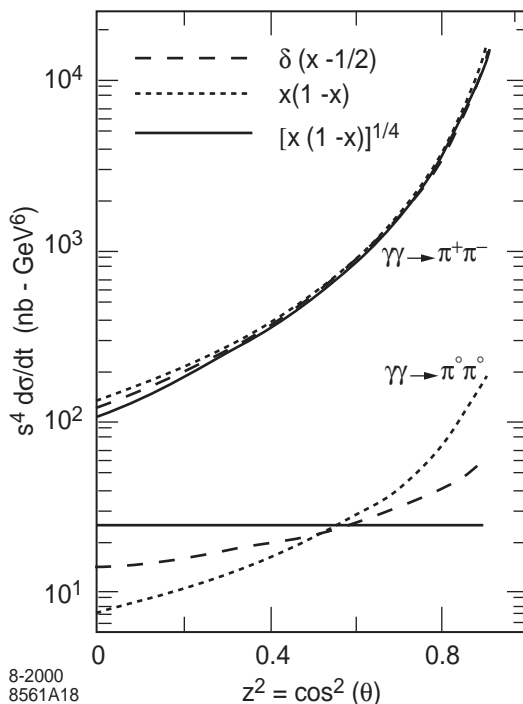
Figure 9: Perturbative QCD predictions for the angular distribution of $\gamma\gamma \to \pi^+\pi^-$ and $\gamma\gamma \to \pi^0\pi^0$ at leading twist.[54] The predictions are shown for three different models for the pion distribution amplitude $\phi(x, Q)$.

Similar predictions are possible for other helicity-zero mesons. The normalization of $\gamma\gamma \to M\overline{M}$ relative to the $\gamma\gamma \to \pi^+\overline{\pi}^-$ cross section is completely determined by the ratio of meson decay constants $(f_M/f_\pi)^4$ and by the flavor-symmetry of the wave functions, provided only that meson and pion distribution amplitudes are similar in shape.

The neutral pion pair production cross section is predicted to be much smaller than that of charged pion pairs. See Fig. 9. This would not be true if only diagrams in which the photon couples to both quarks dominates. Furthermore, there is strong sensitivity of the QCD prediction $\gamma\gamma \to \pi^0\pi^0$ angular distribution to the pion distribution amplitude. Thus measurements of the ratio

$$\frac{\frac{d\sigma}{dt}\left(\gamma\gamma \to \pi^0\pi^0\right)}{\frac{d\sigma}{dt}\left(\gamma\gamma \to \pi^+\pi^-\right)}$$

are crucial for QCD. Notice also that the production cross section for charged ρ-pairs (with any helicity) is much larger that for that of neutral ρ pairs, particularly at large $\theta_{\mathrm{c.m.}}$ angles.

Exclusive two-photon processes probe the basic Born structure of QCD; they thus provide detailed checks of scaling behavior of the quark and gluon propaga-
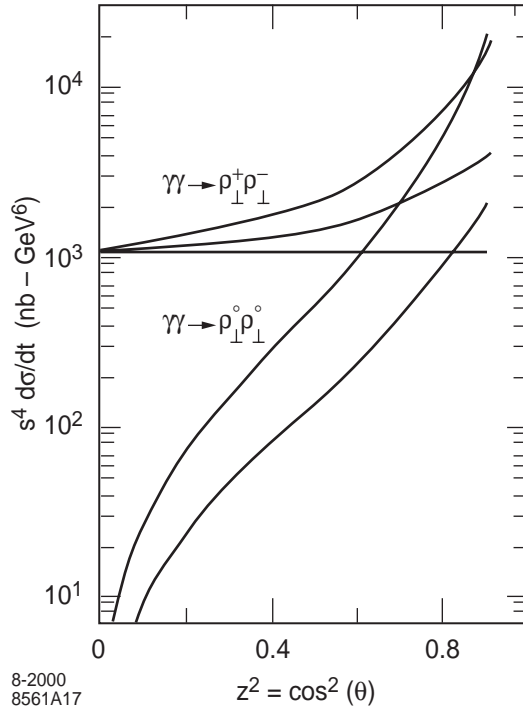
19

Figure 10: PQCD predictions for the leading twist angular distribution of the $\gamma\gamma \to \rho^+\rho^-$ production cross section.[54]

tors and interactions as well as their charges and spins. Conversely, the angular dependence of the $\gamma\gamma \to H\overline{H}$ amplitudes can be used to determine the shape of the process-independent distribution amplitude $\phi_H(x, Q)$ for valence quarks in the hadron Fock state. The $\theta_{\mathrm{c.m.}}$ dependence of the $\gamma\gamma$ amplitudes determines the light cone x-dependence of the meson distribution amplitude in much the same way that the x_{bj} dependence of deep inelastic cross sections determines the light-cone x-dependence of the structure functions. The form of the leading twist predictions are exact to leading order in α_s. Power-law (m/Q) corrections can arise from mass insertions, higher Fock states, pinch singularities, and nonperturbative effects. In particular, the predictions are only valid when s-channel resonance effects can be neglected. It is likely that the background due to resonances can be reduced relative to the leading order QCD contributions if one measures the two-photon processes with at least one of the photons tagged at moderate spacelike momentum q^2, since resonance contributions are expected to be strongly damped by form factor effects.

Finally, note that the amplitudes given above have simple crossing properties. In particular, we can analyze the Compton amplitude $\gamma M \to \gamma M$ in the region of large t with $s \gg |t|$ in order to study the leading Regge behavior in the large momentum transfer domain. In the case of helicity ± 1 mesons, the leading contribution to the
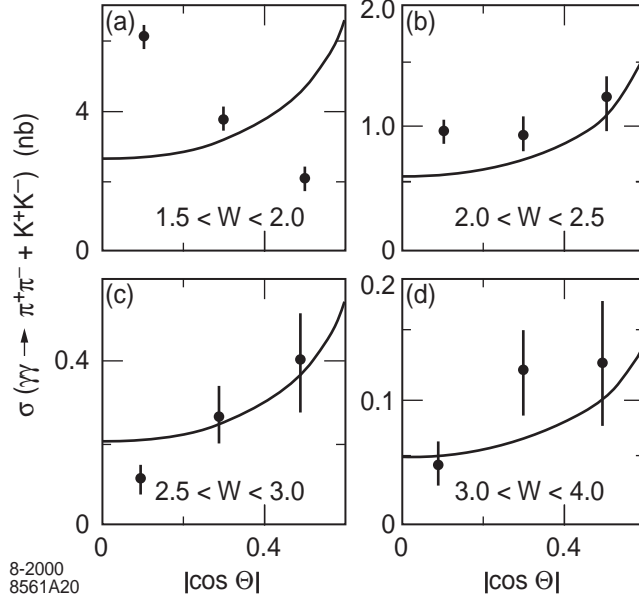
20

Figure 11: Comparison of the angular distribution of the sum of $\gamma\gamma \to \pi^+\pi^-$ and $\gamma\gamma \to K^+K^-$ meson pair production cross sections with the perturbative QCD prediction of Brodsky and Lepage.[54] The data are from the CLEO collaboration.[55]

Compton amplitude has the form $s \gg |t|$

$$\mathcal{M}_{\gamma M \to \gamma M} = 16\pi\alpha F_{M_\perp}(t)(e_1^2 + e_2^2) \tag{20}$$

for $\lambda_\gamma = \lambda_\gamma', \lambda_M = \lambda_M'$. which corresponds to a fixed Regge singularity at $J = 0$. In the case of helicity zero mesons, this singularity decouples, and the leading J-plane singularity is at $J = -2$.

2.4 Perturbative QCD Calculation of Baryon Form Factors

The baryon form factor at large momentum transfer provides another important example of the application of perturbative QCD to exclusive processes. Its factorized structure is illustrated in Fig. 12.

Away from possible special points in the x_i integrations (which are suppressed by Sudakov form factors) the form factor can be written to leading order in $1/Q^2$ as a convolution of a connected hard-scattering amplitude T_H convoluted with the baryon distribution amplitudes:

$$\phi_B(x_i, Q) = \int^{|\mathcal{E}| < \overline{Q}^2} [d^2 k_\perp] \psi_{qqq}(x_i, \vec{k}_{\perp i}) , \tag{21}$$
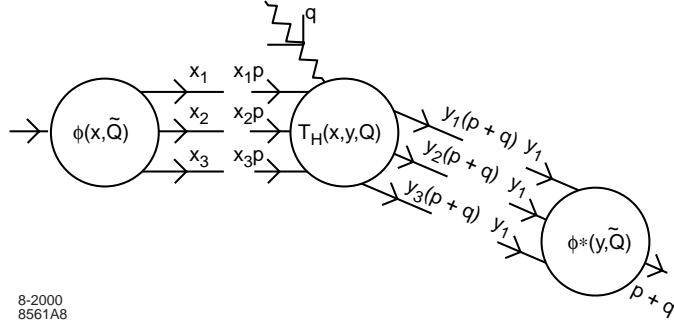
21

Figure 12: Factorization of the baryon form factor in perturbative QCD at large momentum transfer. The hard scattering amplitude T_H is computed perturbatively for incident and final state valence quarks collinear with the respective hadrons.

where $\mathcal{E} = \mathcal{M}_3^2 - M_p^2$ is the invariant mass squared of the three quarks relative to the bound state mass. The hard scattering amplitude T_H is computed by replacing each external hadron line by massless valence quarks each collinear with the hadron's momentum $p_i^\mu \cong x_i p_H^\mu$. Thus the baryon form factor at large Q^2 takes the form [57]

$$G_M(Q^2) = \int [dx][dy] \phi^*(y_i, \overline{Q}) T_H(x, y; Q^2) \phi(x, \overline{Q}) \tag{22}$$

where T_H is the $3q + \gamma \to 3q'$ amplitude. For the proton and neutron we have to leading order $[C_B = 2/3]$

$$T_p = \frac{128\pi^2 C_B^2}{(Q^2 + M_0^2)^2} \, T_1, \tag{23}$$

and

$$T_n = \frac{128\pi^2 C_B^2}{3(Q^2 + M_0^2)^2} \, [T_1 - T_2] \tag{24}$$

where

$$\begin{aligned} T_1 \;\; = \;\; & -\frac{\alpha_s(x_3 y_3 Q^2) \, \alpha_s(1 - x_1)(1 - y_1)Q^2)}{x_3(1 - x_1)^2 \, y_3(1 - y_1)^2} \\ & +\frac{\alpha_s(x_2 y_2 Q^2) \, \alpha_s\left((1 - x_1)(1 - y_1)Q^2\right)}{x_2(1 - x_1)^2 \, y_2(1 - y_1)^2} \\ & -\frac{\alpha_s(x_2 y_2 Q^2) \, \alpha_s(x_3 y_3 Q^2)}{x_2 x_3(1 - x_3) \, y_2 y_3(1 - y_1)} \,, \end{aligned} \tag{25}$$

and

$$T_2 = -\frac{\alpha_s(x_1 y_1 Q^2) \, \alpha_s(x_3 y_3 Q^2)}{x_1 x_3(1 - x_1) \, y_1 y_3(1 - y_3)} \quad . \tag{26}$$

T_1 corresponds to the amplitude where the photon interacts with the quarks (1) and (2) which have helicity parallel to the nucleon helicity, and T_2 corresponds to the

22

amplitude where the quark with opposite helicity is struck. The running coupling constants have arguments $\hat{Q}^2$ corresponding to the gluon momentum transfer of each diagram. Only the large Q^2 behavior is predicted by the theory; we utilize the parameter M_0 to represent the effect of power-law suppressed terms from mass insertions, higher Fock states, *etc.*

The Q^2-evolution of the baryon distribution amplitude can be derived from the operator product expansion of three quark fields or from the gluon exchange kernel. The baryon evolution equation to leading order in $\alpha_s(Q^2)$,[57]

$$x_1 x_2 x_3 \left\{ \frac{\partial}{\partial \zeta} \tilde{\phi}(x_i, Q) + \frac{3}{2} \frac{C_F}{\beta_0} \tilde{\phi}(x_i, Q) \right\} = \frac{C_B}{\beta_0} \int_0^1 [dy] V(x_i, y_i) \tilde{\phi}(y_i, Q). \qquad (27)$$

Here $\phi = x_1 x_2 x_3 \tilde{\phi}$, $\zeta = \log(\log Q^2/\Lambda^2)$, $C_F = (n_c^2 - 1)/2n_c = 4/3$, $C_B = (n_c + 1)/2n_c = 2/3$, $\beta = 11 - (2/3)n_f$, and $V(x_i, y_i)$ is computed to leading order in α_s from the single-gluon-exchange kernel:

$$
\begin{aligned}
V(x_i, y_i) &= 2 x_1 x_2 x_3 \sum_{i \neq j} \theta(y_i - x_i) \delta(x_k - y_k) \frac{y_j}{x_j} \left(\frac{\delta_{h_i \bar{h}_j}}{x_i + x_j} + \frac{\Delta}{y_i - x_i} \right) \qquad (28) \\
&= V(y_i, x_i) \quad .
\end{aligned}
$$

The infrared singularity at $x_i = y_i$ is canceled because the baryon is a color singlet.

The evolution equation automatically sums to leading order in $\alpha_s(Q^2)$ all of the contributions from multiple gluon exchange which determine the tail of the valence wavefunction and thus the Q^2-dependence of the distribution amplitude. The general solution of this equation is

$$\phi(x_i, Q) = x_1 x_2 x_3 \sum_{n=0}^{\infty} a_n \left(\ell n \frac{Q^2}{\Lambda^2} \right)^{-\gamma_n} \phi_n(x_i) \quad , \qquad (29)$$

where the anomalous dimensions γ_n and the eigenfunctions $\tilde{\phi}_n(x_i)$ satisfy the characteristic equation:

$$x_1 x_2 x_3 \left(-\gamma_n + \frac{3 C_F}{2\beta} \right) \tilde{\phi}_n(x_i) = \frac{C_B}{\beta} \int_0^1 [dy] \, V(x_i, y_i) \tilde{\phi}_n(y_i) \quad . \qquad (30)$$

A useful technique [58] for obtaining the solution to the evolution equations is to construct completely antisymmetric representations as a polynomial orthonormal basis for the distribution amplitude of multi-quark bound states. In this way one obtain a distinctive classification of nucleon (N) and Delta (Δ) wave functions and the corresponding Q^2 dependence which discriminates N and Δ form factors.

More recently Braun and collaborators have shown how one can use conformal symmetry to classify the eigensolutions of the baryon distribution amplitude.[59] They identify a new 'hidden' quantum number which distinguishes components in the $\lambda = 3/2$ distribution amplitudes with different scale dependence. They are able

to find analytic solution of the evolution equation for $\lambda = 3/2$ and $\lambda = 1/2$ baryons where the two lowest anomalous dimensions for the $\lambda = 1/2$ operators (one for each parity) are separated from the rest of the spectrum by a finite 'mass gap'. These special states can be interpreted as baryons with scalar diquarks. Their results may support Carlson's solution[60] to the puzzle that the proton to Δ form factor falls faster[61] than other $p \to N^*$ amplitudes if the Δ distribution amplitude has a symmetric $x_1 x_2 x_3$ form.

Taking into account the evolution of the baryon distribution amplitude, the nucleon magnetic form factors at large Q^2, has the form[24, 35, 57]

$$G_M(Q^2) \to \frac{\alpha_s^2(Q^2)}{Q^4} \sum_{n,m} b_{nm} \left(\log\frac{Q^2}{\Lambda^2}\right)^{\gamma_n^B - \gamma_n^B} \left[1 + \mathcal{O}\left(\alpha_s(Q^2), \frac{m^2}{Q^2}\right)\right] \quad . \quad (31)$$

where the γ_n are computable anomalous dimensions of the baryon three-quark wave function at short distance and the b_{mn} are determined from the value of the distribution amplitude $\phi_B(x, Q_0^2)$ at a given point Q_0^2 and the normalization of T_H. The anomalous dimensions of three quark operators have also been computed by Peskin from the operator product expansion.[62] Asymptotically, the dominant term has the minimum anomalous dimension. The dominant part of the proton form factor comes from the region of the x_i integration where each quark has a finite fraction of the light cone momentum. The contribution from the endpoint regions of integration, $x \sim 1$ and $y \sim 1$, at finite $k_\perp$ is Sudakov suppressed [34, 35, 24]; however, it can play a significant role in phenomenology.

One can also use PQCD to predict ratios of various baryon and isobar form factors assuming isospin or $SU(3)$-flavor symmetry for the basic wave function structure. Results for the neutral weak and charged weak form factors assuming standard $SU(2) \times U(1)$ symmetry can also be derived. [63]

A critical input for predicting the normalization of the proton form factor is the value of f_N, the coefficient of the asymptotic contribution to the baryon distribution amplitude. The first analysis from QCD sum rules was carried out by Ioffe and Belyaev,[64] giving the value $f_N = (8 \pm 3) \times 10^{-3}\text{GeV}^2$. In an updated analysis, Chernyak and Zhitnitsky find $f_N = (5.3 \pm 0.5) \times \times 10^{-3}\text{GeV}^2$.[65, 66] The same parameter enters the computation of proton decay. The proton distribution amplitude has to be evolved to the appropriate scale controlling the decay processes in the grand unified theory.[67]

Phenomenologically, the leading order QCD prediction explains the observed approximate $Q^4 G_M(Q^2) \approx \text{const}$ behavior, modulo the logarithmic corrections from the evolution of the coupling and distribution amplitude. The shape of the distribution amplitude is critical: if one assumes that the proton distribution amplitude is the asymptotic form: $\phi_N = C x_1 x_2 x_3$, then the convolution with the leading order form for T_H gives zero! If one takes a non-relativistic form peaked at $x_i = 1/3$, the sign is negative, requiring a crossing point zero in the form factor at some finite Q^2. The broad asymmetric distribution amplitudes deduced by Chernyak and Zhitnitsky in

their QCD sum rule analysis gives a more satisfactory result. If one assumes a constant value of $\alpha_s = 0.3$, and $f_N = 5.3 \times 10^{-3} \text{GeV}^2$, the leading order prediction is below the data by a factor of ≈ 3. However, since the form factor is proportional to $\alpha_s^2 f_N^2$. One can obtain agreement by a simple renormalization of the parameters. For example, if one uses the central value of Ioffe's determination $f_N = 8 \times 10^{-3} \text{GeV}^2$, then good agreement is obtained. A detailed comparison with the data is given in a recent review by Stefanis.[6]

2.5 The Onset of Leading-Twist Contributions in Exclusive Reactions

Is a perturbative QCD analysis of form factors, Compton scattering, and other hard exclusive processes at the present experimentally accessible momentum transfer justified? The situation is not totally clear, and there is an active debate in literature.

In general, the applicability of a perturbative analysis depends on the convergence of the series. In the case of Compton scattering, the number of diagrams contributing to the hard radiative corrections to T_H is very large even, at one-loop order. Furthering, the overall momentum transfer Q is divided among several exchanged gluons, so the regime where leading twist perturbative QCD becomes applicable would be expected to be at larger momentum scales than that typical of inclusive reactions.

Ioffe and Smilga [68] were the first to use QCD sum rules to predict the behavior of exclusive amplitudes at intermediate momentum transfer. More recently Braun, Khodjamirian, and Maul [69] calculated the pion form factor in QCD at intermediate momentum transfers in the light-cone sum rule approach, including radiative corrections and higher-twist effects. Assuming the asymptotic pion, they find a strong numerical cancelation between the soft (end point) contribution and power suppressed hard contributions of higher twist, so that the total nonperturbative correction to the leading twist PQCD result turns out to be only of order 30% for $Q^2 \sim 1 \text{ GeV}^2$.

The transition from soft to hard QCD could be related to the QCD scale anomaly.[70]. At small momentum transfers, one can identify by duality the anomalous contribution $\frac{\beta}{2g}G^{\mu\nu}G_{\mu\nu}$ to the trace of the stress tensor θ_μ^μ with the corresponding meson pair contributions to the θ_μ^μ given by chiral Lagrangian. This implies an effective coupling of two gluons to meson pairs at zeroth order in the QCD coupling g. See e.g., Fujii and Kharzeev [71] For example, in case of the proton form factor, tree diagram contributions to $T_H(qqq\gamma^* \to qqq)$ will be strongly modified at low momentum transfer by the propagation of low mass $I = O$ meson pairs between the exchanged gluons. At high momentum transfer the meson exchange effects are suppressed. It would be interesting to study the effect of these hadronic corrections on the nucleon form factors at intermediate scales.

The proton form factor appears to scale at $Q^2 > 5 \text{ GeV}^2$ according to the PQCD predictions. See Fig. 13. Nucleon form factors are approximately described phe-

nomenologically by the well-known dipole form

$$G_M(Q^2) \simeq \frac{1}{(1 + Q^2/0.71 \, \text{GeV}^2)^2} \tag{32}$$

which behaves asymptotically as

$$G_M(Q^2) \simeq \frac{1}{Q^4}\left(1 - 2\frac{0.71 \text{GeV}^2}{Q^2} + \cdots\right).$$

This provides some evidence that the corrections to leading twist in the proton form factor and similar exclusive processes involving protons become important in the range $Q^2 < 1.4 \, \text{GeV}^2$.
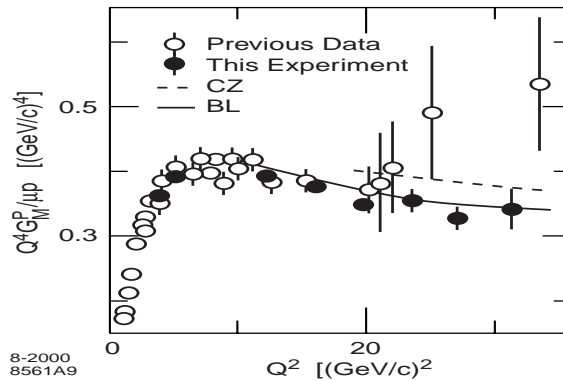

Figure 13: Predictions for the normalization and sign of the proton form factor at high Q^2 using perturbative QCD factorization and QCD sum rule predictions for the proton distribution amplitude (From Ji *et al.*[72] The curve labeled BL has arbitrary normalization and incorporates the fall-off of two powers of the running coupling. The dotted line is the QCD sum rule prediction of given by Chernyak and Zhitnitsky.[65, 66] The results are similar for the model distribution amplitudes of King and Sachrajda,[73] and Gari and Stefanis.[74]

2.6 Applications of Perturbative QCD to Two-Body Reactions

We can also apply perturbative QCD factorization to exclusive hadron scattering processes such as $A + B \to C + D$ scattering at fixed θ_{cm}, where A, B, C, D can be leptons, gauge bosons, or hadrons. See Fig. 14. In such cases the exclusive amplitude typically factorizes at leading order in the momentum transfer scale Q as a convolution

$$\mathcal{M} = \int [dx] T_H(x_j, Q) \prod_{H_I} \phi_{H_I}(x_j, Q) \tag{33}$$
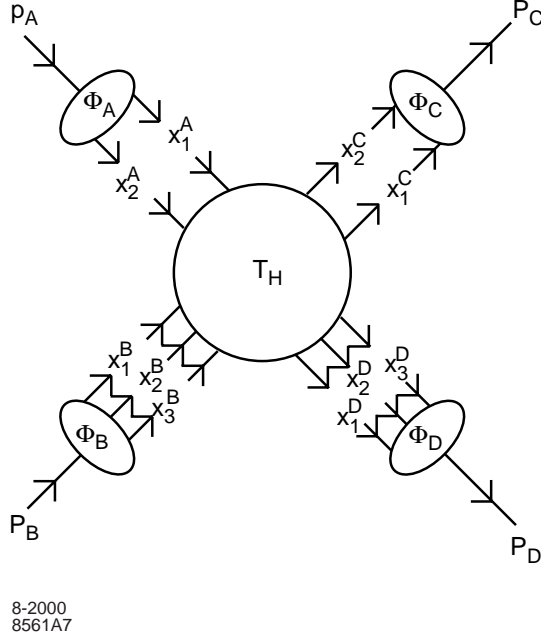
26

8-2000
8561A7

Figure 14: Factorization of the meson-baryon scattering in perturbative QCD at large momentum transfer. The hard scattering amplitude T_H is computed perturbatively for incident and final state valence quarks collinear with the respective hadrons.

where

$$[dx] = \prod_{j=1}^{n_I} \delta(1 - \sum_{j=1}^{n_I} x_j). \tag{34}$$

Here T_H is the hard scattering amplitude which is computed by replacing each of the incident and final hadrons by collinear massless valence quarks with momentum fractions $k_i^\mu = x_i P_H$ $0 < x_i < 1, \sum_i x_i = 1$, respectively. The fractions x_j are the boost-invariant light-cone momentum fractions $x_j = k_j^+/P^+$ carried by the quarks. The light-cone metric is taken as $k^+ = k^0 \pm k^3, 2k \cdot p = k^+ p^- + k^- p^+ - 2\vec{k}_\perp \cdot p_\perp$.

A critical complication in the analysis of two-body elastic scattering reactions is the presence of pinch singularities; *i.e.*, regions of integration in which the intermediate state can approach on-shell configurations. For example, consider $\pi^+ \pi^+$ elastic scattering. The pion can scatter to large angles via the successive elastic scattering of two quark pairs to the same angle. Only the soft configurations of the wavefunction are required. The intermediate state between the two scattering is close to on-shell. As shown by Landshoff, [75] the integration over this domain gives an amplitude

$$M_{\pi\pi\to\pi\pi}^{pinch} \propto M_{qq\to qq} M_{\overline{qq}\to\overline{qq}} \times \frac{i}{\sqrt{stu}}. \tag{35}$$

The suppression in the amplitude for scattering the pairs through the same angle

27

thus decreases as $\frac{i}{\sqrt{stu}}$ and has simultaneous cuts in each of the three Mandelstam variables. In the case of baryon-baryon scattering, the result is

$$M_{BB \to BB}^{pinch} \propto M_{qq \to qq} M_{qq \to qq} M_{qq \to qq} \times \left[\frac{i}{\sqrt{stu}} \right]^2 . \qquad (36)$$

These contributions thus apparently have slower fall-off than the leading twist dimensional scaling contributions. It is shown, however, by Duncan and Mueller,[76, 77] that the soft integration domain of the pinch contribution is suppressed at large momentum transfer by Sudakov form factors since the scattering of nearly-on-shell quarks implies gluonic radiation which is suppressed for elastic hadron-hadron scattering. The result, assuming logarithmic fall-off of the running coupling is a suppression of the pinch amplitude which nearly reproduces dimensional counting rules. For example the leading contribution to meson-meson scattering arises from the region $k_i^2 \sim (Q^2)^{1-\epsilon}$ where $\epsilon = (2c-1)^{-1}, c = C_F/(11 - 2/3 n_f)$. For four flavors $\epsilon \simeq 0.281$. The net result of the pinch contributions is

$$M_{\pi\pi \to \pi\pi}^{\text{pinch}} \sim (Q^2)^{-3/2 - c \ln(2c+1)/2c} \simeq (Q^2)^{-1.922}, \qquad (37)$$

compared to $(Q^2)^{-2}$ from the nominal dimensional counting factor. Thus pinch contributions could account for the apparent simple dimensional scaling of amplitudes such as $\gamma p \to \pi^+ n$ and elastic scattering at fixed angles. If one assumes that the coupling is effectively constant in the integration domain, the Sudakov corrections give a result which has a faster power fall-off than PQCD.

2.7 Diminished Final State Interactions and Color Transparency

The factorization of a hard hadronic exclusive amplitude $\mathcal{M}$ into a product of separate distributions ϕ_H for each hadron is only possible if there are no corrections at leading order in $1/Q$ due to the initial or final state hadronic interactions. In fact, QCD predicts strong suppression of final state interactions, a remarkable property considering that hadrons normally interact strongly!

The physical picture which leads to diminished final state interactions is as follows: We assume that pinch contributes are effectively suppressed by Sudakov effects. Then each hadron emitted from a hard exclusive reaction initially emerges with high momentum and small transverse size $b_\perp = \mathcal{O}(1/\tilde{Q})$. A fundamental feature of gauge theory is that soft gluons decouple from the small color-dipole moment of the compact fast-moving color-singlet wavefunction configurations of the incident and final-state hadrons.

The transversely compact color-singlet configurations can effectively persist over a distance of order $\ell_{\text{Ioffe}} = \mathcal{O}(E_{\text{lab}}/Q^2)$, the Ioffe coherence length. Thus if we study hard quasi-elastic processes in a nuclear target such as $eA \to e'p'(A-1)$ or $pA \to p'(A-1)$, the outgoing and ingoing hadrons will have minimal absorption in a nucleus. The

diminished absorption of hadrons produced in hard exclusive reactions implies additivity of the nuclear cross section in nucleon number A and is the theoretical basis the "color transparency" of hard quasi-elastic reactions. [78, 79, 80] Since such a state stays small over a distance ℓ_{Ioffe} proportional to its energy, this implies that quasi-elastic hadron-nucleon scattering at large momentum transfer can occur additively on all of the nucleons in a nucleus with minimal attenuation due to elastic or inelastic final state interactions in the nucleus, $i.e.$ the nucleus becomes "transparent." In contrast, in conventional Glauber scattering, one predicts strong, nearly energy-independent initial and final state attenuation. Similarly, in hard diffractive high energy processes, such as $\gamma^*(Q^2)p \to \rho p$ [30] only small transverse size $b_\perp \sim 1/Q$ of the vector meson distribution amplitude is involved. The hadronic interactions are minimal, and thus the $\gamma^*(Q^2)N \to \rho N$ reaction can occur coherently throughout a nuclear target in reactions without absorption or shadowing. The $\gamma^*A \to VA$ process is thus a laboratory for testing QCD color transparency.

The most convincing demonstration of color transparency has been reported by the E791 group at FermiLab[81] in measurements of diffractive dissociation of a high energy pions to high transverse momentum dijets; $\pi A \to jet\ jet\ A$; the forward diffractive amplitude is observed to grow in proportion to the total number of nucleons in the nucleus, in strong contrast to standard Glauber theory which predicts that only the front surface of the nucleus should be effective. This experiment is discussed further in Section 6.

There is also evidence for the onset of color transparency in large angle quasi-elastic pp scattering in nuclear targets, [82, 83, 84] in the regime $6 < s < 25$ GeV^2, indicating that small wavefunction configurations are indeed controlling this exclusive reaction at moderate momentum transfers. However at $p_{\text{lab}} \simeq 12$ GeV, $E_{cm} \simeq 5$ GeV, color transparency dramatically fails. The concept of color transparency is itself not in doubt in view of the E791 results.

It is noteworthy that at the same energy the normal-normal spin asymmetry A_{NN} in elastic $pp \to pp$ scattering at $\theta_{cm} = 90^0$ increases dramatically to $A_{NN} \simeq 0.6$ in the same kinematical regime—it is ~ 4 times more probable that the protons scatter with helicity normal to the scattering plane than anti-normal.[85] The unusual spin and color transparency effects seen in elastic proton-proton scattering at $E_{CM} \sim 5$ GeV and large angles could be related to the charm threshold and the effect of a $|\,uuduudc\bar{c}\rangle$ resonance which would appear as in the $J = L = S = 1$ pp partial wave.[86, 87] The intermediate state $|uuduudc\bar{c}\rangle$ has odd intrinsic parity and couples to the $J = S = 1$ initial state, thus strongly enhancing scattering when the incident projectile and target protons have their spins parallel and normal to the scattering plane. A similar enhancement of A_{NN} is observed at the strangeness threshold. The physical protons coupling at the charm threshold will have normal Glauber interactions, thus explaining the anomalous change in color transparency observed at the same energy in quasi-elastic pp scattering. A crucial test of the charm hypothesis is the observation of open charm production near threshold with a cross section of order of 1μb. [86, 87]

An alternative explanation of the color transparency and spin anomalies in pp

elastic scattering has been postulated by Ralston and Pire [88, 80] collaborators. The oscillatory effects in the large angle $pp \rightarrow pp$ cross section and spin structure is assumed to be due to the interference of Landshoff pinch and perturbative QCD amplitudes. In the case of quasi-elastic reactions, the nuclear medium absorbs and filters out the non-compact pinch contributions, leaving the additive hard contributions unabsorbed. Indeed, Jain, Pire, and Ralston [80, 89] have constructed models in which the pinch and hard scattering contributions can generate an interference pattern in the $pp \rightarrow pp$ amplitude similar to that observed in the data. It is not clear that such a model can successfully account for the sharp rise in the spin correlation in A_{NN} observed near $\sqrt{s} = 5$ GeV. [90]

There are thus two viable models which can explain the unusual features of elastic and quasi-elastic proton-proton scattering; clearly more experiments and analysis are needed.

2.8 Hadron Helicity Conservation and Other General Features of Exclusive Amplitudes at Leading Twist

One can abstract some general features of QCD common to all exclusive processes at large momentum transfer:

(1) All of the nonperturbative bound-state physics in the scattering amplitude is isolated in the process-independent distribution amplitudes. This is an essential feature of QCD factorization.

(2) The nominal power-law behavior of an exclusive amplitude at fixed $\theta_{\text{c.m.}}$ is $(1/Q)^{n-4}$ where n is the number of external elementary particles (quarks, gluons, leptons, photons, etc.) entering the subprocess in T_H.[19, 20, 21] The amplitude T_H is by definition collinear-irreducible, in the sense that all gluon exchange momentum integrations are hard: $k_\perp^2 > \mathcal{O}(Q^2)$; since the soft integration region is incorporated into the definition of the hadron distribution amplitude. Thus all radiative corrections are higher order in $\alpha_s(Q)$. The convolution of T_H with the $\phi_H(x, Q)$ leads to logarithmic corrections $\log^{\gamma_n} Q$ where the fractional powers γ_n are given by the anomalous dimensions of the local operators which control the evolution of the distribution amplitudes. Thus the scaling of the hadronic amplitude closely follows that of the underlying hard quark scattering amplitude T_H, up to computable logarithmic corrections from the anomalous dimensions of the distribution amplitudes and the logarithmic fall-off of the QCD coupling $\alpha_s(Q^2)$ In particular, the nominal power-law fall-off of helicity-conserving form factors is $F_H \propto (1/Q^2)^{1-n_H}$ where n_H is the number of valence quarks of the hadron. In the case of fixed-angle scattering, the nominal power law fall-off of the cross section is

$$\frac{d\sigma}{dt}(A + B \rightarrow C + D) = \frac{F_{A+B \rightarrow C+D}(\theta_{cm})}{s^{n_{tot}-2}},$$ (38)

where $n_{tot} = n_A + n_B + n_C + n_D$ is the number of elementary fields in the initial state and final state. For example, $n_{tot} = n_A + n_B + n_C + n_D = 1 + 3 + 2 + 3 = 9$ for $\gamma p \rightarrow \pi^0 p$,

scaling which agrees remarkably well with the fixed angle pion photoproduction data as seen in Fig. 15.
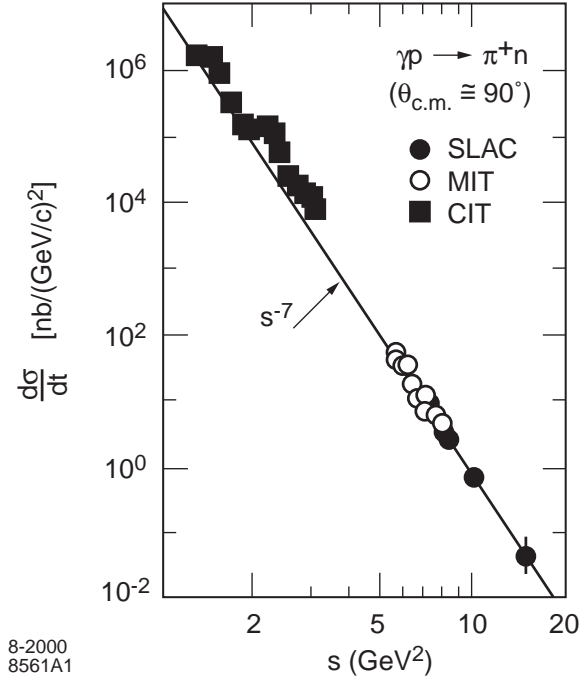

Figure 15: Comparison of photoproduction data with the dimensional counting power-law prediction. The data are summarized in Anderson *et al.*[91]

The dimensional counting rules are expected to be modified by the Q^2-dependence of the factors of $\alpha_s(Q^2)$ in T_H, by the Q^2-evolution of the distribution amplitudes, and possibly by a small power correction associated with the Sudakov suppression of pinch singularities in hadron-hadron scattering. The dimensional counting rules in fact appear to be experimentally well-established for a wide variety of processes.

The approach to scaling of $s^7 d\sigma/dt(\gamma p \to \pi^+ n)$ as shown in Fig. 15 appears to indicate that leading twist PQCD is applicable at momentum transfers exceeding a few GeV. If anything, the scaling appears to work too well, considering that one expects logarithmic deviations from the running of the QCD coupling and logarithmic evolution of the hadron distribution amplitudes. The absence of significant corrections to leading-twist scaling suggests that the running coupling is effectively frozen at the kinematics relevant to the data. This is discussed further in Section 4. If higher-twist soft processes are conspiring to mimic leading twist scaling $s^7 d\sigma/dt(\gamma p \to \pi^+ n)$, then we would have the strange situation of seeing two separate kinematic domains of s^7 scaling of the photoproduction cross section. However, despite the empirical success of the PQCD description, higher twist mechanisms could still complicate the simple hard scattering description.

The success of PQCD scaling of hard exclusive reaction cross sections illustrated here is not atypical. There are a large number of measured exclusive reactions in which the empirical power law fall-off predicted by dimensional counting and PQCD appears to be accurate over a large range of momentum transfer. These include processes such as the proton form factor, time-like meson pair production in e^+e^- and $\gamma\gamma$ annihilation, large-angle scattering processes such as pion photoproduction $\gamma p \to \pi^+ p$, and nuclear processes such as the deuteron form factor at large momentum transfer and deuteron photodisintegration. [92]

An interesting contribution to $K^+ p \to K^+ p$ scattering comes from the exchange of the common u quark. The quark interchange amplitude for $A + B \to C + D$ can be written as a convolution of the four light-cone wavefunctions multiplied by a factor $\Delta^- = P_A^- + P_B^- - \sum_i k_i^-$, the inverse of the central propagator. [93] The interchange amplitude is consistent with PQCD scaling, and often provides a phenomenologically accurate representation of the $\theta_{c.m.}$ angular distribution at large momentum transfer. For example, the angular distribution of processes such as $K^+ p \to K^+ p$ appear to follow the predictions based on hard scattering diagrams based on quark interchange, e.g., $T_H((u_1\overline{s})(u_2 u_3 d) \to (u_2\overline{s})(u_1 u_3 d))$. [93] This mechanism also provides constraints on Regge intercepts $\alpha_R(t)$ for meson exchange trajectories at large $-t$. [23] An extensive review of this phenomenology is given in the review by Sivers et al. [94]

(3) Hadron helicity conservation: [57] since gauge interactions are vector-like, quark chirality is conserved at every vertex. Furthermore, the leading power contribution corresponds to the projection of T_H on the $L_z = 0$ projections of the hadron wavefunctions. Thus the leading amplitude in $1/Q$ conserves hadron helicity: the sum of hadron helicities in the initial state must equal that of the final state.

$$\sum_{\text{initial}} \lambda_{H_{\text{initial}}} = \sum_{\text{final}} \lambda_{H_{\text{final}}}. \tag{39}$$

Notice that the constraint is independent of the photon helicity in the case of photoninduced reactions. Thus in the case of spin-half form factors, perturbative QCD predicts the dominance of the $F_1(q^2)$ Dirac form factor over the helicity-flip $F_2(q^2)$ Pauli form factor at large momentum transfer.

Only flavor-singlet mesons in the O^{-+} nonet can have a two-gluon valence component, and thus even for these states the quark helicity equals the hadronic helicity. Consequently hadronic helicity conservation applies for all amplitudes involving light mesons and baryons. Note that exclusive reactions which involve hadrons with quarks or gluons in higher orbital angular states are suppressed by powers.

The helicity rule is one of the most characteristic features of QCD, being a direct consequence of the gluon's spin. A scalar or tensor gluon-quark coupling flips the quark's helicity. Thus, for such theories, helicity may or may not be conserved in any given diagram contributing to T_H, depending upon the number of interactions involved. Only for a vector theory, like QCD, can we have a helicity selection rule valid to all orders in perturbation theory. In contrast, in inclusive reactions, there are

any number of noninteracting spectator constituent and the spin of the active quarks or gluons is only statistically related to the hadron spin (except at the edge of phase space $x \to 1$).

The study of timelike hadronic form factors using e^+e^- colliding beams can provide very sensitive tests of this rule, since the virtual photon in $e^+e^- \to \gamma^* \to h_A \overline{h}_B$ always has spin ± 1 along the beam axis at high energies. Angular momentum conservation implies that the virtual photon can "decay" with one of only two possible angular distributions in the center of momentum frame: $(1 + \cos^2 \theta)$ for $|\lambda_A - \lambda_B| = 1$ and $\sin^2 \theta$ for $|\lambda_A - \lambda_B| = 0$ where λ_A and λ_B are the helicities of the outgoing hadrons. Hadronic helicity conservation, as required by QCD, greatly restricts the possibilities. It implies that $\lambda_A + \lambda_B = 0$. Consequently, angular momentum conservation requires $|\lambda_A| = |\lambda_B| = l/2$ for baryons, and $|\lambda_A| = |\lambda_B| = 0$ for mesons; thus the angular distributions for any sets of hadron pairs are now completely determined at leading twist:

$$\frac{d\sigma}{d\cos\theta}(e^+e^- = B\overline{B}) \propto 1 + \cos^2 \theta \tag{40}$$

$$\frac{d\sigma}{d\cos\theta}(e^+e^- = M\overline{M}) \propto \sin^2 \theta \ . \tag{41}$$

Verifying these angular distributions for vector mesons and other higher spin mesons and baryons would verify the vector nature of the gluon in QCD and the validity of PQCD applications to exclusive reactions.

2.9   Applications to Exclusive Nuclear Processes

One of the most interesting areas of exclusive processes is to amplitudes where the nuclear wavefunction has to absorb large momentum transfer. For example, the helicity-conserving deuteron form factor is predicted to scale as $F_d(Q^2) \propto (Q^2)^{-5}$ reflecting the minimal six quark component of nuclear wavefunction.

The deuteron form factor at high Q^2 is sensitive to wavefunction configurations where all six quarks overlap within an impact separation $b_{\perp i} < \mathcal{O}(1/Q)$. The leading power-law fall off predicted by QCD is $F_d(Q^2) = f(\alpha_s(Q^2))/(Q^2)^5$, where, asymptotically, $f(\alpha_s(Q^2)) \propto \alpha_s(Q^2)^{5+2\gamma}$. [92] The derivation of the evolution equation for the deuteron distribution amplitude and its leading anomalous dimension γ were calculated by Brodsky, Lepage and Ji. [95] In general, the six-quark wavefunction of a deuteron is a mixture of five different color-singlet states. The dominant color configuration at large distances corresponds to the usual proton-neutron bound state. However at small impact space separation, all five Fock color-singlet components eventually acquire equal weight, *i.e.*, the deuteron wavefunction evolves to 80% "hidden color." [95] The relatively large normalization of the deuteron form factor observed at large Q^2 hints at sizable hidden-color contributions. [96] Hidden color components can also play a predominant role in the reaction $\gamma d \to J/\psi pn$ at threshold if it is dominated by the multi-fusion process $\gamma gg \to J/\psi$. In the case of nuclear structure functions beyond the single nucleon kinematic limit, $1 < x_{bj} < A$, the nuclear

light-cone momentum must be transferred to a single quark, requiring quark-quark correlations between quarks of different nucleons in a compact, far-off-shell regime. This physics is also sensitive to the part of the nuclear wavefunction which contains hidden-color components in distinction from a convolution of separate color-singlet nucleon wavefunctions.

To first approximation the proton and neutron share the deuteron's momentum equally. Since the deuteron form factor contains the probability amplitudes for the proton and neutron to scatter from $p/2$ to $p/2+q/2$; it is natural to define the reduced deuteron form factor[92, 95]

$$f_d(Q^2) \equiv \frac{F_d(Q^2)}{F_{1N}\left(\frac{Q^2}{4}\right) F_{1N}\left(\frac{Q^2}{4}\right)}. \tag{42}$$

The effect of nucleon compositeness is removed from the reduced form factor. QCD then predicts the scaling

$$f_d(Q^2) \sim \frac{1}{Q^2}; \tag{43}$$

i.e. the same scaling law as a meson form factor. Diagrammatically, the extra power of $1/Q^2$ comes from the propagator of the struck quark line, the one propagator not contained in the nucleon form factors. Because of hadron helicity conservation, the prediction is for the leading helicity-conserving deuteron form factor ($\lambda = \lambda' = 0$.) As shown in Fig. 16, this scaling is consistent with experiment for $Q \gtrsim 1$ GeV. In the case of deuteron photodisintegration $\gamma d \to pn$ the amplitude requires the scattering of each nucleon at $t_N = t_d/4$. The perturbative QCD scaling is[97]

$$\frac{d\sigma}{d\Omega_{c.m.}}(\gamma d \to np) = \frac{1}{\sqrt{s(s - M_d^2)}} \frac{F_n^2(t_d/4)F_p^2(t_d/4)f_{red}^2(\theta_{c.m})}{p_\perp^2}. \tag{44}$$

The predicted scaling of the reduced photodisintegration amplitude $f_{red}(\theta_{c.m.}) \simeq$ const is consistent with experiment.[97, 98, 99] See Fig. 17.

2.10 Experimental Conflicts with Perturbative QCD Predictions

There are, however, striking experimental exceptions to the general success of the leading twist PQCD approach, such as

(a) The dominant two-body decay of the J/ψ is $J/\psi \to \rho\pi$ decay which is forbidden by hadron helicity conservation;

(b) One of the most striking anomalies in elastic proton-proton scattering is the large spin correlation A_{NN} observed at large angles.[102] At $\sqrt{s} \simeq 5$ GeV, the rate for scattering with incident proton spins parallel and normal to the scattering plane is four times larger than that for scattering with anti-parallel polarization.
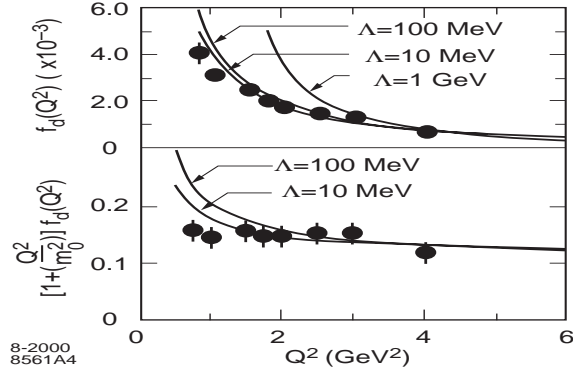
Figure 16: Scaling of the deuteron reduced form factor. The data and theory are summarized by Brodsky and Chertok [92] and by Brodsky and Hiller.[97]
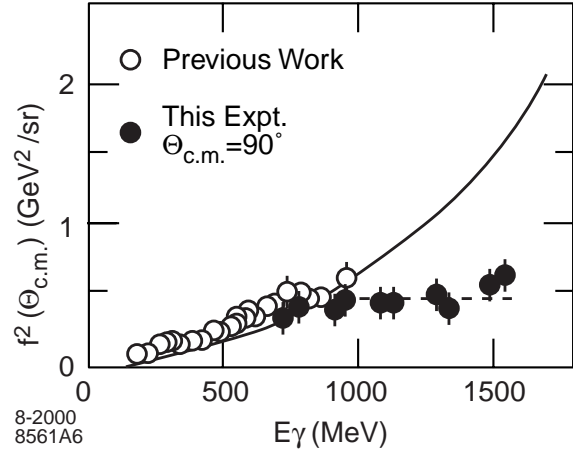

Figure 17: Comparison of deuteron photodisintegration data with the scaling prediction which requires $f^2(\theta_{cm})$ to be at most logarithmically dependent on energy at large momentum transfer. The data in are from Belz *et al.*[100] The solid curve is a nuclear physics prediction.[101]

(c) Surprisingly, the color transparency effect appears to diminish at $s >$ 12 GeV^2, an effect which might be attributed to pinch contributions or the charm threshold.

(d) Recent data from Jefferson laboratory appears to be in conflict with $G_E : G_M$ scaling, which would imply that the helicity-non-conserving Pauli Form factor F_2 is not decreasing much faster than the helicity-conserving Dirac form factor in the Jefferson lab kinematic domain.[103]

These conflicts with leading-twist PQCD predictions could be hinting at new physical effects. For example, It is usually assumed that a heavy quarkonium state such as the J/ψ always decays to light hadrons via the annihilation of its heavy quark constituents to gluons. However, as Karliner and I [104] have recently shown, the transition $J/\psi \to \rho\pi$ can also occur by the rearrangement of the $c\bar{c}$ from the J/ψ into the $|q\bar{q}c\bar{c}\rangle$ intrinsic charm Fock state of the ρ or π. Further discussion will be given in Section 7.

It is clear from these examples that exclusive processes often incorporate a number of physical effects, so that the transition from the soft to hard QCD domain can be very complicated. The contribution of endpoint $x \to 1$ regions of integration where the internal transverse momenta remain soft is a particularly important issue. The integrations over x_i and y_i in the convolution of T_H with the light-cone wavefunctions have potentially significant contributions from the endpoint region $x_2, x_3 \sim \mathcal{O}(m/Q), x_1 \sim 1 - \mathcal{O}(m/Q)$ where the struck quark has nearly all of the proton's light-cone momentum. Since $\sum^n i = 1 x_i = 1$ The spectator quarks must carry small values of the light-cone momentum fraction. In the rest frame $x_i = \frac{k_i^0 + k_i^z}{M}$. Thus in order to have $x_i \to 0$ one must have exactly massless spectators with $m_i = 0$ and $k_{\perp i} = 0_\perp$ or else $k_z \to -\infty$. From this perspective, the end-point domain is a very far-off shell configuration of the light-cone wavefunction. A soft QCD wavefunction would be expected to be exponentially suppressed in this regime, as in the BHL model $\psi_n^{soft}(x_i, k_{\perp i}) = A \exp{-b \, \mathcal{M}_n^2}$.[105]

Bloom-Gilman duality [106, 107] and the Drell-Yan West connection [108, 109] each imply that the contribution to form factors will give a $1/t^2$ fall-off of the nucleon form factors provided that the structure function $F_2(x, Q)$ falls off as $(1-x)^3$.[110] This is, in fact, the nominal power-law behavior predicted from the perturbative hard far-off-shell tail of the light-cone wavefunction, as derived using the spectator counting rules for quarks with helicity parallel to that of the proton.

One can examine the contribution to form factors from the endpoint $x \to 1$ small $k_\perp$ integration region where the struck quark remains near its mass-shell [$k^2 \sim \mathcal{O}(mQ)$] order-by-order in perturbation theory. In the case of spin-zero mesons one can show [237] that the leading power dependence of the two-particle light-cone Fock wavefunction in the endpoint region is $1-x$, giving a meson structure function which falls as $(1-x)^2$ and thus by duality a non-leading contribution to the meson form factor $F(Q^2) \propto 1/Q^3$. Thus the dominant contribution to meson form factors comes from the hard-scattering regime.

In the case of baryon form factors, the endpoint and hard-scattering contributions have the same nominal power-law behavior. However, the endpoint contributions are also suppressed at large Q^2 by a Sudakov form factor, an exponential of a double logarithm, arising from the virtual correction to the $\overline{q}\gamma q$ vertex when the quark legs are nearly-on-shell. [51, 76, 20, 57] Physically, the Sudakov suppression of enedpoint contribuitions to form factors arises since the struck, nearly on-shell quarks tends to radiate gluons; however, in an exclusive process, the gluon radiation into the final state cannot occur. The Sudakov suppression of the endpoint region requires an all orders resummation of perturbative contributions, and thus the dominance of the hard-scattering contribution in baryon form factors is not as rigorous as that for meson form factors.

A detailed analysis of the Sudakov effect has been given by Sterman and Li,[111] and has been extensively developed by Kroll and collaborators [112] and Stefanis and collaborators.[113] The formulation is simplest in the impact representation of the light-cone overlap formula. The vertex corrections give an extra factor [113]

$$S(b_\perp, \zeta) = \exp\left[-\frac{2C_F}{\beta_0} \log \frac{\zeta Q}{\sqrt{2}\Lambda_{QCD}} \log \frac{\frac{\zeta Q}{\sqrt{2}\Lambda_{QCD}}}{\frac{1}{b_\perp \Lambda_{QCD}}}\right], \tag{45}$$

where ζ represents the light-cone fraction of the quarks. The $\log\log\Lambda_{QCD}$ dependence arises from the assumption of the leading logarithmic fall-off of the QCD coupling. The Sudakov fall-off would be stronger if one assumes a fixed coupling.

It is interesting to compare the corresponding calculations of form factors of bound states in QED. The soft wavefunction is the Schrödinger-Coulomb solution $\psi_{1s}(\vec{k}) \propto (1 + \vec{p}^2/(\alpha m_{\text{red}})^2)^{-2}$, and the full wavefunction, which incorporates transversely polarized photon exchange, only differs by a factor $(1 + \vec{p}^2/m_{\text{red}}^2)$. Thus the leading twist dominance of form factors in QED occurs at relativistic scales $Q^2 > m_{\text{red}}^2$.[2, 3] Furthermore, there are no extra relative factors of α in the hard-scattering contribution. If the QCD coupling α_V has an infrared fixed point, then the fall-off of the valence wavefunctions of hadrons will have analogous power-law forms, consistent with the Abelian correspondence principle.[114] If such power-law wavefunctions are indeed applicable to the soft domain of QCD then the transition to leading-twist power law behavior will occur in the nominal hard perturbative QCD domain where $Q^2 \gg \langle k_\perp^2 \rangle, m_q^2$.

In the perturbative QCD analyses, it is helpful to consider the ratio

$$\frac{s^6 d\sigma/dt(\gamma p \to \gamma p)}{t^4 F_1^2(ep \to ep)}$$

where $F_1(t)$ is the elastic helicity-conserving Dirac form factor. The power-law fall-off, the normalization of the valence wavefunctions, and much of the uncertainties from the scales of α_s^4 cancel. Figure 18 shows the result of a recent calculation of the Compton process in PQCD by Brooks and Dixon,[115] which extends and corrects

earlier work. The calculation of T_H for Compton scattering requires the evaluation of 368 helicity-conserving tree diagrams which contribute to $\gamma(qqq) \to \gamma'(qqq)'$ at the Born level and a careful integration over singular intermediate energy denominators. [116, 117, 118] The angular dependence of this ratio is sensitive to the shape of the proton distribution amplitudes, but it appears to be consistent with the distribution amplitudes motivated by QCD sum rules. The normalization at leading order is not predicted correctly. However, it is conceivable that the hard QCD loop corrections to the normalization of the hard scattering Compton amplitude $\gamma(qqq) \to \gamma'(qqq)'$ is significantly larger than that of the elastic form factors in view of the much greater number of Feynman diagrams contributing to T_H in the Compton case relative to T_H for the proton form factor. The perturbative QCD predictions [117] for the Compton amplitude phase can be tested in virtual Compton scattering by interference with Bethe-Heitler processes. [119]
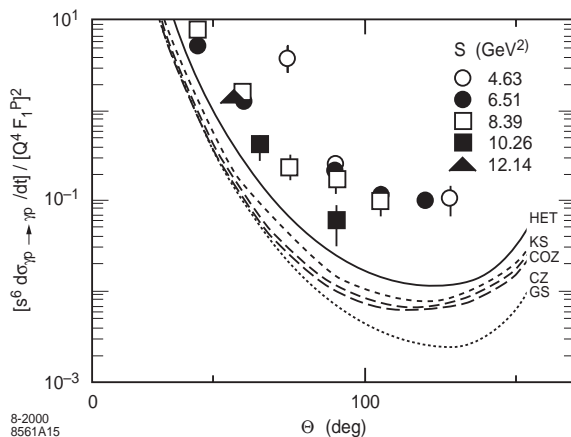

Figure 18: PQCD predictions for Compton scattering $\frac{s^6 d\sigma/dt(\gamma p \to \gamma p)}{t^4 F_1^2(ep \to ep)}$ in PQCD scaled by the Dirac proton form factor for different QCD sum rule-motivated distribution amplitudes. From Brooks and Dixon. [115]

The debate has thus continued [120, 121, 122] on whether processes such as the pion and proton form factors and elastic Compton scattering $\gamma p \to \gamma p$ might be dominated by higher-twist mechanisms until very large momentum transfers. For example, if one assumes that the light-cone wavefunction of the pion has the form $\psi_{\text{soft}}(x, k_\perp) = A \exp(-b \frac{k_\perp^2}{x(1-x)})$, then the Feynman endpoint contribution to the overlap integral at small $k_\perp$ and $x \simeq 1$ will dominate the form factor compared to the hard-scattering contribution until very large Q^2. However, this ansatz for $\psi_{\text{soft}}(x, k_\perp)$ has no suppression at $k_\perp = 0$ for any x; *i.e.*, the wavefunction in the hadron rest frame does not fall-off at all for $k_\perp = 0$ and $k_z \to -\infty$. Thus such wavefunctions do not represent well soft QCD contributions. In addition, as noted above such endpoint contributions will be suppressed by the QCD Sudakov form factor, reflecting

the fact that a near-on-shell quark must radiate if it absorbs large momentum. If the endpoint contribution dominates proton Compton scattering, then both photons will interact on the same quark line as in the handbag diagram in strong contrast to the perturbative QCD predictions.

Radyushkin [121] has argued that the Compton amplitude is dominated by soft end-point contributions of the proton wavefunctions where the two photons both interact on a quark line carrying nearly all of the proton's momentum. This description is dependent on model forms for the soft wavefunctions, but it appears to have some empirical applicability, at least at forward angles where $-t < 10$ GeV^2 From this viewpoint, the dominance of the factorizable PQCD leading twist contributions requires momentum transfers much higher than those currently available. However, a corresponding soft endpoint explanation of the observed $s^7 d\sigma/dt(\gamma p \to \pi^+ n)$ scaling of the pion photoproduction data is not apparent; there is no apparent endpoint contribution which could explain the success of dimensional counting in large-angle pion photoproduction apparent in Fig. 15.

2.11 Additional Theoretical Tools

In addition to perturbative QCD itself, there are additional theoretical tools which can be used to clarify the analytic structure of exclusive amplitudes.

The Conformal Correspondence Principle: Conformal symmetry provides a template for QCD predictions, leading to relations between observables which are present even in a theory which is not scale invariant. Thus an important guide in QCD analyses is to identify the underlying conformal relations of QCD which are manifest if we drop quark masses and effects due to the running of the QCD couplings. In fact, if QCD has an infrared fixed point (vanishing of the Gell Mann-Low function at low momenta), the theory will closely resemble a scale-free conformally symmetric theory in many applications. For example, the natural representation of distribution amplitudes is in terms of an expansion of orthonormal conformal functions multiplied by anomalous dimensions determined by QCD evolution equations. [123, 124, 125, 59]

The Abelian Correspondence Principle. One can consider QCD predictions as analytic functions of the number of colors N_C and flavors N_F. In particular, one can show at all orders of perturbation theory that PQCD predictions reduce to those of an Abelian theory at $N_C \to 0$ with $\hat{\alpha} = C_F \alpha_s$ and $\widehat{N_F} = N_F/TC_F$ held fixed. [114] There is thus a deep connection between QCD processes and their corresponding QED analogs.

The Chiral Correspondence Principle. A particularly interesting constraint on the pion light-cone wavefunction is provided by the $\pi^0 \to \gamma\gamma$ decay amplitude in the chiral $m_\pi^2 \ll 1/R_\pi^2$ limit. The result of matching to the anomaly is[105]

$$\int_0^1 dx \psi_{q\bar{q}}(k_\perp = 0_\perp, x) = \frac{\sqrt{n_c}}{f_\pi} \tag{46}$$

This result, together with the normalization of the integral of $\psi(x, k_\perp)$ from $\pi \to \mu\overline{\nu}$ decay leads to the result that the probability that the pion is in its valence $q\overline{q}$ Fock state is of order $1/4$. Unlike charged particles in QED which have zero probability to be in a given Fock state, neutral charged or color systems have infrared finite wavefunction moments.

3 Light-Cone Fock Representation of Bound State Wavefunctions

We have seen that the physics of exclusive amplitudes is directly tied to the structure of hadron wavefunctions. We thus must confront the fundamental nonperturbative problem in QCD: the solution of the bound state problem; the structure and spectrum of hadrons and nuclei in terms of their quark and gluon degrees of freedom. Ideally, one wants a frame-independent, quantum-mechanical description of hadrons at the amplitude level capable of encoding multi-quark, hidden-color and gluon momentum, helicity, and flavor correlations in the form of universal process-independent hadron wavefunctions. Remarkably, the light-cone Fock expansion allows just such a unifying representation.

Formally, the light-cone expansion is constructed by quantizing QCD at fixed light-cone time [126] $\tau = t + z/c$ and forming the invariant light-cone Hamiltonian: $H_{LC}^{QCD} = P^+P^- - \vec{P}_\perp^2$ where $P^\pm = P^0 \pm P^z$. [127] The operator $P^- = i\frac{d}{d\tau}$ generates light-cone time translations. The P^+ and $\vec{P}_\perp$ momentum operators are independent of the interactions. Each intermediate state consists of particles with light-cone energy $k^- = \frac{\vec{k}_\perp^2 + m^2}{k^+} > 0$ and positive k^+. The procedure for quantizing non-Abelian gauge theory in QCD is well-known.[34, 35, 24, 128, 127] In brief: if one chooses light-cone gauge $A^+ = 0$, the dependent gauge field A^- and quark field $\psi^- = \Lambda^-\psi$ can be eliminated in terms of the physical transverse field $A^\perp$ and $A^+ = \Lambda^+\psi$ fields. Here $\Lambda^\pm = \frac{1}{2}\gamma^\mp\gamma^\pm = \frac{1}{\sqrt{2}}\gamma^0\gamma^\pm$ are hermitian projection operators. Remarkably, no ghosts fields appear in the formalism, since only physical degrees of freedom propagate. The interaction Hamiltonian includes the usual Dirac interactions between the quarks and gluons, the three-point and four-point gluon non-Abelian interactions plus instantaneous light-cone time gluon exchange and quark exchange contributions:[128, 127]

$$
\begin{aligned}
\mathcal{H}_{int} &= -g\,\overline{\psi}^i\gamma^\mu A_\mu^{\ ij}\psi^j \\
&+ \frac{g}{2}f^{abc}\left(\partial_\mu A^a_{\ \nu} - \partial_\nu A^a_{\ \mu}\right)A^{b\mu}A^{c\nu} \\
&+ \frac{g^2}{4}f^{abc}f^{ade}A_{b\mu}A^{d\mu}A_{c\nu}A^{e\nu} \\
&- \frac{g^2}{2}\overline{\psi}^i\gamma^+\left(\gamma^{\perp'}A_{\perp'}\right)^{ij}\frac{1}{i\partial_-}\left(\gamma^\perp A_\perp\right)^{jk}\psi^k
\end{aligned}
$$

$$-\frac{g^2}{2} j^+{}_a \frac{1}{(\partial_-)^2} j^+{}_a \tag{47}$$

where

$$j^+{}_a = \overline{\psi}^i \gamma^+ (t_a)^{ij} \psi^j + f_{abc}(\partial_- A_{b\mu})A^{c\mu} \tag{48}$$

Srivastava and I have recently shown how one can use the Dyson-Wick formalism to construct the Feynman rules in light-cone gauge for QCD. The gauge fields satisfy both the light-cone gauge and the Lorentz condition $\partial_\mu A^\mu = 0$. We have also shown that one can also effectively quantize QCD in the covariant Feynman gauge.[129]

The calculation rules for the Hamiltonian form of light-front-quantized perturbation theory are given in the Appendix.

The eigen-spectrum of H_{LC}^{QCD} in principle gives the entire mass squared spectrum of color-singlet hadron states in QCD, together with their respective light-cone wavefunctions. For example, the proton state satisfies: $H_{LC}^{QCD}|\psi_p\rangle = M_p^2|\psi_p\rangle$. The projection of the proton's eigensolution $|\psi_p\rangle$ on the color-singlet $B = 1$, $Q = 1$ eigenstates $\{|n\rangle\}$ of the free Hamiltonian $H_{LC}^{QCD}(g=0)$ gives the light-cone Fock expansion:

$$\left| \Psi_p; P^+, \vec{P}_\perp, \lambda \right\rangle = \sum_{n \geq 3, \lambda_i} \int \Pi_{i=1}^n \frac{d^2 k_{\perp i} dx_i}{\sqrt{x_i} 16\pi^3} 16\pi^3 \delta\left(1 - \sum_j^n x_j \right) \delta^{(2)}\left(\sum_\ell^n \vec{k}_{\perp\ell} \right)$$

$$\left| n; x_i P^+, x_i \vec{P}_\perp + \vec{k}_{\perp i}, \lambda_i \right\rangle \psi_{n/p}(x_i, \vec{k}_{\perp i}, \lambda_i) . \tag{49}$$

The light-cone Fock wavefunctions $\psi_{n/H}(x_i, \vec{k}_{\perp i}, \lambda_i)$ thus interpolate between the hadron H and its quark and gluon degrees of freedom. The light-cone momentum fractions of the constituents, $x_i = k_i^+/P^+$ with $\sum_{i=1}^n x_i = 1$, and the transverse momenta $\vec{k}_{\perp i}$ with $\sum_{i=1}^n \vec{k}_{\perp i} = \vec{0}_\perp$ appear as the momentum coordinates of the light-cone Fock wavefunctions. A crucial feature is the frame-independence of the light-cone wavefunctions. The x_i and $\vec{k}_{\perp i}$ are relative coordinates independent of the hadron's momentum P^μ. The actual physical transverse momenta are $\vec{p}_{\perp i} = x_i \vec{P}_\perp + \vec{k}_{\perp i}$.

The λ_i label the light-cone spin S^z projections of the quarks and gluons along the z direction. The physical gluon polarization vectors $\epsilon^\mu(k, \ \lambda = \pm 1)$ are specified in light-cone gauge by the conditions $k \cdot \epsilon = 0$, $\eta \cdot \epsilon = \epsilon^+ = 0$. Each light-cone Fock wavefunction satisfies conservation of the z projection of angular momentum: $J^z = \sum_{i=1}^n S_i^z + \sum_{j=1}^{n-1} l_j^z$. The sum over S_i^z represents the contribution of the intrinsic spins of the n Fock state constituents. The sum over orbital angular momenta $l_j^z = -\mathrm{i}(k_j^1 \frac{\partial}{\partial k_j^2} - k_j^2 \frac{\partial}{\partial k_j^1})$ derives from the $n - 1$ relative momenta. This excludes the contribution to the orbital angular momentum due to the motion of the center of mass, which is not an intrinsic property of the hadron.[130]

Light-cone wavefunctions are thus the frame-independent interpolating functions between hadron and quark and gluon degrees of freedom. Hadron amplitudes can be computed from the convolution of the light-cone wavefunctions with irreducible quark-gluon amplitudes. For example, space-like form factors can be represented as

the diagonal $\Delta n = 0$ overlap of light-cone wavefunctions. Time-like form factors such as semi-exclusive B decays can be expressed as the sum of diagonal $\Delta n = 0$ and $\Delta n = 2$ overlap integrals. Structure functions are simply related to the sum over absolute squares of the light-cone wavefunctions. More generally, all multi-quark and gluon correlations in the bound state are represented by the light-cone wavefunctions. Thus in principle, all of the complexity of a hadron is encoded in the light-cone Fock representation, and the light-cone Fock representation is thus a representation of the underlying quantum field theory. The LC wavefunctions $\psi_{n/H}(x_i, \vec{k}_{\perp i}, \lambda_i)$ are universal, process-independent, and thus control all hadronic reactions. In the case of deep inelastic scattering, one needs to evaluate the imaginary part of the virtual Compton amplitude $\mathcal{M}[\gamma^*(q)p \to \gamma^*(q)p]$. The simplest frame choice for electroproduction is $q^+ = 0, q_\perp^2 = Q^2 = -q^2, q^- = 2q \cdot p/P^+, p^+ = P^+, p_\perp = 0_\perp, p^- = M_p^2/P^+$. At leading twist, soft final-state interactions of the outgoing hard quark line are power-law suppressed in light-cone gauge, so the calculation of the virtual Compton amplitude reduces to the evaluation of matrix elements of the products of free quark currents of the free quarks. Given the light-cone wavefunctions, one can compute [34, 35, 24] all of the leading twist helicity and transversity distributions measured in polarized deep inelastic lepton scattering.[131] For example, the helicity-specific quark distributions at resolution Λ correspond to

$$
\begin{aligned}
q_{\lambda_q/\Lambda_p}(x, \Lambda) \quad = \quad & \sum_{n,q_a} \int \prod_{j=1}^n dx_j d^2 k_{\perp j} \sum_{\lambda_i} |\psi_{n/H}^{(\Lambda)}(x_i, \vec{k}_{\perp i}, \lambda_i)|^2 \\
& \times \delta\left(1 - \sum_i^n x_i\right) \delta^{(2)}\left(\sum_i^n \vec{k}_{\perp i}\right) \delta(x - x_q) \delta_{\lambda_a, \lambda_q} \Theta(\Lambda^2 - \mathcal{M}_n^2) \, ,
\end{aligned}
\tag{50}
$$

where the sum is over all quarks q_a which match the quantum numbers, light-cone momentum fraction x, and helicity of the struck quark. Similarly, the transversity distributions and off-diagonal helicity convolutions are defined as a density matrix of the light-cone wavefunctions. This defines the LC factorization scheme [34, 35, 24] where the invariant mass squared $\mathcal{M}_n^2 = \sum_{i=1}^n \left(k_{\perp i}^2 + m_i^2\right)/x_i$ of the n partons of the light-cone wavefunctions are limited to $\mathcal{M}_n^2 < \Lambda^2$.

The light-cone wavefunctions also specify the multi-quark and gluon correlations of the hadron. For example, the distribution of spectator particles in the final state which could be measured in the proton fragmentation region in deep inelastic scattering at an electron-proton collider are in principle encoded in the light-cone wavefunctions. We also note that the high momentum tail of the light-cone wavefunctions can be computed perturbatively in QCD. In particular, the evolution equations for structure functions and distribution amplitudes follow from the perturbative high transverse momentum behavior of the light-cone wavefunctions. The gauge theory features of color transparency and color opacity for color singlet hadrons follows from the distribution of the quarks and gluons in transverse space of the hadron wavefunctions.[78, 79, 80] Light-cone wavefunctions thus are the natural quantities to encode hadron properties and to bridge the gap between empirical constraints and

theoretical predictions for the bound state solutions. One can also obtain guides to
the exact behavior of LC wavefunctions in QCD from analytic or DLCQ solutions
to toy models such as "reduced" $QCD(1+1)$. QCD sum rules, lattice gauge theory
moments, and QCD inspired models such as the bag model, chiral theories, provide
important constraints. We also note that the light-cone and many-body Schrödinger
theory formalisms must match in the heavy quark nonrelativistic limit.

3.1 Light-cone Fock Representation of Current Matrix Elements

The light-cone Fock representation of current matrix elements has a number of sim-
plifying properties. Matrix elements of space-like local operators for the coupling of
photons, gravitons and the deep inelastic structure functions can all be expressed as
overlaps of light-cone wavefunctions with the same number of Fock constituents. This
is possible since one can choose the special frame $q^+ = 0$ [108, 109] for space-like mo-
mentum transfer and take matrix elements of "plus" components of currents such as
J^+ and T^{++}. Since the physical vacuum in light-cone quantization coincides with the
perturbative vacuum, no contributions to matrix elements from vacuum fluctuations
occur. [127]

In the case of a spin-$\frac{1}{2}$ composite system, the Dirac and Pauli form factors $F_1(q^2)$
and $F_2(q^2)$ are defined by

$$\langle P'|J^\mu(0)|P\rangle = \overline{u}(P') \left[F_1(q^2)\gamma^\mu + F_2(q^2)\frac{i}{2M}\sigma^{\mu\alpha}q_\alpha \right] u(P) \ , \tag{51}$$

where $q^\mu = (P'-P)^\mu$ and $u(P)$ is the bound state spinor. In the light-cone formal-
ism it is convenient to identify the Dirac and Pauli form factors from the helicity-
conserving and helicity-flip vector current matrix elements of the J^+ current: [140]

$$\left\langle P+q,\uparrow \left| \frac{J^+(0)}{2P^+} \right| P,\uparrow \right\rangle = F_1(q^2) \ , \tag{52}$$

$$\left\langle P+q,\uparrow \left| \frac{J^+(0)}{2P^+} \right| P,\downarrow \right\rangle = -(q^1 - iq^2)\frac{F_2(q^2)}{2M} \ . \tag{53}$$

The magnetic moment of a composite system is one of its most basic properties. The
magnetic moment is defined at the $q^2 \to 0$ limit,

$$\mu = \frac{e}{2M}\left[F_1(0) + F_2(0) \right], \tag{54}$$

where e is the charge and M is the mass of the composite system. We use the standard
light-cone frame ($q^\pm = q^0 \pm q^3$):

$$\begin{aligned} q &= (q^+, q^-, \vec{q}_\perp) = \left(0, \frac{-q^2}{P^+}, \vec{q}_\perp \right), \\ P &= (P^+, P^-, \vec{P}_\perp) = \left(P^+, \frac{M^2}{P^+}, \vec{0}_\perp \right), \end{aligned} \tag{55}$$

where $q^2 = -2P \cdot q = -\vec{q}_\perp^2$ is 4-momentum square transferred by the photon.

The Pauli form factor and the anomalous magnetic moment $\kappa = \frac{e}{2M}F_2(0)$ can then be calculated from the expression

$$-(q^1 - \mathrm{i}q^2)\frac{F_2(q^2)}{2M} = \sum_a \int \frac{\mathrm{d}^2\vec{k}_\perp \mathrm{d}x}{16\pi^3} \sum_j e_j \; \psi_a^{\uparrow *}(x_i, \vec{k}'_{\perp i}, \lambda_i) \, \psi_a^{\downarrow}(x_i, \vec{k}_{\perp i}, \lambda_i) \; , \qquad (56)$$

where the summation is over all contributing Fock states a and struck constituent charges e_j. The arguments of the final-state light-cone wavefunction are [108, 109]

$$\vec{k}'_{\perp i} = \vec{k}_{\perp i} + (1 - x_i)\vec{q}_\perp \qquad (57)$$

for the struck constituent and

$$\vec{k}'_{\perp i} = \vec{k}_{\perp i} - x_i \vec{q}_\perp \qquad (58)$$

for each spectator. Notice that the magnetic moment must be calculated from the spin-flip non-forward matrix element of the current. It is not given by a diagonal forward matrix element. [132] In the ultra-relativistic limit where the radius of the system is small compared to its Compton scale $1/M$, the anomalous magnetic moment must vanish. [133] The light-cone formalism is consistent with this theorem.

The anomalous moment coupling $B(0)$ to a graviton vanishes for any composite system. This remarkable result, first derived by Okun and Kobzarev, [134, 135, 136, 25, 137] follows directly from the Lorentz boost properties of the light-cone Fock representation. [130]

Exclusive semi-leptonic B-decay amplitudes involving time-like currents such as $B \to A\ell\overline{\nu}$ can also be evaluated exactly in the light-cone framework. [138, 139] In this case, the $q^+ = 0$ frame cannot be used, and the time-like decay matrix elements require the computation of both the diagonal matrix element $n \to n$ where parton number is conserved and the off-diagonal $n + 1 \to n - 1$ convolution such that the current operator annihilates a $q\overline{q}'$ pair in the initial B wavefunction. This term is a consequence of the fact that the time-like decay $q^2 = (p_\ell + p_{\overline{\nu}})^2 > 0$ requires a positive light-cone momentum fraction $q^+ > 0$. A similar result holds for the light-cone wavefunction representation of the deeply virtual Compton amplitude. [29]

Recently Dae Sung Hwang, Bo-Qiang Ma, Ivan Schmidt, and I [130] have shown that the light-cone wavefunctions generated by the radiative corrections to the electron in QED provides a simple system for understanding the spin and angular momentum decomposition of relativistic systems. We have explicitly compute the form factors $F_1(q^2)$ and $F_2(q^2)$ of the electromagnetic current, and the various contributions to the form factors $A(q^2)$ and $B(q^2)$ of the energy-momentum tensor for the model. This perturbative model also illustrates the interconnections between Fock states of different number. The model is patterned after the quantum structure which occurs in the one-loop Schwinger $\alpha/2\pi$ correction to the electron magnetic moment. [140] In effect, we can represent a spin-$\frac{1}{2}$ system as a composite of a spin-$\frac{1}{2}$ fermion

and spin-one vector boson with arbitrary masses. A similar model has been used to illustrate the matrix elements and evolution of light-cone helicity and orbital angular momentum operators.[141] This representation of a composite system is particularly useful because it is based on two constituents but yet is totally relativistic. It can easily be generalized to effectively composite models by assuming Pauli-Villars spectral conditions on the constituent masses, while retaining the spin structure as a consistent template.

3.2 Light-cone Representation of Deeply Virtual Compton Scattering

The virtual Compton scattering process $\frac{d\sigma}{dt}(\gamma^* p \to \gamma p)$ for large initial photon virtuality $q^2 = -Q^2$ (see Fig. 19) has extraordinary sensitivity to fundamental features of the proton's structure. Even though the final state photon is on-shell, the deeply virtual process probes the elementary quark structure of the proton near the light cone as an effective local current. In contrast to deep inelastic scattering, which measures only the absorptive part of the forward virtual Compton amplitude $Im\mathcal{T}_{\gamma^* p \to \gamma^* p}$, deeply virtual Compton scattering allows the measurement of the phase and spin structure of proton matrix elements for general momentum transfer squared t. In addition, the interference of the virtual Compton amplitude and Bethe-Heitler wide angle scattering Bremsstrahlung amplitude where the photon is emitted from the lepton line leads to an electron-positron asymmetry in the $e^{\pm} p \to e^{\pm} \gamma p$ cross section which is proportional to the real part of the Compton amplitude.[142] The deeply virtual Compton amplitude $\gamma^* p \to \gamma p$ is related by crossing to another important process $\gamma^* \gamma \to$ hadron pairs at fixed invariant mass which can be measured in electron-photon collisions.[31, 33]

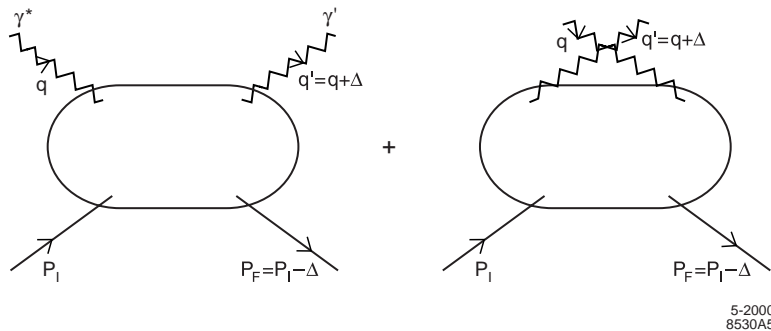

Figure 19: The virtual Compton amplitude $\gamma^*(q) p_I \to \gamma(q') p_F$.

To leading order in $1/Q$, the deeply virtual Compton scattering amplitude factorizes as the convolution in x of the amplitude $t^{\mu\nu}$ for hard Compton scattering on a

quark line with the generalized Compton form factors $H(x,t,\zeta)$, $E(x,t,\zeta)$, $\tilde{H}(x,t,\zeta)$, and $\tilde{E}(x,t,\zeta)$ of the target proton (see Refs. 26–28, 143–151, and 118). Here x is the light-cone momentum fraction of the struck quark, and $\zeta = Q^2/2P\cdot q$ plays the role of the Bjorken variable. The square of the four-momentum transfer from the proton is given by

$$t = \Delta^2 \;=\; 2P\cdot\Delta \;=\; -\frac{(\zeta^2 M^2 + \vec{\Delta}_\perp^2)}{(1-\zeta)} \;, \tag{59}$$

where Δ is the difference of initial and final momenta of the proton ($P = P'+\Delta$). The form factor $H(x,t,\zeta)$ describes the proton response when the helicity of the proton is unchanged, and $E(x,t,\zeta)$ is for the case when the proton helicity is flipped. Two additional functions $\tilde{H}(x,t,\zeta)$, and $\tilde{E}(x,t,\zeta)$ appear, corresponding to the dependence of the Compton amplitude on quark helicity.

Each of the Compton generalized form factors $E,\tilde{E},H,\tilde{H}$ evolve in $\log Q^2$ due to radiative processes associated with struck quark. Our emphasis here, however, will be on the non-perturbative structure of the Compton densities and how they reflect the wavefunctions of proton target. We will also show that the definition and interpretation of the Compton densities $E,\tilde{E},H,\tilde{H}$ and their arguments are frame-dependent.

Virtual Compton scattering with $Q^2 \neq 0$ always involves non-zero momentum transfer, so that a probabilistic interpretation of the skewed distributions is not possible. However, as we shall show, these distributions can be constructed directly from specific overlap integrals of the light-cone Fock-state wavefunctions of the target proton. As in the case of the form factors which control time-like semi-leptonic B decay, one obtains contributions to the virtual Compton amplitude from both diagonal $n = n'$ and off-diagonal $n = n'+2$ parton-number-changing contributions.[138] Nevertheless, despite this complication, there are remarkable sum rules connecting the chiral-conserving and chiral-flip form factors $H(x,t,\zeta)$ and $E(x,t,\zeta)$ which appear in deeply virtual Compton scattering with the corresponding spin-conserving and spin-flip electromagnetic form factors $F_1(t)$ and $F_2(t)$ and gravitational form factors $A_{\rm q}(t)$ and $B_{\rm q}(t)$ for each quark and anti-quark constituent.[143] For example, the gravitational form factors are given by

$$\int_0^1 \frac{{\rm d}x}{1-\frac{\zeta}{2}} \frac{x-\frac{\zeta}{2}}{1-\frac{\zeta}{2}} \left[H(x,\zeta,t) + E(x,\zeta,t)\right] \;=\; A_q(t) + B_q(t) \;. \tag{60}$$

Thus deeply virtual Compton scattering is related to the quark contribution to the form factors of a proton scattering in a gravitational field. Another remarkable feature of these sum rules is the fact that the resulting form factors are independent of the value of ζ. This invariance is due to the Lorentz frame-independence of the light-cone Fock representation of space-like local operator matrix elements which in turn reflects the underlying connections between Fock states of different parton number implied by the QCD equations of motion.

The kinematics of virtual Compton scattering $\gamma^*(q)p(P) \to \gamma(q')p(P')$ are illustrated in Fig. 20. We specify the frame by choosing a convenient parameterization of the light-cone coordinates for the initial and final proton:

$$P_I = (P^+ , \vec{P}_\perp , P^-) = \left(P^+ , \vec{0}_\perp , \frac{M^2}{P^+} \right) , \tag{61}$$

$$P_F = (P'^+ , \vec{P}'_\perp , P'^-) = \left((1-\zeta)P^+ , -\vec{\Delta}_\perp , \frac{(M^2 + \vec{\Delta}_\perp^2)}{(1-\zeta)P^+} \right) . \tag{62}$$

(Our metric is specified by $V^\pm = V^0 \pm V^z$ and $V^2 = V^+ V^- - V_\perp^2$.) The four-momentum transfer from the target is

$$\Delta = P_I - P_F = (\Delta^+ , \vec{\Delta}_\perp , \Delta^-) = \left(\zeta P^+ , \vec{\Delta}_\perp , \frac{(t + \vec{\Delta}_\perp^2)}{\zeta P^+} \right) ,$$

where $\Delta^2 = t$. In addition, overall energy-momentum conservation requires $\Delta^- = P_I^- - P_F^-$.

As in the case of space-like form factors, it is convenient to choose a frame where the incident space-like photon carries $q^+ = 0$ and $q^2 = -Q^2 = -\vec{q}_\perp^2$:

$$q = (q^+ , \vec{q}_\perp , q^-) = \left(0 , \vec{q}_\perp , \frac{(\vec{q}_\perp + \vec{\Delta}_\perp)^2}{\zeta P^+} + \frac{(\zeta M^2 + \vec{\Delta}_\perp^2)}{(1-\zeta)P^+} \right) , \tag{63}$$

$$q' = (q'^+ , \vec{q}'_\perp , q'^-) = \left(\zeta P^+ , (\vec{q}_\perp + \vec{\Delta}_\perp) , \frac{(\vec{q}_\perp + \vec{\Delta}_\perp)^2}{\zeta P^+} \right) = q + \Delta. \tag{64}$$

Thus no light-cone time-ordered amplitudes involving the splitting of the incident photon can occur. The connection between $\vec{\Delta}_\perp^2$, ζ, and t is given by Eq. (59). The variable ζ is fixed from (61) and (64)

$$2P_I \cdot q = \frac{(\vec{q}_\perp + \vec{\Delta}_\perp)^2}{\zeta} + \frac{(\zeta M^2 + \vec{\Delta}_\perp^2)}{(1-\zeta)} . \tag{65}$$

Given the $\psi_{n/H}^{(\Lambda)}$, one can construct space-like electromagnetic, electroweak, gravitational couplings, or any local operator product matrix element from the diagonal overlap of the LC wavefunctions [140]. However, as noted above, in the case of deeply virtual Compton scattering, the proton matrix elements require the computation of not only the diagonal matrix element $n \to n$ for $\zeta < x < 1$, where parton number is conserved, but also an off-diagonal $n+1 \to n-1$ convolution for $0 < x < \zeta$. This second domain occurs since the current operator of the final-state photon with
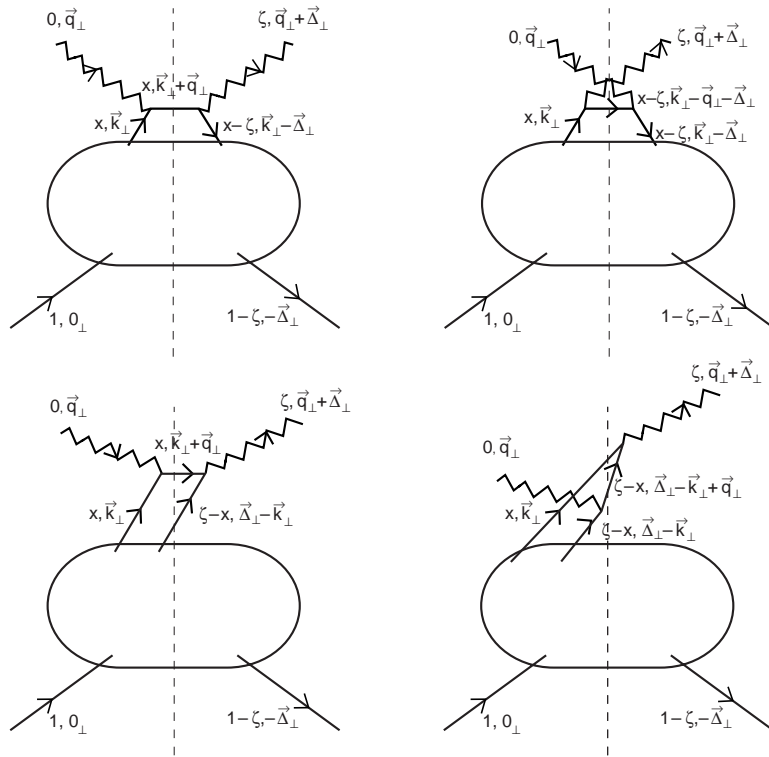
Figure 20: Light-cone time-ordered contributions to deeply virtual Compton scattering. Only the contributions of leading twist in $1/q^2$ are illustrated. These contributions illustrate the factorization property of the leading twist amplitude.

positive light-cone momentum fraction ζ can annihilate a $q\overline{q}'$ pair in the initial proton wavefunction. The off-diagonal terms are referred to in the literature as the "ERBL" contributions, since they resemble virtual Compton scattering on an exchanged mesonic system $\gamma^* q\overline{q}' \to \gamma$ and thus obey the same evolution equations in $\log q^2$ as the meson distribution amplitudes. [35, 46, 24, 47] In fact, the light cone Fock representation shows that there are underlying relations between Fock states of different particle number which interrelate the two domains.

In deeply virtual Compton scattering q^2 is large compared to the masses and t. Then, to leading order in $1/Q^2$, we can take

$$\frac{-q^2}{2P_I \cdot q} = \zeta \ . \tag{66}$$

Thus ζ plays the role of the Bjorken variable in deeply virtual Compton scattering. For a fixed value of $-t$, the allowed range of ζ is given by

$$0 \ \leq \ \zeta \ \leq \ \frac{(-t)}{2M^2} \ \left(\sqrt{1 + \frac{4M^2}{(-t)}} \ - \ 1 \right) \ . \tag{67}$$

The choice of parameterization of the light-cone frame is of course arbitrary. For example, one can also conveniently utilize a "symmetric" frame for the ingoing and outgoing proton which has manifest $\Delta \to -\Delta$ symmetry.

In the case of circularly polarized initial and final photons I and J (I, J are $\uparrow$ or $\downarrow$),

$$M^{IJ}(\vec{q}_\perp, \vec{\Delta}_\perp, \zeta) \ = \ -e_{\mathrm{q}}^2 \ \int_0^1 dx \tag{68}$$

$$\times \left[\ \overline{t}^{IJ}(x,\zeta) \left(H(x,t,\zeta) \, \overline{U}(P')\frac{\gamma^+}{2P^+}U(P) \right. \right.$$

$$+ \ E(x,t,\zeta) \, \overline{U}(P')\frac{i}{2M}\frac{\sigma^{+\alpha}}{2P^+}(-\Delta_\alpha)U(P) \Bigg)$$

$$\overline{s}^{IJ}(x,\zeta) \left(\widetilde{H}(x,t,\zeta) \, \overline{U}(P')\frac{\gamma^+\gamma_5}{2P^+}U(P) \right.$$

$$+ \ \widetilde{E}(x,t,\zeta) \, \overline{U}(P')\frac{1}{2M}\frac{\gamma_5}{2P^+}(-\Delta^+)U(P) \Bigg) \ \Bigg] \ ,$$

where

$$\overline{t}^{\ \uparrow\uparrow}(x,\zeta) \ = \ \overline{t}^{\ \downarrow\downarrow}(x,\zeta) \ = \ \left(\frac{1}{x - i\epsilon} \ + \ \frac{1}{x - \zeta + i\epsilon} \right) \ , \tag{69}$$

$$\overline{s}^{\ \uparrow\uparrow}(x,\zeta) \ = \ - \, \overline{s}^{\ \downarrow\downarrow}(x,\zeta) \ = \ -\left(-\frac{1}{x - i\epsilon} \ + \ \frac{1}{x - \zeta + i\epsilon} \right) \ ,$$

$$\overline{t}^{\ \uparrow\downarrow}(x,\zeta) \ = \ \overline{t}^{\ \downarrow\uparrow}(x,\zeta) \ = \ 0 \ , \qquad \overline{s}^{\ \uparrow\downarrow}(x,\zeta) \ = \ \overline{s}^{\ \downarrow\uparrow}(x,\zeta) \ = \ 0 \ .$$

The two boson polarization vectors in light-cone gauge are $\epsilon^\mu = (\epsilon^+ = 0 \; , \epsilon^- = \frac{\vec{\epsilon}_\perp \cdot \vec{k}_\perp}{2k^+}, \vec{\epsilon}_\perp)$ where $\vec{\epsilon} = \vec{\epsilon}_\perp^{\uparrow, \downarrow} = \mp (1/\sqrt{2})(\widehat{x^1} \pm i\widehat{x^2})$. The polarization vectors also satisfy the Lorentz condition $k \cdot \epsilon = 0$. It is useful to define generalized form factors,

$$F_1(t) = \int_\zeta^1 dx \; f_{1\,(n \to n)}(x, t, \zeta) + \int_0^\zeta dx \; f_{1\,(n+1 \to n-1)}(x, t, \zeta) = \int_0^1 dx \; f_1(x, t, \zeta), \quad (70)$$

$$H(x, t, \zeta) = f_1(x, t, \zeta) = f_{1\,(n \to n)}(x, t, \zeta)\theta(x - \zeta) + f_{1\,(n+1 \to n-1)}(x, t, \zeta)\theta(\zeta - x), \quad (71)$$

and

$$F_2(t) = \int_\zeta^1 dx \; f_{2\,(n \to n)}(x, t, \zeta) + \int_0^\zeta dx \; f_{2\,(n+1 \to n-1)}(x, t, \zeta) = \int_0^1 dx \; f_2(x, t, \zeta), \quad (72)$$

$$E(x, t, \zeta) = f_2(x, t, \zeta) = f_{2\,(n \to n)}(x, t, \zeta)\theta(x - \zeta) + f_{2\,(n+1 \to n-1)}(x, t, \zeta)\theta(\zeta - x). \quad (73)$$

Recently, Diehl, Hwang, and I [29] have shown how the generalized form factors of deeply virtual Compton amplitude can be evaluated explicitly in the Fock state representation using the matrix elements of the currents and the boost properties of the light-cone wavefunctions.

For the $n \to n$ diagonal term ($\Delta n = 0$), the relevant current matrix element at quark level is

$$\int \frac{dy^-}{8\pi} \, e^{ixP^+ y^-/2} \quad (74)$$
$$\times \left\langle 1; x_1' P'^+, \vec{p}_{\perp 1}', \lambda_1' \left| \overline{\psi}(0) \, \gamma^+ \, \psi(y) \right| 1; x_1 P^+, \vec{p}_{\perp 1}, \lambda_1 \right\rangle \Big|_{y^+ = 0, y_\perp = 0}$$
$$= \sqrt{x_1 x_1'} \sqrt{1 - \zeta} \, \delta(x - x_1) \, \delta_{\lambda_1' \lambda_1} \; ,$$

where for definiteness we have labeled the struck quark with the index $i = 1$. We thus obtain formulae for the diagonal (parton-number-conserving) contributions to H and E in the domain $\zeta \leq x \leq 1$ [28]:

$$\frac{\sqrt{1 - \zeta}}{1 - \frac{\zeta}{2}} H_{(n \to n)}(x, \zeta, t) - \frac{\zeta^2}{4(1 - \frac{\zeta}{2})\sqrt{1 - \zeta}} E_{(n \to n)}(x, \zeta, t) \quad (75)$$
$$= \sqrt{1 - \zeta}^{\,2-n} \sum_{n, \lambda_i} \int \prod_{i=1}^n \frac{dx_i \, d^2\vec{k}_{\perp i}}{16\pi^3}$$
$$\times 16\pi^3 \delta \left(1 - \sum_{j=1}^n x_j \right) \delta^{(2)} \left(\sum_{j=1}^n \vec{k}_{\perp j} \right)$$
$$\times \delta(x - x_1) \, \psi_{(n)}^{\uparrow *}(x_i', \vec{k}_{\perp i}', \lambda_i) \, \psi_{(n)}^{\uparrow}(x_i, \vec{k}_{\perp i}, \lambda_i) \; ,$$

$$\frac{1}{\sqrt{1 - \zeta}} \frac{\Delta^1 - i\Delta^2}{2M} E_{(n \to n)}(x, \zeta, t) \quad (76)$$
$$= \sqrt{1 - \zeta}^{\,2-n} \sum_{n, \lambda_i} \int \prod_{i=1}^n \frac{dx_i \, d^2\vec{k}_{\perp i}}{16\pi^3}$$

$$\times \, 16\pi^3 \delta \left(1 - \sum_{j=1}^{n} x_j \right) \delta^{(2)} \left(\sum_{j=1}^{n} \vec{k}_{\perp j} \right)$$

$$\times \, \delta(x - x_1) \, \psi_{(n)}^{\uparrow \, *}(x_i', \vec{k}_{\perp i}', \lambda_i) \, \psi_{(n)}^{\downarrow}(x_i, \vec{k}_{\perp i}, \lambda_i) \, ,$$

where the arguments of the final-state wavefunction are given by

$$x_1' = \frac{x_1 - \zeta}{1 - \zeta} \, , \quad \vec{k}_{\perp 1}' = \vec{k}_{\perp 1} - \frac{1 - x_1}{1 - \zeta} \vec{\Delta}_\perp \quad \text{for the struck quark,} \qquad (77)$$

$$x_i' = \frac{x_i}{1 - \zeta} \, , \qquad \vec{k}_{\perp i}' = \vec{k}_{\perp i} + \frac{x_i}{1 - \zeta} \vec{\Delta}_\perp \quad \text{for the spectators } i = 2, \cdots, n.$$

One easily checks that $\sum_{i=1}^{n} x_i' = 1$ and $\sum_{i=1}^{n} \vec{k}_{\perp i}' = \vec{0}_\perp$. In Eqs. (75) and (76) one has to sum over all possible combinations of helicities λ_i and over all parton numbers n in the Fock states. We also imply a sum over all possible ways of numbering the partons in the n-particle Fock state so that the struck quark has the index $i = 1$.

Analogous formulae hold in the domain $\zeta - 1 < x < 0$, where the struck parton in the target is an antiquark instead of a quark. Some care has to be taken regarding overall signs arising because fermion fields anti-commute.[28, 152]

For the $n + 1 \to n - 1$ off-diagonal term ($\Delta n = -2$), let us consider the case where quark 1 and antiquark $n + 1$ of the initial wavefunction annihilate into the current leaving $n - 1$ spectators. Then $x_{n+1} = \zeta - x_1$ and $\vec{k}_{\perp n+1} = \vec{\Delta}_\perp - \vec{k}_{\perp 1}$. The remaining $n - 1$ partons have total plus-momentum $(1 - \zeta)P^+$ and transverse momentum $-\vec{\Delta}_\perp$. The current matrix element now is

$$\int \frac{dy^-}{8\pi} \, e^{ixP^+ y^-/2} \qquad (78)$$

$$\left\langle 0 \left| \overline{\psi}(0) \, \gamma^+ \, \psi(y) \right| 2; \; x_1 P^+, x_{n+1} P^+, \; \vec{p}_{\perp 1}, \vec{p}_{\perp n+1}, \; \lambda_1, \lambda_{n+1} \right\rangle \Big|_{y^+=0, y_\perp=0}$$

$$= \; \sqrt{x_1 x_{n+1}} \, \delta(x - x_1) \, \delta_{\lambda_1 - \lambda_{n+1}} \, ,$$

and we thus obtain the formulae for the off-diagonal contributions to H and E in the domain $0 \leq x \leq \zeta$:

$$\frac{\sqrt{1 - \zeta}}{1 - \frac{\zeta}{2}} \, H_{(n+1 \to n-1)}(x, \zeta, t) - \frac{\zeta^2}{4(1 - \frac{\zeta}{2})\sqrt{1 - \zeta}} \, E_{(n+1 \to n-1)}(x, \zeta, t) \qquad (79)$$

$$= \; \sqrt{1 - \zeta}^{\, 3-n} \sum_{n, \lambda_i} \int \prod_{i=1}^{n+1} \frac{dx_i \, d^2 \vec{k}_{\perp i}}{16\pi^3}$$

$$\times 16\pi^3 \delta \left(1 - \sum_{j=1}^{n+1} x_j \right) \delta^{(2)} \left(\sum_{j=1}^{n+1} \vec{k}_{\perp j} \right)$$

$$\times \, 16\pi^3 \delta(x_{n+1} + x_1 - \zeta) \, \delta^{(2)} \left(\vec{k}_{\perp n+1} + \vec{k}_{\perp 1} - \vec{\Delta}_\perp \right)$$

$$\times \, \delta(x - x_1) \, \psi_{(n-1)}^{\uparrow \, *}(x_i', \vec{k}_{\perp i}', \lambda_i) \, \psi_{(n+1)}^{\uparrow}(x_i, \vec{k}_{\perp i}, \lambda_i) \, \delta_{\lambda_1 - \lambda_{n+1}} \, ,$$

$$\frac{1}{\sqrt{1-\zeta}} \frac{\Delta^1 - i\Delta^2}{2M} E_{(n+1 \rightarrow n-1)}(x, \zeta, t) \tag{80}$$

$$= \sqrt{1-\zeta}^{3-n} \sum_{n, \lambda_i} \int \prod_{i=1}^{n+1} \frac{\mathrm{d}x_i \, \mathrm{d}^2 \vec{k}_{\perp i}}{16\pi^3}$$

$$\times 16\pi^3 \delta \left(1 - \sum_{j=1}^{n+1} x_j\right) \delta^{(2)} \left(\sum_{j=1}^{n+1} \vec{k}_{\perp j}\right)$$

$$\times 16\pi^3 \delta(x_{n+1} + x_1 - \zeta) \delta^{(2)} \left(\vec{k}_{\perp n+1} + \vec{k}_{\perp 1} - \vec{\Delta}_\perp\right)$$

$$\times \delta(x - x_1) \, \psi_{(n-1)}^{\uparrow \, *}(x_i', \vec{k}_{\perp i}', \lambda_i) \, \psi_{(n+1)}^{\downarrow}(x_i, \vec{k}_{\perp i}, \lambda_i) \, \delta_{\lambda_1 - \lambda_{n+1}} \ ,$$

where $i = 2, \cdots, n$ label the $n-1$ spectator partons which appear in the final-state hadron wavefunction with

$$x_i' = \frac{x_i}{1-\zeta}, \qquad \vec{k}_{\perp i}' = \vec{k}_{\perp i} + \frac{x_i}{1-\zeta} \vec{\Delta}_\perp \ . \tag{81}$$

We can again check that the arguments of the final-state wavefunction satisfy $\sum_{i=2}^{n} x_i' = 1$, $\sum_{i=2}^{n} \vec{k}_{\perp i}' = \vec{0}_\perp$. In (79) and (80) the sum is over all possible ways of numbering the partons in the initial wavefunction such that the quark with index 1 and the antiquark with index $n+1$ annihilate into the current.

The powers of $\sqrt{1-\zeta}$ in (75), (76) and (79), (80) have their origin in the integration measures in the Fock state decomposition for the outgoing proton. The fractions x_i' appearing there refer to the light-cone momentum $P'^+ = (1-\zeta) P^+$, whereas the fractions x_i in the incoming proton wavefunction refer to P^+. Transforming all fractions so that they refer to P^+ as in our final formulae thus gives factors of $\sqrt{1-\zeta}$. Different powers appear in the $n \rightarrow n$ and $n+1 \rightarrow n-1$ overlaps because of the different parton numbers in the final state wavefunctions.

The above representation is the general form for the generalized form factors of the deeply virtual Compton amplitude for any composite system. Thus given the light-cone Fock state wavefunctions of the eigensolutions of the light-cone Hamiltonian, we can compute the amplitude for virtual Compton scattering including all spin correlations. The formulae are accurate to leading order in $1/Q^2$. Radiative corrections to the quark Compton amplitude of order $\alpha_s(Q^2)$ from diagrams in which a hard gluon interacts between the two photons have also been neglected.

The QCD scattering amplitude for deeply virtual exclusive meson production $\gamma^* p \rightarrow Mp$ also factorizes into a hard subprocess and soft universal hadronic matrix elements.[153, 32, 154] For example, consider exclusive meson electroproduction such as $ep \rightarrow e\pi^+ n$ (Fig. 21a). Here one takes (as in DIS) the Bjorken limit of large photon virtuality, with $x_B = Q^2/(2m_p\nu)$ fixed, while the momentum transfer $t = (p_p - p_n)^2$ remains small. These processes also involve 'skewed' parton distributions, which are generalizations of the usual parton distributions measured in DIS. The skewed distribution in this case describes the emission of a u-quark from the proton target

52

together with the formation of the final neutron from the d-quark and the proton remnants. As the subenergy $\hat{s}$ of the scattering process $\gamma^* u \to \pi^+ d$ is not fixed, the amplitude involves an integral over the u-quark momentum fraction x.
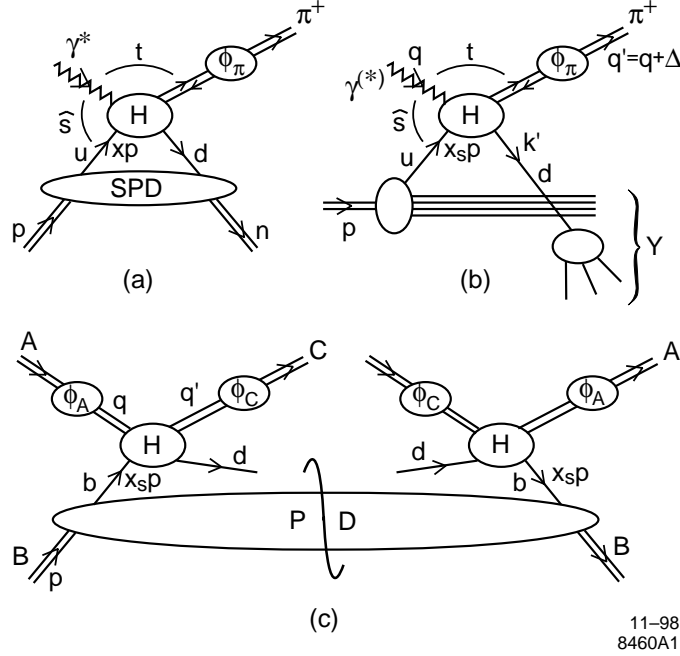

Figure 21:   (a): Factorization of $\gamma^* p \to \pi^+ n$ into a skewed parton distribution (SPD), a hard scattering H and the pion distribution amplitude ϕ_π. (b): Semi-exclusive process $\gamma^{(*)} p \to \pi^+ Y$. The d-quark produced in the hard scattering H hadronizes independently of the spectator partons in the proton. (c): Diagram for the cross section of a generic semi-exclusive process. It involves a hard scattering H, distribution amplitudes ϕ_A and ϕ_C and a parton distribution (PD) in the target B.

3.3   Electroweak Matrix Elements and Light-Cone Wavefunctions

Another remarkable advantage of the light-cone formalism is that exclusive semileptonic B-decay amplitudes such as $B \to A\ell\overline{\nu}$ can be evaluated exactly. [138] The time-like decay matrix elements require the computation of the diagonal matrix element $n \to n$ where parton number is conserved, and the off-diagonal $n+1 \to n-1$ convolution where the current operator annihilates a $q\overline{q'}$ pair in the initial B wavefunction. See Fig. 22. This term is a consequence of the fact that the time-like decay $q^2 = (p_\ell + p_{\overline{\nu}})^2 > 0$ requires a positive light-cone momentum fraction $q^+ > 0$.
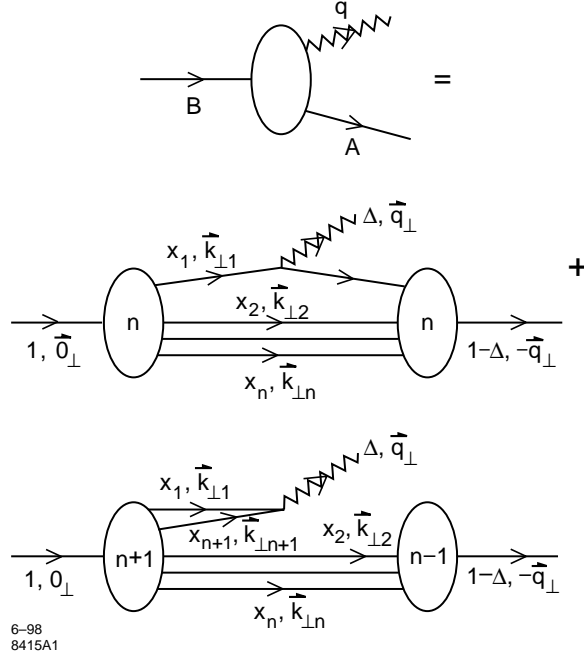
Figure 22: Exact representation of electroweak decays and time-like form factors in the light-cone Fock representation.

Conversely for space-like currents, one can choose $q^+ = 0$, as in the Drell-Yan-West representation of the space-like electromagnetic form factors. However, as can be seen from the explicit analysis of the form factor in a perturbative model, the off-diagonal convolution can yield a nonzero q^+/q^+ limiting form as $q^+ \to 0$. This extra term appears specifically in the case of "bad" currents such as J^- in which the coupling to $q\bar{q}$ fluctuations in the light-cone wavefunctions are favored. In effect, the $q^+ \to 0$ limit generates $\delta(x)$ contributions as residues of the $n + 1 \to n - 1$ contributions. The necessity for such "zero mode" $\delta(x)$ terms has been noted by Chang, Root and Yan,[155] Burkardt,[156] and Ji and Choi.[157]

The off-diagonal $n + 1 \to n - 1$ contributions give a new perspective for the physics of B-decays. A semileptonic decay involves not only matrix elements where a quark changes flavor, but also a contribution where the leptonic pair is created from the annihilation of a $q\bar{q}'$ pair within the Fock states of the initial B wavefunction. The semileptonic decay thus can occur from the annihilation of a nonvalence quark-antiquark pair in the initial hadron. This feature will carry over to exclusive hadronic B-decays, such as $B^0 \to \pi^- D^+$. In this case the pion can be produced from the coalescence of a $d\bar{u}$ pair emerging from the initial higher particle number Fock wavefunction of the B. The D meson is then formed from the remaining quarks after the internal exchange of a W boson.

In principle, a precise evaluation of the hadronic matrix elements needed for B-

decays and other exclusive electroweak decay amplitudes requires knowledge of all of the light-cone Fock wavefunctions of the initial and final state hadrons. In the case of model gauge theories such as QCD(1+1) [158] or collinear QCD [159] in one-space and one-time dimensions, the complete evaluation of the light-cone wavefunction is possible for each baryon or meson bound-state using the DLCQ method. It would be interesting to use such solutions as a model for physical B-decays.

3.4 Proofs of Factorization for Hard QCD Exclusive Processes using the Light-Cone Fock Representation

The light-cone formalism provides a physical factorization scheme which conveniently separates and factorizes soft non-perturbative physics from hard perturbative dynamics in both exclusive and inclusive reactions. [24, 35] The proof of factorization begins with the exact representation of the process in terms of the light-cone Fock representation. The LC wavefunctions are the interpolating functions between the quark and gluon states and the hadronic states. Using light-cone Hamiltonian theory, the sum over each intermediate state can be divided according to $\mathcal{M}_n^2 < \Lambda^2$ and $\mathcal{M}_n^2 > \Lambda^2$ domains where $\mathcal{M}_n^2$ is the invariant mass of the intermediate state. All of the dynamics associated with $\mathcal{M}_n^2 < \Lambda^2$ is thus summed into the cutoff light-cone wavefunctions $\psi_n^{\mathcal{M}_n^2 < \Lambda^2}(x_i, k_{i\perp}, \lambda_i)$. In the high invariant mass regime $\mathcal{M}_n^2 > \Lambda^2$, intrinsic transverse momenta can be ignored, so that the structure of the process at leading power has the form of hard scattering on collinear quark and gluon constituents, as in the parton model. The attachment of gluons from the LC wavefunction to a propagator in a hard subprocess is power-law suppressed in LC gauge, so that the minimal quark-gluon particle-number subprocesses dominate. The light-cone Fock representation thus provides an explicit realization of the operator product representation. For example, in the case of inclusive reactions such as deep inelastic lepton scattering, the hard domain corresponds to virtual Compton scattering on the quark constituents. All intermediate states of loop diagrams are in the hard regime $\mathcal{M}_n^2 > \Lambda^2$. The coefficient functions, the quark $q(x, \Lambda)$ and gluon distributions $g(x, \Lambda)$ of the proton are then given absolute squares of the proton's cutoff LC wavefunctions with $\mathcal{M}_n^2 < \Lambda^2$. It is then straightforward to derive the DGLAP equations from the evolution of the distributions with $\log \Lambda^2$. The anomaly contribution to isospin-singlet helicity structure function $g_1(x, Q)$ can be explicitly identified in the LC factorization scheme as due to the $\gamma^* g \to q\bar{q}$ fusion process. The anomaly contribution would be zero if the gluon is on shell. However, if the off-shellness of the state is larger than the quark pair mass, one can derive the usual anomaly contribution. [160]

In the case of an exclusive amplitude involving a hard scale Q^2, all intermediate states can again divided according to $\mathcal{M}_n^2 < \Lambda^2 < Q^2$ and $\mathcal{M}_n^2 < \Lambda^2$ invariant mass domains. The high invariant mass contributions to the amplitude has the structure of a hard scattering process T_H in which the hadrons are replaced by their respective (collinear) quarks and gluons. In light-cone gauge only the minimal Fock states

contribute to the leading power-law fall-off of the exclusive amplitude. The wave-functions in the lower invariant mass domain can be integrated up to the invariant mass cutoff Λ, thus defining the distribution amplitudes. Final-state and initial state corrections from gluon attachments to lines connected to the color-singlet distribution amplitudes cancel at leading twist.

The key non-perturbative input for exclusive processes is thus the gauge and frame independent hadron distribution amplitude [35, 24] defined as the integral of the valence (lowest particle number) Fock wavefunction; *e.g.* for the pion

$$\phi_\pi(x_i, \Lambda) \equiv \int d^2 k_\perp \, \psi_{q\bar{q}/\pi}^{(\Lambda)}(x_i, \vec{k}_{\perp i}, \lambda) \tag{82}$$

where the global cutoff Λ is identified with the resolution Q. The distribution ampli-tude controls leading-twist exclusive amplitudes at high momentum transfer, and it can be related to the gauge-invariant Bethe-Salpeter wavefunction at equal light-cone time. Given the solution for the hadronic wavefunctions $\psi_n^{(\Lambda)}$ with $\mathcal{M}_n^2 < \Lambda^2$, one can also construct the wavefunction in the hard regime with $\mathcal{M}_n^2 > \Lambda^2$ using projection operator techniques. [34, 35, 24] The construction can be done perturbatively in QCD since only high invariant mass, far off-shell matrix elements are involved. One can use this method to derive the physical properties of the LC wavefunctions and their matrix elements at high invariant mass. Since $\mathcal{M}_n^2 = \sum_{i=1}^n \left(\frac{k_\perp^2 + m^2}{x} \right)_i$, this method also allows the derivation of the asymptotic behavior of light-cone wavefunctions at large $k_\perp$, and $x \to 1$. The logarithmic evolution of hadron distribution amplitudes $\phi_H(x_i, Q)$ can also be derived from the perturbatively-computable tail of the va-lence light-cone wavefunction in the high transverse momentum regime. [35, 24] The conformal basis for the evolution of the three-quark distribution amplitudes for the baryons [34] has recently been obtained by V. Braun *et al.*[59]

Thus at high transverse momentum an exclusive amplitudes factorizes into a con-volution of a hard quark-gluon subprocess amplitudes T_H with the hadron distribution amplitudes $\phi(x_i, \Lambda)$.[34, 35, 24] The T_H satisfy the dimensional counting rules. The logarithmic evolution of hadron distribution amplitudes $\phi_H(x_i, Q)$ can be derived from the perturbatively-computable tail of the valence light-cone wavefunction in the high transverse momentum regime. [34, 35, 24]

3.5   Applications to Hard Exclusive Heavy Hadron Decays

The existence of an exact formalism provides a basis for systematic approximations and a control over neglected terms. For example, one can analyze exclusive semi-leptonic and exclusive two-body hadronic B-decays which involve hard internal mo-mentum transfer using the perturbative QCD formalism. [161, 162, 163, 164, 165, 166] The hard-scattering analysis again proceeds by writing each hadronic wavefunction as a sum of soft and hard contributions $\psi_n = \psi_n^{\text{soft}}(\mathcal{M}_n^2 < \Lambda^2) + \psi_n^{\text{hard}}(\mathcal{M}_n^2 > \Lambda^2)$, where $\mathcal{M}_n^2$ is the invariant mass of the partons in the n-particle Fock state and Λ is the sep-aration scale. The high internal momentum contributions to the wavefunction ψ_n^{hard}

can be calculated systematically from QCD perturbation theory by iterating the gluon exchange kernel. The contributions from high momentum transfer exchange to the B-decay amplitude in the heavy $b-$ quark limit can then be written as a convolution of a hard-scattering quark-gluon scattering amplitude T_H with the distribution amplitudes $\phi(x_i, \Lambda)$, the valence wavefunctions obtained by integrating the constituent momenta up to the separation scale $\mathcal{M}_n < \Lambda < Q$. Furthermore in processes such as $B \to \pi D$ where the pion is effectively produced as a rapidly moving small Fock state with a small color-dipole interactions, final state interactions are suppressed by color transparency. In the most recent analyses by Beneke *et al.* [164] a careful separation is given of the hard PQCD and soft contribution from the convolution of the light-cone wavefunctions and verified thorough two-loop order.

3.6   Evolution of the Meson Distribution Amplitude

The meson distribution amplitude $\phi_M(x, Q)$ evolves with $\log Q^2$ in analogy to the DGLAP evolution of quark structure functions. Note that non-singlet quark distribution in the meson is the diagonal meson to meson matrix element of the same bilocal operator $\overline{\psi}(0)\gamma^+\gamma_5\psi(z)$ which appear in the vacuum to meson matrix element defining the meson distribution amplitude. The separation between the fields is very nearly on the light cone: $z^2 = z^+z^- - z_\perp^2 = \mathcal{O}(1/Q^2)$. Both matrix elements thus have the same operator product expansion near the light-cone. Since the scale dependence is determined by the operators in the OPE expansion, the anomalous dimensions γ_n of $q_M(x, Q)$ for non-singlet quark distributions and $\phi_M(x, Q)$ for non-singlet mesons are identical to all orders. However, the coefficients $C_n(x)$ which appear in the OPE expansion of the distribution amplitude must be functions of the light-cone momentum fraction. These coefficients can be determined from conformal symmetry since the non-conformal dynamics is already incorporated into the evolution of the local operators. [37, 62] The consistency of the conformal symmetry approach was verified to higher order by Müller. [125] The extension of this approach to baryon distribution amplitudes is due to Braun *et al.* [59]

The physics of the evolution of the meson distribution amplitudes is most easily seen in the light-cone Fock wavefunction formalism. Differentiating the integral representation of $\phi(x, Q)$ Eq. (5) with respect to $\log Q^2$ brings in two contributions, one from the integrand at the upper limit of transverse momentum $\psi(x, k_\perp^2 = Q^2)$ and the other from the Q^2 dependence of the wavefunction renormalization of the external lines defining the two-particle wavefunction. The large $k_\perp^2$ dependence of the wavefunction can be obtained by iterating the Hamiltonian equation of motion which has the form of a gluon exchange kernel $V_{1g}(x, y)$ convoluted again with the distribution amplitude $\phi(y, Q^2)$. The wavefunction renormalization contributions provide a subtraction term for color-singlet mesons. $y = x$ which eliminates a potentially infrared divergent contribution. The one-gluon exchange contribution represents the change in the probability amplitude ϕ due to the addition of more $q\overline{q}$ states as the cutoff Q is increased, while the wavefunction renormalization takes into account the

loss of probability from those already present.

The net result is

$$Q \frac{\partial}{\partial Q} \phi(x, Q) = \frac{\alpha_s(Q^2)}{4\pi} \left\{ \int_0^1 dy \, \frac{V(x, y)}{y(1 - y)} \, \phi(y, Q) - 2\phi(x, Q) \right\} \qquad (83)$$

where the evolution potential is

$$V(x, y) = 4C_F \left\{ x(1 - y) \, \theta(y - x) \left(\delta_{-h, \overline{h}} + \frac{\Delta}{y - x} \right) + \left(\begin{matrix} x \leftrightarrow 1 - x \\ y \leftrightarrow 1 - y \end{matrix} \right) \right\} = V(y, x). \qquad (84)$$

The operator Δ in the potential is defined by

$$\Delta \frac{\phi(y, Q)}{y(1 - y)} \equiv \frac{\phi(y, Q)}{y(1 - y)} - \frac{\phi(x, Q)}{x(1 - x)}. \qquad (85)$$

The indices h and $\overline{h}$ indicate the helicities of the quark and antiquark ($\delta_{-h, \overline{h}} = 1$ for pions).

The evolution equation completely specifies the Q dependence of $\phi(x, Q)$; still it is instructive to exhibit explicitly its general Q dependence. The evolution potential $V(x, y)$ can be treated as an integral operator. Being symmetric it has real eigenvalues $\tilde{\gamma}_n$ and eigensolutions $\phi_n(y)$ which satisfy $\int dy \, V(x, y) \, w(y) \, \phi_n(y) = \tilde{\gamma}_n \, \phi_n(x)$ where integration weight $w(y) \equiv 1/(y(1 - y))$. The eigensolutions must be orthogonal with respect to weight $w(x)$, from which it immediately follows that $\phi_n(x) \propto x(1 - x) \, C_n^{3/2}(2x - 1)$ where $C_n^{3/2}$ is a Gegenbauer polynomial. A general solution of the evolution equation can be written down as an expansion on the complete set of eigensolutions of $V(x, y)$:

$$\phi(x, Q) = x(1 - x) \sum_{n=0}^{\infty} a_n \, C_n^{3/2}(2x - 1) \left(\log \frac{Q^2}{\Lambda_{QCD}^2} \right)^{-\gamma_n/2\beta_0} \qquad (86)$$

where as usual $C_F = 4/3$ and $\beta_0 = 11 - 2n_f/3$ where n_f is the number of effective quark flavors. The eigenvalues of V give the anomalous dimensions

$$\gamma_n = 2C_F \left\{ 1 + 4 \sum_{k=2}^{n+1} \frac{1}{k} - \frac{2\delta_{-h, \overline{h}}}{(n + 1)(n + 2)} \right\} \geq 0. \qquad (87)$$

By combining the orthogonality condition for the Gegenbauer polynomials and the operator definition of ϕ, we can project out the expansion constants:

$$a_n \left(\log \frac{Q^2}{\Lambda_{QCD}^2} \right)^{-\gamma_n/2\beta_0} = \frac{4(2n+1)}{(2+n)(1+n)} \int_0^1 dx \, C_n^{3/2}(2x - 1) \, \phi(x, Q)$$

$$= \frac{4(2n+3)}{(2+n)(1+n)} \, \langle 0 \mid \overline{\psi} \, \frac{\gamma^+ \gamma_5}{2\sqrt{2}n_c} \, C_n^{3/2}(\overleftrightarrow{D}^+) \, \psi \mid \pi \rangle^{(Q)} \ .$$

$$(88)$$

58

The coefficients a_n's contain the non-perturbative physics of the meson; from the OPE point of view they are the vacuum-to-meson matrix elements of the nonsinglet local operators. They thus can be determined from lattice gauge theory or QCD sum rules. An extensive review of the application of QCD sum rules to exclusive processes is given by Chernyak and Zhitnitski. [3]

The Gegenbauer polynomials also appear very naturally in this context, as a consequence of the residual conformal symmetry of QCD at short distances. All of the dimensionful couplings in the QCD Lagrangian can be dropped at very short distances, and so the classical theory (*i.e.* tree order in perturbation theory) becomes invariant under conformal mappings of the space-time coordinates. This conformal symmetry is destroyed in the quantum field theory by renormalization, which necessarily introduces a dimensionful parameter such as the cutoff Λ.

The operator-product analysis of the distribution amplitude suggests an important constraint on ϕ. The $n = 0$ Gegenbauer moment of the distribution amplitude is proportional to the amplitude for pion decay:

$$\int_0^1 dx \, \phi(x, Q) = \frac{f_\pi}{2\sqrt{n_c}}. \tag{89}$$

Given the shape of $\phi(x, Q)$ this equation normalizes it for any Q. Note that the value of this moment is Q independent. This is because the $n = 0$ operator is just the axial-vector current operator. As far as its ultraviolet behavior is concerned, this operator is conserved and so its anomalous dimension vanishes: $\gamma_{n=0} = 0$. Notice also that $\gamma_n > 0$ for all other n. Thus only the $n = 0$ asymptotic term in the expansion of $\phi(x, Q)$ survives:

$$\phi(x, Q) \to \frac{3 f_\pi}{\sqrt{n_c}} \, x(1 - x) \tag{90}$$

as $Q \to \infty$. Thus the shape and normalization of $\phi(x, Q)$ is completely determined for the pion when Q is asymptotically large. In contrast, the quark structure functions $q(x, Q)$ evolve to $C\delta(x)$ in the same limit. It should be emphasized that $\psi^{(\Lambda)}(x, k_\perp)$ does in fact fall as $1/k_\perp^2$, up to logarithms, as $k_\perp$ grows. The $x \to 1$ and $x \to 0$ dependence is also determined. Thus the high-momentum, short-distance behavior of the Fock-state wavefunctions is thus perturbative in nature.

3.7 Non-Perturbative Computation of Light-Cone Wavefunctions

Is there any hope of computing light-cone wavefunctions from first principles? In the discretized light-cone quantization method (DLCQ),[167] periodic boundary conditions are introduced in $b_\perp$ and x^- so that the momenta $k_{\perp i} = n_\perp \pi / L_\perp$ and $x_i^+ = n_i / K$ are discrete. A global cutoff in invariant mass of the partons in the Fock expansion is also introduced. Solving the quantum field theory then reduces to the problem of diagonalizing the finite-dimensional hermitian matrix H_{LC} on a finite discrete Fock

basis. The DLCQ method has now become a standard tool for solving both the spectrum and light-cone wavefunctions of one-space one-time theories—virtually any $1+1$ quantum field theory, including "reduced QCD" (which has both quark and gluonic degrees of freedom) can be completely solved using DLCQ.[168, 159] The method yields not only the bound-state and continuum spectrum, but also the light-cone wavefunction for each eigensolution. The solutions for the model 1+1 theories can provide an important theoretical laboratory for testing approximations and QCD-based models.

In the case of theories in 3+1 dimensions, Hiller, McCartor, and I [169, 170] have recently shown that the use of covariant Pauli-Villars regularization with DLCQ allows one to obtain the spectrum and light-cone wavefunctions of simplified theories, such as (3+1) Yukawa theory. Dalley *et al.* have shown how one can use DLCQ in one space-one time, with a transverse lattice to solve mesonic and gluonic states in $3 + 1$ QCD.[171] The spectrum obtained for gluonium states is in remarkable agreement with lattice gauge theory results, but with a huge reduction of numerical effort. Hiller and I [172] have shown how one can use DLCQ to compute the electron magnetic moment in QED without resort to perturbation theory. Light-cone gauge $A^+ = 0$ allows one to utilize only the physical degrees of freedom of the gluon field to appear. However, light-cone quantization in Feynman gauge has a number of attractive features, including manifest covariance and a straightforward passage to the Coulomb limit in the case of static quarks. [129]

One can also formulate DLCQ so that supersymmetry is exactly preserved in the discrete approximation, thus combining the power of DLCQ with the beauty of supersymmetry.[173, 174, 175] The "SDLCQ" method has been applied to several interesting supersymmetric theories, to the analysis of zero modes, vacuum degeneracy, massless states, mass gaps, and theories in higher dimensions, and even tests of the Maldacena conjecture.[173]

Broken supersymmetry is interesting in DLCQ, since it may serve as a method for regulating non-Abelian theories.[170] Another remarkable advantage of light-cone quantization is that the vacuum state $|0\rangle$ of the full QCD Hamiltonian coincides with the free vacuum. For example, as discussed by Bassetto,[176] the computation of the spectrum of $QCD(1 + 1)$ in equal time quantization requires constructing the full spectrum of non perturbative contributions (instantons). However, light-cone methods with infrared regularization give the correct result without any need for vacuum-related contributions. The role of instantons and such phenomena in light-cone quantized $QCD(3 + 1)$ is presumably more complicated and may reside in zero modes;[177] *e.g.*, zero modes are evidently necessary to represent theories with spontaneous symmetry breaking.[178]

3.8 Computation of the Pion Distribution Amplitude in QCD using the Transverse Lattice

The transverse lattice approach [179, 180] to non-perturbative light-front Hamiltonian QCD combines attractive elements of both lattice gauge theory and discretized light-cone quantization.[181] Recently Dalley [182] has reported the first application of this method to the computation of the valence pion's distribution amplitude.

In Dalley's approach, the x^- and x^+ coordinates are treated as in DLCQ. The physics of the transverse dimensions $x_\perp$ are treated as a lattice theory with transverse lattice spacing a. As in the work of Bardeen and Pearson [179] a linear sigma model approximation is used Instead of formulating the lattice part of the theory in terms of link variables $U \in \mathrm{SU}(N)$, one uses link variables $M \in GL(N)$, where the complex matrices M transform in the same way under gauge transformation. The Hamiltonian is then augmented by operators which restore the Poincare and other continuum symmetries even at finite a. Chiral symmetry is explicitly broken in the light-front Hamiltonian while preserving the stability of the vacuum. The effective light-front Hamiltonian is approximately Lorentz covariant, and is compatible with a massless pion.

In fact, it is advantageous to work at finite a, rather than the limit $a \to 0$ and choose the parameters of the Hamiltonian in a region of renormalization group stability. Thus one tunes the effective theory to respect the continuum symmetries (gauge, Poincaré, chiral) required of the theory. Ideally, after DLCQ and Tamm-Dancoff cut-offs are extrapolated, the theory should exhibit enhanced Lorentz covariance on an approximately one-dimensional trajectory of couplings, along which a varies. This trajectory represents the best approximation to the (unique) renormalized trajectory in the infinite-dimensional space of couplings.

The method was first used for a successful series of glueball studies by Dalley and van de Sande.[183, 184] Preliminary results for the pion have recently been presented by Dalley, but are not to be considered definitive.

The resulting DLCQ/transverse lattice pion wavefunction at $a = 0.35$ and DLCQ resolution $K = 8$ is shown in Fig. 23. It can be fit to the conformal expansion [185, 186] of the distribution amplitude

$$
\begin{aligned}
\phi_\pi(x, Q^2 \sim 1 GeV^2) &= \frac{2.653}{a} x(1-x) \Big\{ C_0^{3/2} + 0.237 C_2^{3/2} - 0.102 C_4^{3/2} \\
&\quad -0.05 C_6^{3/2} + \cdots \Big\} \ .
\end{aligned}
\tag{91}
$$

The transverse scale 1GeV is a rough estimate based on π/a, and $C_n^{3/2}(1 - 2x^2)$ are the appropriate Gegenbauer polynomials. The conformal expansion appears convergent. The overall normalization yields $f_\pi = 101$ MeV compared with the experimental value $f_\pi(exp.) = 93$ MeV. However, it should be noted that recent lattice results from Del Debbio *et al.*[40] predict a much narrower shape for the pion distribution amplitude than the distribution predicted by the transverse lattice.
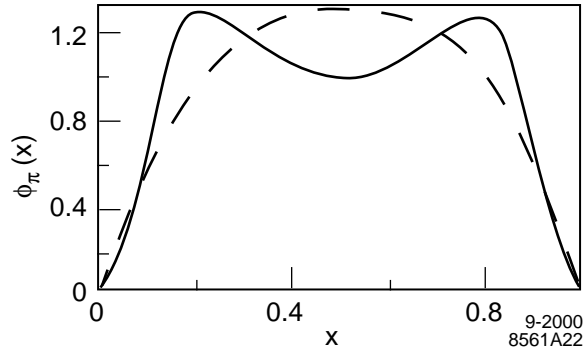
Figure 23: Preliminary transverse lattice results for the pion distribution amplitude at $Q^2 \sim 10 GeV^2$. The solid line is the theoretical prediction from the combined DLCQ transverse lattice method [182]; the chain line is experimental deduction (each with unknown systematic errors). Both are normalized to area 1 for comparison.

The results can be compared with direct and indirect experimental measurements, using leading order perturbative QCD evolution to the appropriate scales Q^2, and assuming leading order perturbative QCD factorization. The scaled $\gamma\gamma^* \to \pi^0$ transition form factor $Q^2 F_{\pi^0}$ measured at CLEO-II [187] is approximately constant in the range 1 GeV$^2 < Q^2 < 10$ GeV^2 and at the higher end $Q^2 F_{\pi^0}(Q^2 = 8$ GeV$^2) = 0.16 \pm 0.03$ GeV. This compares with the leading order theoretical result

$$Q^2 F_{\pi^0}(Q^2 = 8 \text{GeV}^2) = \frac{4}{\sqrt{3}} \int_0^1 dx \frac{\phi_\pi(x, Q^2 \sim 8 \text{GeV}^2)}{x} = 0.21 \text{ GeV} \qquad (92)$$

As discussed in the next section, higher order QCD corrections will reduce the magnitude of the theory prediction.

As discussed in Section 6, direct measurements of ϕ_π are possible from measurements of diffractive dissociation on a nucleus $\pi + A \to A +$ jets. [81] Figure 23 compares the quark amplitude with the best fit to the jet data after hadronization and experimental acceptance. [81] Although hadronization tends to wash out any fine structure in the quark amplitude, making an accurate comparison difficult, the theoretical curve is somewhat broader than the experimental result. The lattice calculation can be improved by taking the resolution K in the DLCQ expansion larger. There are also uncertainties introduced from the use of a nearly massless pion, ambiguities in setting the factorization scale Q^2, as well as errors in the evolution of the distribution amplitude from 1 to 10 GeV^2.

62

4 Renormalization Scale and Scheme for Exclusive Processes

The scale ambiguities for the underlying quark-gluon subprocesses are particularly acute in the case of QCD predictions for exclusive processes since the running coupling α_s enters at a high power. Furthermore, since each external momentum entering an exclusive reaction is partitioned among the many propagators of the underlying hard-scattering amplitude, the physical scales that control these processes are inevitably smaller than the overall momentum transfer. Exclusive process phenomenology is further complicated by the fact that the scales of the running couplings in the hard-scattering amplitude depend on the shape of the hadronic wavefunctions.

The renormalization scale ambiguity problem can be resolved if one can optimize the choices of scale and scheme according to some sensible criteria. In the BLM procedure,[188] the renormalization scales are chosen such that all vacuum polarization effects from the QCD β function are re-summed into the running couplings. The coefficients of the perturbative series are thus identical to the perturbative coefficients of the corresponding conformally invariant theory with $\beta = 0$. The BLM method has the important advantage of "pre-summing" the large and strongly divergent terms in the PQCD series which grow as $n!(\alpha_s\beta_0)^n$, *i.e.*, the infrared renormalons associated with coupling constant renormalization [189, 190] are avoided. Furthermore, the renormalization scales Q^* in the BLM method are physical in the sense that they reflect the mean virtuality of the gluon propagators. [188, 190, 191, 192] In fact, in the $\alpha_V(Q)$ scheme, where the QCD coupling is defined from the heavy quark potential, the renormalization scale is by definition the momentum transfer caused by the gluon.

The BLM procedure can be used to fix the renormalization scale of the QCD coupling in exclusive hadronic amplitudes such as the pion form factor, the photon-to-pion transition form factor and $\gamma\gamma \to \pi^+\pi^-$ at large momentum transfer.[193] Renormalization-scheme-independent commensurate scale relations can be established which connect the hard scattering subprocess amplitudes that control these exclusive processes to other QCD observables such as the heavy quark potential and the electron-positron annihilation cross section. Because the renormalization scale is small, one can argue that the effective coupling is nearly constant, thus accounting for the nominal scaling behavior of the data. [194, 195, 193]

The heavy-quark potential $V(Q^2)$ is defined as the two-particle-irreducible scattering amplitude of an infinitely-heavy quark and antiquark at momentum transfer $t = -Q^2$. The relation

$$V(Q^2) = -\frac{4\pi C_F \alpha_V(Q^2)}{Q^2},\tag{93}$$

with $C_F = (N_C^2 - 1)/2N_C = 4/3$, then defines the effective charge $\alpha_V(Q)$. This coupling provides a physically-based alternative to the usual $\overline{MS}$ scheme. As in the corresponding case of Abelian QED, the scale Q of the coupling $\alpha_V(Q)$ is identified

with the exchanged momentum. All vacuum polarization corrections due to fermion pairs are incorporated in the usual vacuum polarization kernels defined in terms of physical mass thresholds. The first two terms $\beta_0 = 11 - 2n_f/3$ and $\beta_1 = 102 - 38n_f/3$ in the expansion of the β function defined from the logarithmic derivative of $\alpha_V(Q)$ are universal, $i.e.$, identical for all effective charges at $Q^2 \gg 4m_f^2$. The coefficient β_2 for α_V has recently been calculated in the $\overline{MS}$ scheme.[196] All vacuum polarization corrections due to fermion pairs are then automatically and analytically incorporated into the Gell Mann-Low function, thus avoiding the problem of explicitly computing and resumming quark mass corrections related to the running of the coupling.[197] The use of a finite effective charge such as α_V as the expansion parameter also provides a basis for regulating the infrared nonperturbative domain of the QCD coupling. A similar coupling and scheme can be based on an assumed skeleton expansion of the theory.[198, 199, 200] Lattice calculations have provided strong constraints on the normalization and shape of $\alpha_V(Q^2)$:

$$\alpha_V^{(3)}(8.2 \text{ GeV}) = 0.196(3), \tag{94}$$

where the effective number of light flavors is $n_f = 3$. The corresponding modified minimal subtraction coupling evolved to the Z mass using Eq. (96) is given by

$$\alpha_{\overline{MS}}^{(5)}(M_Z) = 0.115(2). \tag{95}$$

Commensurate scale relations (see Refs. 201 and 202) are perturbative QCD predictions which relate observable to observable at fixed relative scale, such as the "generalized Crewther relation" [203], which connects the Bjorken and Gross-Llewellyn Smith deep inelastic scattering sum rules to measurements of the e^+e^- annihilation cross section. The relations have no renormalization scale or scheme ambiguity. The coefficients in the perturbative series for commensurate scale relations are identical to those of conformal QCD; thus no infrared renormalons are present.[200] One can identify the required conformal coefficients at any finite order by expanding the coefficients of the usual PQCD expansion around a formal infrared fixed point, as in the Banks-Zak method.[198] All non-conformal effects are absorbed by fixing the ratio of the respective momentum transfer and energy scales. In the case of fixed-point theories, commensurate scale relations relate both the ratio of couplings and the ratio of scales as the fixed point is approached. [200]

The scale-fixed relation between α_V and the conventional $\overline{MS}$ coupling is

$$\alpha_V(Q) = \alpha_{\overline{MS}}(e^{-5/6}Q)\left(1 - \frac{2C_A}{3}\frac{\alpha_{\overline{MS}}}{\pi} + \cdots\right), \tag{96}$$

above or below any quark mass threshold. The factor $e^{-5/6} \simeq 0.4346$ is the ratio of commensurate scales between the two schemes to this order. It arises because of the conventions used in defining the modified minimal subtraction scheme. The scale in the $\overline{MS}$ scheme is thus a factor ~ 0.4 smaller than the physical scale. The coefficient

$2C_A/3$ in the NLO term is a feature of the non-Abelian couplings of QCD; the same coefficient would occur even if the theory were conformally invariant with $\beta_0 = 0$. The coupling α_V thus provides a natural scheme for computing exclusive amplitudes. Once we relate, *e.g.*, form factors to effective charges based on observables, there are no ambiguities due to scale or scheme conventions.

It is straightforward to obtain the commensurate scale relation between F_π and α_V. The appropriate BLM scale for F_π is determined from the explicit calculations of the NLO corrections given by Dittes and Radyushkin [204] and Field *et al.*[205] These may be written in the form $(A(\mu)n_f + B(\mu))\alpha_s/\pi$, where A is independent of the separation scale $\tilde{Q}$. The n_f dependence allows one to uniquely identify the dependence on β_0, which is then absorbed into the running coupling by a shift to the BLM scale $Q^* = e^{3A(\mu)}\mu$. An important check of self-consistency is that the resulting value for Q^* is independent of the choice of the starting scale μ.

Combining this result with the BLM scale-fixed expression for α_V, and eliminating the intermediate coupling, we find

$$
\begin{aligned}
F_\pi(Q^2) &= \int_0^1 dx\phi_\pi(x) \int_0^1 dy\phi_\pi(y) \frac{16\pi C_F \alpha_V(Q_V)}{(1-x)(1-y)Q^2} \left(1 + C_V \frac{\alpha_V(Q_V)}{\pi}\right) \\
&= -4 \int_0^1 dx\phi_\pi(x) \int_0^1 dy\phi_\pi(y) V(Q_V^2) \left(1 + C_V \frac{\alpha_V(Q_V)}{\pi}\right),
\end{aligned}
\tag{97}
$$

where $C_V = -1.91$ is the same coefficient one would obtain in a conformally invariant theory with $\beta = 0$, and $Q_V^2 \equiv (1-x)(1-y)Q^2$. In this analysis we have assumed that the pion distribution amplitude has the asymptotic form $\phi_\pi = \sqrt{3}f_\pi x(1-x)$, where the pion decay constant is $f_\pi \simeq 93$ MeV. In this simplified case the distribution amplitude does not evolve, and there is no dependence on the separation scale $\tilde{Q}$. This commensurate scale relation between $F_\pi(Q^2)$ and $\langle\alpha_V(Q_V)\rangle$ represents a general connection between the form factor of a bound-state system and the irreducible kernel that describes the scattering of its constituents.

If we expand the QCD coupling about a fixed point in NLO [191]: $\alpha_s(Q_V) \simeq \alpha_s(Q_0)[1 - (\beta_0\alpha_s(Q_0)/2\pi)\ln(Q_V/Q_0)]$, then the integral over the effective charge in Eq. (97) can be performed explicitly. Thus, assuming the asymptotic distribution amplitude, the pion form factor at NLO is

$$
Q^2 F_\pi(Q^2) = 16\pi f_\pi^2 \alpha_V(Q^*) \left(1 - 1.91\frac{\alpha_V(Q^*)}{\pi}\right),
\tag{98}
$$

where $Q^* = e^{-3/2}Q$. In this approximation $\ln Q^{*2} = \langle\ln(1-x)(1-y)Q^2\rangle$, in agreement with the explicit calculation. A striking feature of this result is that the physical scale controlling the meson form factor in the α_V scheme is very low: $e^{-3/2}Q \simeq 0.22Q$, reflecting the characteristic momentum transfer experienced by the spectator valence quark in lepton-meson elastic scattering.

The transition form factor between a photon and a neutral hadron such as $F_{\gamma\pi}(Q^2)$, which has now been measured up to $Q^2 < 8$ GeV^2 in the tagged two-photon collisions

$e\gamma \to e'\pi^0$ by the CLEO and CELLO collaborations. In this case the amplitude has the factorized form

$$F_{\gamma M}(Q^2) = \frac{4}{\sqrt{3}} \int_0^1 dx \phi_M(x, Q^2) T_{\gamma \to M}^H(x, Q^2), \tag{99}$$

where the hard scattering amplitude for $\gamma \gamma^* \to q\overline{q}$ is

$$T_{\gamma M}^H(x, Q^2) = \frac{1}{(1-x)Q^2} \left(1 + \mathcal{O}(\alpha_s)\right). \tag{100}$$

The leading QCD corrections have been computed by Braaten; [206] however, the NLO corrections are necessary to fix the BLM scale at LO. Thus it is not yet possible to rigorously determine the BLM scale for this quantity. It is reasonable to assume that this scale is the same as that occurring in the prediction for F_π. For the asymptotic distribution amplitude one thus predicts [193]

$$Q^2 F_{\gamma\pi}(Q^2) = 2f_\pi \left(1 - \frac{5}{3} \frac{\alpha_V(Q^*)}{\pi}\right). \tag{101}$$

An important prediction resulting from the factorized form of these results is that the normalization of the ratio [193]

$$R_\pi(Q^2) \equiv \frac{F_\pi(Q^2)}{4\pi Q^2 |F_{\pi\gamma}(Q^2)|^2} \tag{102}$$

$$= \alpha_{\overline{MS}}(e^{-14/6}Q) \left(1 - 0.56 \frac{\alpha_{\overline{MS}}}{\pi}\right) \tag{103}$$

$$= \alpha_V(e^{-3/2}Q) \left(1 + 1.43 \frac{\alpha_V}{\pi}\right) \tag{104}$$

$$= \alpha_R(e^{5/12 - 2\zeta_3}Q) \left(1 - 0.65 \frac{\alpha_R}{\pi}\right) \tag{105}$$

is formally independent of the form of the pion distribution amplitude. The $\alpha_{\overline{MS}}$ correction follows from combined references. [204, 205, 206] The next-to-leading correction given here assumes the asymptotic distribution amplitude. It should be noted that when one relates R_π to α_V or α_R we relate observable to observable and thus there is no scheme ambiguity. The coefficients -0.56, 1.43 and -0.65 in Eqs. (103)–(105) are identical to those one would have in a theory with $\beta = 0$, $i.e.$, conformally invariant theory.

Effective charges such as α_V and α_R are defined from physical observables and thus must be finite even at low momenta. The conventional solutions of the renormalization group equation for the QCD coupling which are singular at $Q \simeq \Lambda_{\rm QCD}$ are not accurate representations of the effective couplings at low momentum transfer. A number of proposals have been suggested for the form of the QCD coupling in the low-momentum regime. For example, Parisi and Petronzio [207] have argued that the coupling must freeze at low momentum transfer in order that perturbative QCD

loop integrations are well defined. Similar ideas may be found in Curci, Greco and Srivastava. [208] Mattingly and Stevenson [209] have incorporated such behavior into their parameterizations of α_R at low scales. Gribov [210] has presented novel dynamical arguments related to the nature of confinement for a fixed coupling at low scales. Born *et al.*[211] have noted the heavy quark potential must saturate to a Yukawa form since the light-quark production processes will screen the linear confining potential at large distances. Cornwall [212] and others [213, 214] have argued that the gluon propagator will acquire an effective gluon mass m_g from non-perturbative dynamics, which again will regulate the form of the effective couplings at low momentum. In this work we shall adopt the simple parameterization

$$
\alpha_V(Q) = \frac{4\pi}{\beta_0 \ln\left(\frac{Q^2 + 4m_g^2}{\Lambda_V^2}\right)},
\tag{106}
$$

which effectively freezes the α_V effective charge to a finite value for $Q^2 \leq 4m_g^2$.

We can use the non-relativistic heavy quark lattice results [215, 216] to fix the parameters. A fit to the lattice data of the above parameterization gives $\Lambda_V = 0.16$ GeV if we use the well-known momentum-dependent n_f. [217, 197] Furthermore, the value $m_g^2 = 0.19$ GeV^2 gives consistency with the frozen value of α_R advocated by Mattingly and Stevenson. [209] Their parameterization implies the approximate constraint $\alpha_R(Q)/\pi \simeq 0.27$ for $Q = \sqrt{s} < 0.3$ GeV, which leads to $\alpha_V(0.5$ GeV$) \simeq 0.37$ using the NLO commensurate scale relation between α_V and α_R. The resulting form for α_V is shown in Fig. 24. A complimentary method for determining α_V at low momentum is to use the angular anisotropy of $e^+e^- \to Q\overline{Q}$ at the heavy quark thresholds. [218] The corresponding predictions for α_R and $\alpha_{\overline{MS}}$ using the CSRs at NLO are also shown. Note that for low Q^2 the couplings, although frozen, are large. Thus the NLO and higher-order terms in the CSRs are large, and inverting them perturbatively to NLO does not give accurate results at low scales. In addition, higher-twist contributions to α_V and α_R, which are not reflected in the CSR relating them, may be expected to be important for low Q^2. [219]

Exclusive processes are sensitive to the magnitude and shape of the QCD couplings at quite low momentum transfer: $Q_V^{*2} \simeq e^{-3}Q^2 \simeq Q^2/20$ and $Q_R^{*2} \simeq Q^2/50$. [220, 120] The fact that the data for exclusive processes such as form factors, two photon processes such as $\gamma\gamma \to \pi^+\pi^-$, and photoproduction at fixed $\theta_{c.m.}$ are consistent with the nominal scaling of the leading-twist QCD predictions (dimensional counting) at momentum transfers Q up to the order of a few GeV can be immediately understood if the effective charges α_V and α_R are slowly varying at low momentum. The scaling of the exclusive amplitude then follows that of the subprocess amplitude T_H with effectively fixed coupling. Note also that the Sudakov effect of the endpoint region is the exponential of a double log series if the coupling is frozen, and thus is strong.

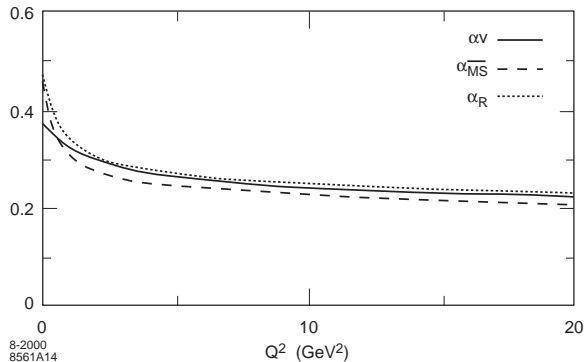In Fig. 6, the CLEO data [41] for the photon-to-pion transition form factor is

Figure 24: The coupling function $\alpha_V(Q^2)$ as given in Eq. (106). Also shown are the corresponding predictions for $\alpha_{\overline{MS}}$ and α_R following from the NLO commensurate scale relations.

compared with the prediction

$$Q^2 F_{\gamma\pi}(Q^2) = 2f_\pi \left(1 - \frac{5}{3} \frac{\alpha_V(e^{-3/2}Q)}{\pi} \right). \tag{107}$$

The flat scaling of the $Q^2 F_{\gamma\pi}(Q^2)$ data from $Q^2 = 2$ to $Q^2 = 8$ GeV^2 provides an important confirmation of the applicability of leading twist QCD to this process. The magnitude of $Q^2 F_{\gamma\pi}(Q^2)$ is remarkably consistent with the predicted form assuming the asymptotic distribution amplitude and including the LO QCD radiative correction with $\alpha_V(e^{-3/2}Q)/\pi \simeq 0.12$. Radyushkin, [43, 221] Ong, [222] and Kroll [42] have also noted that the scaling and normalization of the photon-to-pion transition form factor tends to favor the asymptotic form for the pion distribution amplitude and rules out broader distributions such as the two-humped form suggested by QCD sum rules. [3] One cannot obtain a unique solution for the non-perturbative wavefunction from the $F_{\pi\gamma}$ data alone. However, we have the constraint that

$$\frac{1}{3} \left\langle \frac{1}{1-x} \right\rangle \left[1 - \frac{5}{3} \frac{\alpha_V(Q^*)}{\pi} \right] \simeq 0.8 \tag{108}$$

(assuming the renormalization scale we have chosen in Eq. (101) is approximately correct). Thus one could allow for some broadening of the distribution amplitude, such as indicated by the transverse lattice results, [182] with a corresponding increase in the value of α_V at low scales.

In Fig. 25 the existing measurements of the space-like pion form factor $F_\pi(Q^2)$ [223, 224] (obtained from the extrapolation of $\gamma^* p \to \pi^+ n$ data to the pion pole) are compared with the QCD prediction (98), again assuming the asymptotic form of the pion distribution amplitude. The scaling of the pion form factor data is again important
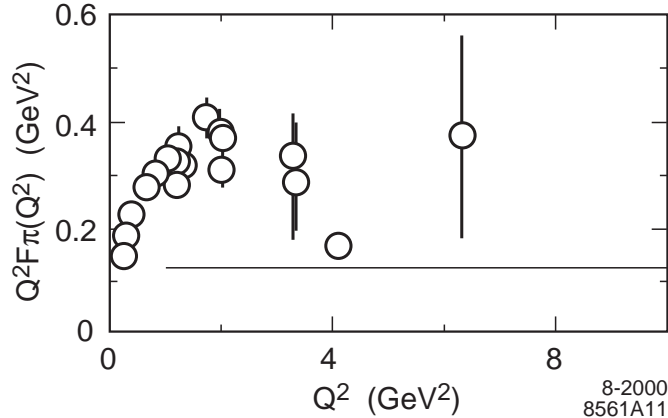
Figure 25: The space-like pion form factor. The data are obtained from an extrapolation of electroproduction data.

evidence for the nominal scaling of the leading twist prediction. However, the prediction is lower than the data by approximately a factor of 2. What is actually measured in electroproduction is a transition form factor from a spacelike mesonic system to the physical pion. The discrepancy could thus be due to the extrapolation of the electroproduction data which becomes increasingly problematic at large Q^2.

One can estimate the sensitivity of these results to the choice of distribution amplitude by comparing the results for the asymptotic amplitude to, $e.g.$, those obtained using the Chernyak-Zhitnitsky (CZ) form. At LO, we find that F_π is increased by roughly a factor of three for the CZ amplitude (relative to the LO result for the asymptotic amplitude, of course), while $F_{\gamma\pi}$ increases by a factor of about 1.5. These estimates are probably quite crude, but give an indication of the typical range over which the results can vary.

If the pion distribution amplitude is close to its asymptotic form, then one can predict the normalization of exclusive amplitudes such as the spacelike pion form factor $Q^2 F_\pi(Q^2)$. Next-to-leading order predictions are now becoming available which incorporate higher order corrections to the pion distribution amplitude as well as the hard scattering amplitude.[125, 225, 226] However, the normalization of the PQCD prediction for the pion form factor depends directly on the value of the effective coupling $\alpha_V(Q^*)$ at momenta $Q^{*2} \simeq Q^2/20$. Assuming $\alpha_V(Q^*) \simeq 0.4$, the QCD LO prediction appears to remain smaller by approximately a factor of 2 compared to the presently available data extracted from the original pion electroproduction experiments from CEA [227]; however, it should be emphasized that this discrepancy may be due to systematic errors introduced by the extrapolation procedure.[228] A recent review has been given by Volmer[229] What is at best measured in electroproduction is the transition amplitude between a mesonic state with an effective space-like mass $m^2 = t < 0$ and the physical pion. It is theoretically possible that the off-shell form

factor $F_\pi(Q^2, t)$ is significantly larger than the physical form factor because of its bias towards more point-like $q\bar{q}$ valence configurations within its Fock state structure. The extrapolation to the pole at $t = m_\pi^2$ also requires knowing the analytic dependence of $F_\pi(Q^2, t)$ on t.

If we assume that there are no significant errors induced by the electroproduction extrapolation, then one must look for other sources for the discrepancy in normalization. Note that the NLO corrections in Eqs. (98) and (104) are of order 20–30%. Thus there may be large contributions from NNLO and higher corrections which need to be re-summed. There are also possible corrections from pion rescattering in the final state of the electroproduction process. In addition, it is possible that pre-asymptotic contributions from higher-twist or soft endpoint physics are important.

A comprehensive analysis of the pion form factors at next-to-leading order assuming the Shirkov-Solovtsov [230] analytic form of the QCD coupling, Sudakov suppression, and transverse momentum effects has recently been given by Stefanis $et\ al$.[113] Like the Cornwall form used for α_V, The Shirkov-Solovtsov ansatz provides an infrared stable, running strong coupling $\alpha_s(Q^2)$ which has no the Landau singularity at $Q^2 = \Lambda_{\rm QCD}^2$. An improved ansatz for the pion wavefunction of the Brodsky-Huang-Lepage type [105] is employed, which includes an effective (constituent-like) quark mass, $m_q = 0.33$ GeV. BLM commensurate scale setting is also used. Stefanis et $al.$ find that the perturbative hard contribution to the pion form factor prevails at momentum transfers above about 20 GeV ^{2}, while at lower Q^2-values it is dominated by Feynman-type end-point contributions.

The analytic parameterization of the QCD coupling suggested by Shirkov in fact predicts a considerably larger value of $\alpha_s(0)$. [231] than implied by the α_V scheme analysis. This would also require a broadening of the pion distribution amplitude compared to its asymptotic form since one needs to raise the expectation value of $1/(1-x)$ in order to maintain consistency with the magnitude of the $F_{\gamma\pi}(Q^2)$ data. A full analysis will also require consideration of the evolution of the distribution amplitude.

The $\gamma\gamma \to \pi^+\pi^-$ data appear to exhibit true leading-twist scaling (See Fig. 8), so that one would expect this process to be a good test of theory. One can show [54] that, to LO,

$$\frac{\frac{d\sigma}{dt}\left(\gamma\gamma \to \pi^+\pi^-\right)}{\frac{d\sigma}{dt}\left(\gamma\gamma \to \mu^+\mu^-\right)} = \frac{4|F_\pi(s)|^2}{1 - \cos^4\theta_{c.m.}} \tag{109}$$

in the c.m. system (CMS), where $dt = (s/2)d(\cos\theta_{c.m.})$ and here $F_\pi(s)$ is the $time$-$like$ pion form factor. The ratio of the time-like to space-like pion form factor for the asymptotic distribution amplitude is given by

$$\frac{|F_\pi^{(\text{timelike})}(-Q^2)|}{F_\pi^{(\text{spacelike})}(Q^2)} = \frac{|\alpha_V(-Q^{*2})|}{\alpha_V(Q^{*2})}. \tag{110}$$

If one simply continues Eq. (106) to negative values of Q^2, then for $1 < Q^2 < 10$ GeV^2, and hence $0.05 < Q^{*2} < 0.5$ GeV^2, the ratio of couplings in Eq. (110) is of

order 1.5. Assuming the asymptotic form for the distribution amplitude, this predicts $F_\pi^{\text{(timelike)}}(-Q^2) \simeq (0.3 \text{ GeV}^2)/Q^2$ and hence

$$\frac{\frac{d\sigma}{dt}\left(\gamma\gamma \to \pi^+\pi^-\right)}{\frac{d\sigma}{dt}\left(\gamma\gamma \to \mu^+\mu^-\right)} \simeq \frac{.36}{s^2}\frac{1}{1 - \cos^4\theta_{c.m.}}. \tag{111}$$

The contribution from kaons can be obtained at this order simply by re-scaling the prediction for pions by a factor $(f_K/f_\pi)^4 \simeq 2.2$. The resulting prediction for the combined cross section $\sigma(\gamma\gamma \to \pi^+\pi^-, K^+K^-)$ is shown in Fig. 8. Considering the possible contribution of the resonance $f_2(1270)$, the agreement is reasonable.

One can also predict the normalization of the timelike pion form factor

$$\begin{aligned} F_\pi^{\text{(timelike)}}(-Q^2) &= \frac{16\pi f_\pi^2}{Q^2}\alpha_V(-Q^{*2})\left(1 - 1.9\frac{\alpha_V}{\pi}\right) \tag{112} \\ &\simeq \frac{0.3 \text{ GeV}^2}{Q^2} \end{aligned}$$

assuming the asymptotic form for the pion distribution amplitude and the form of α_V given in Eq. (106), with the parameters $m_g^2 = 0.19 \text{ GeV}^2$ and $\Lambda_V = 0.16 \text{ GeV}$. This leading-twist prediction $Q^2 F_\pi^{\text{(timelike)}}(-Q^2) = 0.3 \text{ GeV}^2$ is a factor of two below the measurement of the pion form factor obtained from the $J/\psi \to \pi^+\pi^-$ branching ratio.[232] The time-like pion form factor data obtained from $e^+e^- \to \pi^+\pi^-$ annihilation does not have complications from off-shell extrapolations or rescattering, but it is also more sensitive to nearby vector meson poles in the t channel. The J/ψ analysis assumes that the $\pi^+\pi^-$ is created only through virtual photons. However, if the $J/\psi \to \pi^+\pi^-$ amplitude proceeds through channels such as γgg, then the branching ratio is not a precise method for obtaining $F_\pi^{\text{(timelike)}}$. It is thus important to have direct measurement of the $e^+e^- \to \pi^+\pi^-$ amplitude off-resonance.

5 Semi-Exclusive Processes: New Probes of Hadron Structure

A new class of hard "semi-exclusive" processes of the form $A + B \to C + Y$, have been proposed as new probes of QCD [233, 234, 235] These processes are characterized by a large momentum transfer $t = (p_A - p_C)^2$ and a large rapidity gap between the final state particle C and the inclusive system Y. Here A, B and C can be hadrons or (real or virtual) photons. The cross sections for such processes factorize in terms of the distribution amplitudes of A and C and the parton distributions in the target B. For example, $\gamma^* p \to \pi^+ X$ can be described as the convolution of the exclusive $\gamma^* u \to \pi^+ d$ reaction with the u quark structure function in the proton. Because of this factorization, semi-exclusive reactions provide a novel array of generalized currents, which not only give insight into the dynamics of hard scattering QCD processes, but

also allow experimental access to new combinations of the universal quark and gluon distributions including novel types of quark structure functions of specific flavor. One can also analyze the timelike analog, semi-exclusive production of energetic mesons in e^+e^- collisions. [236]

An essential condition for the factorization of the deeply virtual meson production amplitude of Fig. 21a is the existence of a large rapidity gap between the produced meson and the neutron. This factorization remains valid if the neutron is replaced with a hadronic system Y of invariant mass $M_Y^2 \ll W^2$, where W is the c.m. energy of the $\gamma^* p$ process. For $M_Y^2 \gg m_p^2$ the momentum k' of the d-quark in Fig. 21b is large with respect to the proton remnants, and hence it forms a jet. This jet hadronizes independently of the other particles in the final state if it is not in the direction of the meson, $i.e.$, if the meson has a large transverse momentum $q'_\perp = \Delta_\perp$ with respect to the photon direction in the $\gamma^* p$ c.m. Then the cross section for an inclusive system Y can be calculated as in DIS, by treating the d-quark as a final state particle.

The large $\Delta_\perp$ furthermore allows only transversally compact configurations of the projectile A to couple to the hard subprocess H of Fig. 21b, as it does in exclusive processes. [237] Hence the above discussion applies not only to incoming virtual photons at large Q^2, but also to real photons ($Q^2 = 0$) and in fact to any hadron projectile.

Let us then consider the general process $A + B \to C + Y$, where B and C are hadrons or real photons, while the projectile A can also be a virtual photon. In the semi-exclusive kinematic limit $\Lambda_{QCD}^2, M_B^2, M_C^2 \ll M_Y^2, \Delta_\perp^2 \ll W^2$ we have a large rapidity gap $|y_C - y_d| = \log \frac{W^2}{\Delta_\perp^2 + M_Y^2}$ between C and the parton d produced in the hard scattering (see Fig. 21c). The cross section then factorizes into the form

$$
\frac{d\sigma}{dt\,dx_S}(A + B \to C + Y)
$$
$$
= \sum_b f_{b/B}(x_S, \mu^2)\frac{d\sigma}{dt}(Ab \to Cd)\,, \qquad (113)
$$

where $t = (q - q')^2$ and $f_{b/B}(x_S, \mu^2)$ denotes the distribution of quarks, antiquarks and gluons b in the target B. The momentum fraction x_S of the struck parton b is fixed by kinematics to the value $x_S = \frac{-t}{M_Y^2 - t}$ and the factorization scale μ^2 is characteristic of the hard subprocess $Ab \to Cd$.

It is conceptually helpful to regard the hard scattering amplitude H in Fig. 21c as a generalized current of momentum $q - q' = p_A - p_C$, which interacts with the target parton b. For $A = \gamma^*$ we obtain a close analogy to standard DIS when particle C is removed. With $q' \to 0$ we thus find $-t \to Q^2$, $M_Y^2 \to W^2$, and see that x_S goes over into $x_B = Q^2/(W^2 + Q^2)$. The possibility to control the value of q' (and hence the momentum fraction x_S of the struck parton) as well as the quantum numbers of particles A and C should make semi-exclusive processes a versatile tool for studying hadron structure. The cross section further depends on the distribution amplitudes ϕ_A, ϕ_C ($cf.$ Fig. 21c), allowing new ways of measuring these quantities.

6 Self-Resolved Diffractive Reactions and Light Cone Wavefunctions

Diffractive multi-jet production in heavy nuclei provides a novel way to measure the shape of the LC Fock state wavefunctions and test color transparency. For example, consider the reaction [238, 239, 240] $\pi A \rightarrow \text{Jet}_1 + \text{Jet}_2 + A'$ at high energy where the nucleus A' is left intact in its ground state. The transverse momenta of the jets balance so that $\vec{k}_{\perp i} + \vec{k}_{\perp 2} = \vec{q}_\perp < R^{-1}{}_A$. The light-cone longitudinal momentum fractions also need to add to $x_1 + x_2 \sim 1$ so that $\Delta p_L < R_A^{-1}$. The process can then occur coherently in the nucleus. Because of color transparency, the valence wavefunction of the pion with small impact separation, will penetrate the nucleus with minimal interactions, diffracting into jet pairs. [238] The $x_1 = x$, $x_2 = 1 - x$ dependence of the di-jet distributions will thus reflect the shape of the pion valence light-cone wavefunction in x; similarly, the $\vec{k}_{\perp 1} - \vec{k}_{\perp 2}$ relative transverse momenta of the jets gives key information on the derivative of the underlying shape of the valence pion wavefunction. [239, 240, 241] The diffractive nuclear amplitude extrapolated to $t = 0$ should be linear in nuclear number A if color transparency is correct. The integrated diffractive rate should then scale as $A^2/R_A^2 \sim A^{4/3}$. Preliminary results on a diffractive dissociation experiment of this type E791 at Fermilab using 500 GeV incident pions on nuclear targets. [81] appear to be consistent with color transparency. [81] The momentum fraction distribution of the jets is consistent with a valence light-cone wavefunction of the pion consistent with the shape of the asymptotic distribution amplitude, $\phi_\pi^{\text{asympt}}(x) = \sqrt{3} f_\pi x (1-x)$. Data from CLEO [41] for the $\gamma\gamma^* \rightarrow \pi^0$ transition form factor also favor a form for the pion distribution amplitude close to the asymptotic solution [35, 24] to the perturbative QCD evolution equation.

The diffractive dissociation of a hadron or nucleus can also occur via the Coulomb dissociation of a beam particle on an electron beam (*e.g.* at HERA or eRHIC) or on the strong Coulomb field of a heavy nucleus (*e.g.* at RHIC or nuclear collisions at the LHC). [241] The amplitude for Coulomb exchange at small momentum transfer is proportional to the first derivative $\sum_i e_i \frac{\partial}{\vec{k}_{Ti}} \psi$ of the light-cone wavefunction, summed over the charged constituents. The Coulomb exchange reactions fall off less fast at high transverse momentum compared to pomeron exchange reactions since the light-cone wavefunction is effective differentiated twice in two-gluon exchange reactions.

It will also be interesting to study diffractive tri-jet production using proton beams $pA \rightarrow \text{Jet}_1 + \text{Jet}_2 + \text{Jet}_3 + A'$ to determine the fundamental shape of the 3-quark structure of the valence light-cone wavefunction of the nucleon at small transverse separation. [239] For example, consider the Coulomb dissociation of a high energy proton at HERA. The proton can dissociate into three jets corresponding to the three-quark structure of the valence light-cone wavefunction. We can demand that the produced hadrons all fall outside an opening angle θ in the proton's fragmentation region. Effectively all of the light-cone momentum $\sum_j x_j \simeq 1$ of the proton's fragments will thus be produced outside an "exclusion cone". This then limits the invariant

mass of the contributing Fock state $\mathcal{M}_n^2 > \Lambda^2 = P^{+2} \sin^2 \theta / 4$ from below, so that perturbative QCD counting rules can predict the fall-off in the jet system invariant mass $\mathcal{M}$. At large invariant mass one expects the three-quark valence Fock state of the proton to dominate. The segmentation of the forward detector in azimuthal angle ϕ can be used to identify structure and correlations associated with the three-quark light-cone wavefunction. [241] An interesting possibility is that the distribution amplitude of the $\Delta(1232)$ for $J_z = 1/2, 3/2$ is close to the asymptotic form $x_1 x_2 x_3$, but that the proton distribution amplitude is more complex. This ansatz can also be motivated by assuming a quark-diquark structure of the baryon wavefunctions. The differences in shapes of the distribution amplitudes could explain why the $p \to \Delta$ transition form factor appears to fall faster at large Q^2 than the elastic $p \to p$ and the other $p \to N^*$ transition form factors. [242] One can use also measure the dijet structure of real and virtual photons beams $\gamma^* A \to \text{Jet}_1 + \text{Jet}_2 + A'$ to measure the shape of the light-cone wavefunction for transversely-polarized and longitudinally-polarized virtual photons. Such experiments will open up a direct window on the amplitude structure of hadrons at short distances. The light-cone formalism is also applicable to the description of nuclei in terms of their nucleonic and mesonic degrees of freedom. [243, 244] Self-resolving diffractive jet reactions in high energy electron-nucleus collisions and hadron-nucleus collisions at moderate momentum transfers can thus be used to resolve the light-cone wavefunctions of nuclei.

7 Higher Fock States and the Intrinsic Sea

The main features of the heavy sea quark-pair contributions of the higher particle number Fock state states of light hadrons can be derived from perturbative QCD. One can identify two contributions to the heavy quark sea, the "extrinsic" contributions which correspond to ordinary gluon splitting, and the "intrinsic" sea which is multi-connected via gluons to the valence quarks. The leading $1/m_Q^2$ contributions to the intrinsic sea of the proton in the heavy quark expansion are proton matrix elements of the operator [245] $\eta^\mu \eta^\nu G_{\alpha\mu} G_{\beta\nu} G^{\alpha\beta}$ which in light-cone gauge $\eta^\mu A_\mu = A^+ = 0$ corresponds to three or four gluon exchange between the heavy-quark loop and the proton constituents in the forward virtual Compton amplitude. The intrinsic sea is thus sensitive to the hadronic bound-state structure. [246, 247] The maximal contribution of the intrinsic heavy quark occurs at $x_Q \simeq m_{\perp Q} / \sum_i m_\perp$ where $m_\perp = \sqrt{m^2 + k_\perp^2}$; *i.e.* at large x_Q, since this minimizes the invariant mass $\mathcal{M}_n^2$. The measurements of the charm structure function by the EMC experiment are consistent with intrinsic charm at large x in the nucleon with a probability of order $0.6 \pm 0.3\%$. [248] which is consistent with recent estimates based on instanton fluctuations. [245]

It is usually assumed that a heavy quarkonium state such as the J/ψ always decays to light hadrons via the annihilation of its heavy quark constituents to gluons. However, as Karliner and I [104] have shown, the transition $J/\psi \to \rho\pi$ can also occur by the rearrangement of the $c\bar{c}$ from the J/ψ into the $| q\bar{q}c\bar{c} \rangle$ intrinsic charm Fock state

of the ρ or π. On the other hand, the overlap rearrangement integral in the decay $\psi' \to \rho\pi$ will be suppressed since the intrinsic charm Fock state radial wavefunction of the light hadrons will evidently not have nodes in its radial wavefunction. This observation provides a natural explanation of the long-standing puzzle [249] why the J/ψ decays prominently to two-body pseudoscalar-vector final states, breaking hadron helicity conservation,[57] whereas the ψ' does not.

An important consequence of intrinsic charm is the possibility that hadronic decays may not necessarily proceed via the annihilation of the charm quarks. For example, in $J/\psi \to \pi\pi$ the charm quarks may simply flow to the final state higher Fock wavefunctions.

8 Other Applications of Light-Cone Quantization to QCD Phenomenology

Structure functions at large x_{bj}. The behavior of structure functions where one quark has the entire momentum requires the knowledge of LC wavefunctions with $x \to 1$ for the struck quark and $x \to 0$ for the spectators. This is a highly off-shell configuration, and thus one can rigorously derive quark-counting and helicity-retention rules for the power-law behavior of the polarized and unpolarized quark and gluon distributions in the $x \to 1$ endpoint domain.

DGLAP evolution at $x \to 1$ Usually one expects that structure functions are strongly suppressed at large x because of the momentum lost by gluon radiation: the predicted change of the power law behavior at large x is [250]

$$\frac{F_2(x,Q^2)}{F_2(x,Q_0^2)} \underset{x \to 1}{=} (1-x)^{\zeta(Q^2,Q_0^2)} \tag{114}$$

where

$$\zeta(q^2, Q_0^2) = \frac{1}{4\pi} \int_{Q_0^2}^{Q^2} \frac{d\ell^2}{\ell^2} \, \alpha_s(\ell^2) \ . \tag{115}$$

Because of asymptotic freedom, this implies a $\log \log Q^2$ increase in the effective power $\zeta(Q^2, Q_0^2)$. However, this derivation assumes that the struck quark is on its mass shell. The off-shell effect is profound, greatly reducing the PQCD radiation.[251, 105] We can take into account the main effect of the struck quark virtuality by modifying the propagator in Eq. (115):

$$\zeta(Q^2, Q_0^2) = \frac{1}{4\pi} \int_{Q_0^2}^{Q^2} \frac{d\ell^2}{\ell^2 + |k_f^2|} \, \alpha_s(\ell^2). \tag{116}$$

Thus at large x, there is effectively no DGLAP evolution until $Q^2 \gtrsim |k_f^2|$! One can also see that DGLAP evolution at large x at fixed Q^2 must be suppressed in order to have duality at fixed $W^2 = Q^2(1 - x_{bj})/x_{bj}$ between the inclusive electroproduction and

exclusive resonance contributions. [34, 35, 24] Thus evolution of structure functions is minimal in this domain because the struck quark is highly virtual as $x \to 1$; *i.e.* the starting point Q_0^2 for evolution cannot be held fixed, but must be larger than a scale of order $(m^2 + k_\perp^2)/(1-x)$. [34, 35, 24, 2, 252] The absence of structure function evolution at $x \to 1$ and fixed Q^2 is necessary in order to understand duality between the exclusive $p \to N^*$ channels and the inclusive cross section at fixed W^2.

9 Conclusions

Exclusive processes are particularly challenging to compute in QCD because of their sensitivity to the unknown non-perturbative bound state dynamics of the hadrons. However, in some important cases, the leading power-law behavior of an exclusive amplitude at large momentum transfer can be computed rigorously via a factorization theorem which separates the soft and hard dynamics. The key ingredient is the factorization of the hadronic amplitude at leading twist, order-by-order in perturbation theory. As in the case of inclusive reactions, factorization theorems for exclusive processes allow the analytic separation of the perturbatively-calculable short-distance contributions from the long-distance non-perturbative dynamics associated with hadronic binding. One of the most promising new areas of applications is to the study of exclusive B decays, where the heavy quark of the b meson allows a systematic factorization and identification of hard and soft contributions.

Testing quantum chromodynamics to high precision in exclusive processes is not easy. Virtually all QCD processes are complicated by the presence of dynamical higher twist effects, including power-law suppressed contributions due to multi-parton correlations, intrinsic transverse momentum, and finite quark masses. Many of these effects are inherently nonperturbative in nature and require detailed knowledge of hadron wavefunctions themselves. The problem of interpreting perturbative QCD predictions is further compounded by theoretical ambiguities due to the apparent freedom in the choice of renormalization schemes, renormalizations scales, and factorization procedures.

In this review, I have discussed how the universal, process-independent and frame-independent light-cone Fock-state wavefunctions encode the properties of a hadron in terms of its fundamental quark and gluon degrees of freedom. Light-cone wavefunctions provide a systematic framework for evaluating exclusive hadronic matrix elements, including time-like heavy hadron decay amplitudes and form factors. This formalism also provides a physical factorization scheme for separating hard and soft contributions for hard exclusive, semi-exclusive, and diffractive processes. I have also discussed how the ambiguities of renormalization scale and scheme choices can be resolved using the ansatz of a conformal template.

The success of dimensional counting rules and scaling for exclusive processes at present experimentally accessible momentum transfers can be understood if the effective coupling $\alpha_V(Q^*)$ is approximately constant at the relatively small scales Q^*

relevant to the hard scattering amplitudes. In the low-Q^* domain, the evolution of the quark distribution amplitudes also needs to be minimal. Furthermore, Sudakov suppression of the long-distance contributions is strengthened if the coupling is frozen because of the exponentiation of a double logarithmic series. However, it should be stressed that the Ansatz of a frozen coupling at small momentum transfer has not been demonstrated from first principles.

The scaling and normalization of the photon-to-pion transition form factor are fundamental features of QCD. The theory has been calculated to NLO. The prediction is in excellent agreement with empirical normalization of the $\gamma e \to \pi^0 e$ data assuming that the pion distribution amplitude is close to its asymptotic form $\sqrt{3} f_\pi x (1 - x)$. We also reproduce the scaling and normalization of the $\gamma\gamma \to \pi^+\pi^-$ data at large momentum transfer. However, the normalization of the space-like pion form factor $F_\pi(Q^2)$ obtained from electroproduction experiments is somewhat higher than that predicted by the corresponding commensurate scale relation. This discrepancy may be due to systematic errors introduced by the extrapolation of the $\gamma^* p \to \pi^+ n$ electroproduction data to the pion pole.

A new type of jet production reaction, diffractive dijet production has yielded strong empirical constraints on the pion distribution amplitude. These "self-resolving" diffractive processes can also provide direct experimental information on the light-cone wavefunctions of the photon and hadrons in terms of their QCD degrees of freedom, as well as the composition of nuclei in terms of their nucleon and mesonic degrees of freedom. There are now real prospects of computing the hadron wavefunctions and distribution amplitudes from first principles in QCD as exemplified by Dalley's computation [182] of the pion distribution amplitude using a combination of DLCQ and the transverse lattice methods and recent results from traditional lattice gauge theory.[40] Instanton models predict a pion distribution amplitude close to the asymptotic form.[253] A new result for the proton distribution amplitude treating nucleons as chiral solitons has recently been derived by Diakonov and Petrov.[254] Dyson-Schwinger models [255] of hadronic Bethe-Salpeter wavefunctions can also be used to predict light-cone wavefunctions and hadron distribution amplitudes by integrating over the relative k^- momentum. There is a possibility of deriving Bethe-Salpeter wavefunctions within light-cone gauge quantized QCD [129] in order to properly match the light-cone gauge Fock state decomposition.

Even without full non-perturbative solutions of QCD, one can envision a program to construct the light-cone wavefunctions using measured moments constraints from QCD sum rules, lattice gauge theory, hard exclusive and inclusive processes. One is guided by theoretical constraints from perturbation theory which dictates the asymptotic form of the wavefunctions at large invariant mass, $x \to 1$, and high $k_\perp$. One can also use constraints from ladder relations which connect Fock states of different particle number; perturbatively-motivated numerator spin structures; conformal symmetry; guidance from toy models such as "reduced" $QCD(1 + 1)$; and the correspondence to Abelian theory for $N_C \to 0$, and the many-body Schrödinger theory in the nonrelativistic domain.

10 Appendix: Light-Front Quantization and Perturbation Theory

In this Appendix, we outline the canonical quantization of QCD in the ghost-free $A^+ = 0$ light-cone gauge. The discussion follows that given in references previously.[24, 2, 105] The corresponding quantization of QCD in Feynman gauge is given by Srivastava.[256]

The front-form quantization of QCD proceeds in several steps. First one identifies the independent dynamical degrees of freedom in the Lagrangian. The theory is quantized by defining commutation relations for these dynamical fields at a given light-cone time $\tau = t + z = 0$. These commutation relations lead immediately to the definition of the Fock state basis. Expressing dependent fields in terms of the independent fields, one can then derive a light-cone Hamiltonian, which determines the evolution of the state space with changing τ. The rules for τ-ordered perturbation theory are given below, illustrating the origins and nature of the Fock state expansion, and of light-cone perturbation theory. Subtleties due to zero modes, the large scale structure of non-Abelian gauge fields (*e.g.* 'instantons'), chiral symmetry breaking, and the like are ignored. Although these have a profound effect on the structure of the vacuum, the theory can still be described with a Fock state basis and some sort of effective Hamiltonian. Furthermore, the short-distance interactions of the theory are unaffected by this structure, or at least this is the central ansatz of perturbative QCD.

Quantization

The Lagrangian (density) for QCD can be written

$$\mathcal{L} = -\frac{1}{2} \,\text{Tr}\,(F^{\mu\nu}\, F_{\mu\nu}) + \overline{\psi}\,(i\,\slashed{D} - m)\,\psi \tag{117}$$

where $F^{\mu\nu} = \partial^\mu A^\nu - \partial^\nu A^\mu + ig[A^\mu, A^\nu]$ and $iD^\mu = i\partial^\mu - gA^\mu$. Here the gauge field A^μ is a trace-less 3×3 color matrix ($A^\mu \equiv \sum_a A^{a\mu}T^a$, $\text{Tr}(T^aT^b) = 1/2\delta^{ab}$, $[T^a, T^b] = ic^{abc}T^c, \ldots$), and the quark field ψ is a color triplet spinor (for simplicity, we include only one flavor). At a given light-cone time, say $\tau = 0$, the independent dynamical fields are $\psi_\pm \equiv \Lambda_\pm \psi$ and $A^i_\perp$ with conjugate fields $i\psi^\dagger_+$ and $\partial^+ A^i_\perp$, where $\Lambda_\pm = \gamma^o\gamma^\pm/2$ are projection operators ($\Lambda_+\Lambda_- = 0$, $\Lambda^2_\pm = \Lambda_\pm$, $\Lambda_+ + \Lambda_- = 1$) and $\partial^\pm = \partial^0 \pm \partial^3$. Using the equations of motion, the remaining fields in $\mathcal{L}$ can be expressed in terms of ψ_+, $A^i_\perp$:

$$\psi_- \equiv \Lambda_-\psi = \frac{1}{i\partial^+}\left[i\vec{D}_\perp \cdot \vec{\alpha}_\perp + \beta m\right]\psi_+$$

$$= \tilde{\psi}_- - \frac{1}{i\partial^+}\,g\vec{A}_\perp \cdot \vec{\alpha}_\perp\,\psi_+\ ,$$

$$A^+ = 0\ ,$$

$$A^- = \frac{2}{i\partial^+}\,i\vec{\partial}_\perp \cdot \vec{A}_\perp + \frac{2g}{(i\partial^+)^2}\left\{\left[i\partial^+ A^i_\perp, A^i_\perp\right] + 2\psi^\dagger_+ T^a\,\psi_+ T^a\right\}$$

$$\equiv \tilde{A}^- + \frac{2g}{(i\partial^+)^2} \left\{ \left[i\partial^+ A_\perp^i, A_\perp^i \right] + 2\psi_+^\dagger \, T^a \, \psi_+ \, T^a \right\} \; , \tag{118}$$

with $\beta = \gamma^o$ and $\vec{\alpha}_\perp = \gamma^o \vec{\gamma}$.

To quantize, we expand the fields at $\tau = 0$ in terms of creation and annihilation operators,

$$\begin{aligned}
\psi_+(x) &= \int_{k^+>0} \frac{dk^+ \, d^2 k_\perp}{k^+ \, 16\pi^3} \sum_\lambda \left\{ b(\underline{k}, \lambda) \, u_+(\underline{k}, \lambda) \, e^{-ik\cdot x} \right. \\
&\qquad\qquad \left. + \, d^\dagger(\underline{k}, \lambda) \, v_+(\underline{k}, \lambda) \, e^{ik\cdot x} \right\} \; , \quad \tau = x^+ = 0 \\
A_\perp^i(x) &= \int_{k^+>0} \frac{dk^+ \, d^2 k_\perp}{k^+ \, 16\pi^3} \sum_\lambda \left\{ a(\underline{k}, \lambda) \, \epsilon_\perp^i(\lambda) \, e^{-ik\cdot x} + c\cdot c \right\} \; , \\
\tau &= x^+ = 0 \; ,
\end{aligned} \tag{119}$$

with commutation relations ($\underline{k} = (k^+, \vec{k}_\perp)$):

$$\begin{aligned}
\left\{ b(\underline{k}, \lambda), \, b^\dagger(\underline{p}, \lambda) \right\} &= \left\{ d(\underline{k}, \lambda), \, d^\dagger(\underline{p}, \lambda') \right\} \\
&= \left[a(\underline{k}, \lambda), \, a^\dagger(\underline{p}, \lambda') \right] \\
&= 16\pi^3 \, k^+ \, \delta^3(\underline{k} - \underline{p}) \, \delta_{\lambda\lambda'} \; , \\
\{b, b\} = \{d, d\} &= \ldots = 0 \; ,
\end{aligned} \tag{120}$$

where λ is the quark or gluon helicity. These definitions imply canonical commutation relations for the fields with their conjugates ($\tau = x^+ = y^+ = 0, \underline{x} = (x^-, x_\perp), \ldots$):

$$\begin{aligned}
\left\{ \psi_+(\underline{x}), \, \psi_+^\dagger(\underline{y}) \right\} &= \Lambda_+ \, \delta^3(\underline{x} - \underline{y}) \; , \\
\left[A^i(\underline{x}), \, \partial^+ A_\perp^j(\underline{y}) \right] &= i\delta^{ij} \, \delta^3(\underline{x} - \underline{y}) \; .
\end{aligned} \tag{121}$$

The creation and annihilation operators define the Fock state basis for the theory at $\tau = 0$, with a vacuum $|0\rangle$ defined such that $b|0\rangle = d|0\rangle = a|0\rangle = 0$. The evolution of these states with τ is governed by the light-cone Hamiltonian, $H_{LC} = P^-$, conjugate to τ. The Hamiltonian can be readily expressed in terms of ψ_+ and $A_\perp^i$:

$$H_{LC} = H_0 + V \; , \tag{122}$$

where

$$\begin{aligned}
H_0 &= \int d^3 x \left\{ \text{Tr} \left(\partial_\perp^i A_\perp^j \partial_\perp^i A_\perp^j \right) \right. \\
&\quad + \left. \psi_+^\dagger \, (i\partial_\perp \cdot \alpha_\perp + \beta m) \frac{1}{i\partial^+} (i\partial_\perp \cdot \alpha_\perp + \beta m) \psi_+ \right\} \\
&= \sum_{\substack{\lambda \\ \text{colors}}} \int \frac{dk^+ \, d^2 k_\perp}{16\pi^3 \, k^+} \left\{ a^\dagger(\underline{k}, \lambda) \, a(\underline{k}, \lambda) \frac{k_\perp^2}{k^+} + b^\dagger(\underline{k}, \lambda) \, b(\underline{k}, \lambda) \right. \\
&\quad \times \left. \frac{k_\perp^2 + m^2}{k^+} + d^\dagger(\underline{k}, \lambda) \, b(\underline{k}, \lambda) \frac{k_\perp^2 + m^2}{k^+} \right\} + \text{constant}
\end{aligned} \tag{123}$$

79

is the free Hamiltonian and V the interaction:

$$
\begin{aligned}
V \;=\;& \int d^3x \;\Big\{ 2g \operatorname{Tr}\left(i\partial^\mu \widetilde{A}^\nu \left[\widetilde{A}_\mu, \widetilde{A}_\nu\right]\right) - \frac{g^2}{2}\operatorname{Tr}\left(\left[\widetilde{A}^\mu, \widetilde{A}^\nu\right]\left[\widetilde{A}_\mu, \widetilde{A}_\nu\right]\right) \\
&+\; g\overline{\widetilde{\psi}}\;\widetilde{\slashed{A}}\,\widetilde{\psi} + g^2 \operatorname{Tr}\left(\left[i\partial^+ \widetilde{A}^\mu, \widetilde{A}_\mu\right]\frac{1}{(i\partial^+)^2}\left[i\partial^+ \widetilde{A}^\nu, \widetilde{A}_\nu\right]\right) \\
&+\; g^2\overline{\widetilde{\psi}}\;\widetilde{\slashed{A}}\,\frac{\gamma^+}{2i\partial^+}\;\widetilde{\slashed{A}}\,\widetilde{\psi} - g^2\overline{\widetilde{\psi}}\gamma^+\left(\frac{1}{(i\partial^+)^2}\left[i\partial^+ \widetilde{A}^\nu, \widetilde{A}_\nu\right]\right)\widetilde{\psi} \\
&+\; \frac{g^2}{2}\;\overline{\widetilde{\psi}}\gamma^+\,T^a\psi\,\frac{1}{(i\partial^+)^2}\,\overline{\widetilde{\psi}}\gamma^+\,T^a\psi\Big\}\;,
\end{aligned}
\tag{124}
$$

with $\widetilde{\psi} = \widetilde{\psi}_- + \psi_+\;(\to \psi$ as $g\to 0)$ and $\widetilde{A}^\mu = (0, \widetilde{A}^-, A_\perp^i)\;(\to A^\mu$ as $g\to 0)$. The Fock states are obviously eigenstates of H_0 with

$$
H_0\big|\,n: k_i^+, k_{\perp i}\big\rangle = \sum_i \left(\frac{k_\perp^2 + m^2}{k^+}\right)_i \big|\,n: k_i^+, k_{\perp i}\big\rangle\;.
\tag{125}
$$

It is equally obvious that they are not eigenstates of V, though any matrix element of V between Fock states is trivially evaluated.
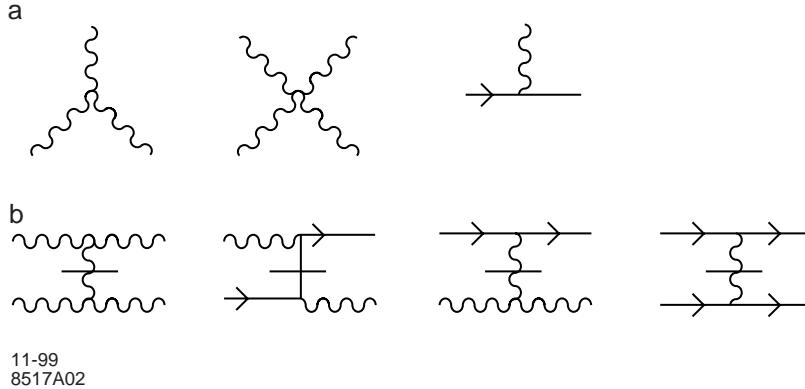

11-99
8517A02

Figure 26: Diagrams which appear in the interaction Hamiltonian for QCD on the light cone. The propagators with horizontal bars represent "instantaneous" gluon and quark exchange which arise from reduction of the dependent fields in $A^+ = 0$ gauge. (a) Basic interaction vertices in QCD. (b) "Instantaneous" contributions.

The first three terms in V correspond to the familiar three and four gluon vertices, and the gluon-quark vertex [Fig. 26(a)]. The remaining terms represent new four-quanta interactions containing instantaneous fermion and gluon propagators [Fig. 26(b)]. All terms conserve total three-momentum $\underline{k} = (k^+, \vec{k}_\perp)$, because of the integral over $\underline{x}$ in V. Furthermore, all Fock states other than the vacuum have total $k^+ >$

0, since each individual bare quantum has $k^+ > 0$. Consequently the Fock state vacuum must be an eigenstate of V and therefore an eigenstate of the full light-cone Hamiltonian.

Light-Cone Perturbation Theory

We define light-cone Greens functions to be the probability amplitudes that a state starting in Fock state $|i\rangle$ ends up in Fock state $|f\rangle$ a (light-cone) time τ later

$$
\begin{aligned}
\langle f|i\rangle\, G(f, i; \tau) &\equiv \langle f|e^{-iH_{LC}\tau/2}|i\rangle \\
&= i \int \frac{d\epsilon}{2\pi}\, e^{-i\epsilon\tau/2}\, G(f, i; \epsilon)\, \langle f|i\rangle\ ,
\end{aligned} \tag{126}
$$

where Fourier transform $G(f, i; \epsilon)$ can be written

$$
\begin{aligned}
\langle f|i\rangle\, G(f, i; \epsilon) &= \left\langle f\left|\frac{1}{\epsilon - H_{LC} + i0_+}\right| i\right\rangle \\
&= \left\langle f\left|\frac{1}{\epsilon - H_{LC} + i0_+} + \frac{1}{\epsilon - H_0 + i0_+}\, V\, \frac{1}{\epsilon - H_0 + i0_+}\right.\right. \\
&\quad + \left.\frac{1}{\epsilon - H_0 + i0_+}\, V\, \frac{1}{\epsilon - H_0 + i0_+}\, V\, \frac{1}{\epsilon - H_0 + i0_+}\right. \\
&\quad + \left.\ldots\middle| i\right\rangle\ .
\end{aligned} \tag{127}
$$

The rules for τ-ordered perturbation theory follow immediately when $(\epsilon - H_0)^{-1}$ is replaced by its spectral decomposition,

$$
\frac{1}{\epsilon - H_0 + i0_+} = \sum_{n, \lambda_i} \int \widetilde{\prod} \frac{dk_i^+\, d^2 k_{\perp i}}{16\pi^3\, k_i^+}\, \frac{|\, n : \underline{k}_i, \lambda_i\rangle\, \langle n : \underline{k}_i, \lambda_i\,|}{\epsilon - \sum_i (k^2 + m^2)_i / k_i^+ + i0_+} \tag{128}
$$

The sum becomes a sum over all states n intermediate between two interactions.

To calculate $G(f, i; \epsilon)$ perturbatively then, all τ-ordered diagrams must be considered, the contribution from each graph may be computed according to the following rules:[24]

1. Assign a momentum k^μ to each line such that the total $k^+, k_\perp$ are conserved at each vertex, and such that $k^2 = m^2$, i.e. $k^- = (k^2 + m^2)/k^+$. With fermions associate an on-shell spinor.

$$
u(\underline{k}, \lambda) = \frac{1}{\sqrt{k^+}}\left(k^+ + \beta m + \vec{\alpha}_\perp \cdot \vec{k}_\perp\right) \begin{cases} \chi(\uparrow) & \lambda = \uparrow \\ \chi(\downarrow) & \lambda = \downarrow \end{cases} \tag{129}
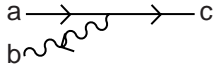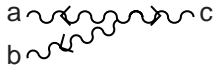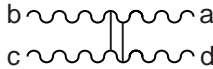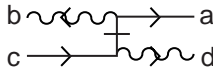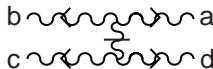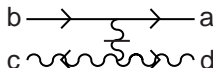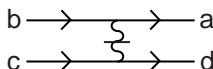$$

or

$$
v(\underline{k}, \lambda) = \frac{1}{\sqrt{k^+}}\left(k^+ - \beta m + \vec{\alpha}_\perp \cdot \vec{k}_\perp\right) \begin{cases} \chi(\downarrow) & \lambda = \uparrow \\ \chi(\uparrow) & \lambda = \downarrow \end{cases} \tag{130}
$$

where $\chi(\uparrow) = 1/\sqrt{2}\,(1, 0, 1, 0)$ and $\chi(\downarrow) = 1/\sqrt{2}\,(0, 1, 0, -1)^T$. For gluon lines, assign a polarization vector $\epsilon^\mu = (0,\ 2\vec{\epsilon}_\perp \cdot \vec{k}_\perp / k^+,\ \vec{\epsilon}_\perp)$ where $\vec{\epsilon}_\perp(\uparrow) = -1/\sqrt{2}\,(1, i)$ and $\vec{\epsilon}_\perp(\downarrow) = 1/\sqrt{2}\,(1, -i)$.

2. Include a factor $\theta(k^+)/k^+$ for each internal line.

3. For each vertex include factors as illustrated in Fig. 27. To convert incoming into outgoing lines or vice versa replace

$$u \leftrightarrow v \ , \qquad \overline{u} \leftrightarrow -\overline{v} \ , \qquad \epsilon \leftrightarrow \epsilon^* \tag{131}$$

in any of these vertices.

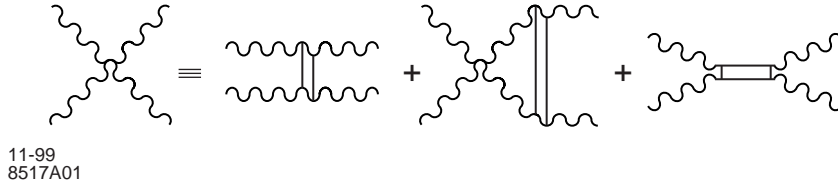|	Vertex Factor	Color Factor
a →→ c, b	$g\bar{u}(c)\,\not{\epsilon}_b\,u(a)$	T^b
a ～～ c, b	$g\{(p_a-p_b)\cdot\varepsilon_c^*\,\varepsilon_a\cdot\varepsilon_b$ + cyclic permutations$\}$	iC^{abc}
b ～ a, c ～ d	$g^2\{\varepsilon_b\cdot\varepsilon_c\,\varepsilon_a^*\cdot\varepsilon_d^* + \varepsilon_a^*\cdot\varepsilon_c\,\varepsilon_b\cdot\varepsilon_d^*\}$	$iC^{abe}\,iC^{cde}$
b ～ a, c → d	$g^2\bar{u}(a)\,\not{\epsilon}_b\,\dfrac{\gamma^+}{2(p_c^+ - p_d^+)}\,\not{\epsilon}_c^*\,u(c)$	$T^b\,T^d$
b ～ a, c ～ d	$g^2\varepsilon_a^*\cdot\varepsilon_b\dfrac{(p_a^+ - p_b^+)(p_c^+ - p_d^+)}{(p_c^+ + p_b^+)}\,\varepsilon_d^*\cdot\varepsilon_c$	$iC^{abe}\,iC^{cde}$
b → a, c ～ d	$g^2\bar{u}(a)\gamma^+u(b)\dfrac{(p_c^+ - p_d^+)}{(p_c^+ + p_d^+)^2}\,\varepsilon_d^*\cdot\varepsilon_c$	$iC^{cde}\,T^e$
b → a, c → d	$g^2\,\dfrac{\bar{u}(a)\gamma^+u(b)\,\bar{u}(d)\gamma^+u(c)}{(p_c^+ - p_d^+)^2}$	$T^e\,T^e$

11-99
8517A01

Figure 27: Graphical rules for QCD in light-cone perturbation theory.

4. For each intermediate state there is a factor

$$\frac{1}{\epsilon - \displaystyle\sum_{\text{interm}} k^- + i0_+} \tag{132}$$

where ϵ is the incident P^-, and the sum is over all particles in the intermediate state.

82

5. Integrate $\int dk^+ d^2k_\perp / 16\pi^3$ over each independent k, and sum over internal helicities and colors.

6. Include a factor -1 for each closed fermion loop, for each fermion line that both begins and ends in the initial state (*i.e.* $\overline{v} \ldots u$), and for each diagram in which fermion lines are interchanged in either of the initial or final states.

As an illustration, the second diagram in Fig. 26 contributes

$$
\frac{1}{\epsilon - \sum\limits_{i=b,d} \left(\frac{k_\perp^2 + m^2}{k^+} \right)_i} \cdot \frac{\theta(k_a^+ - k_b^+)}{k_a^+ - k_b^+}
$$

$$
\times \quad \frac{g^2 \sum\limits_{\lambda} \overline{u}(b)\, \epsilon^*(\underline{k}_a - \underline{k}_b, \lambda)\, u(a)\, \overline{u}(d)\; \not{\epsilon}(\underline{k}_a - \underline{k}_b, \lambda)\, u(c)}{\epsilon - \sum\limits_{i=b,c} \left(\frac{k_\perp^2 + m^2}{k^+} \right)_i - \frac{(k_{\perp a} - k_{\perp b})^2}{k_a^+ - k_b^+}}
$$

$$
2ex \quad \cdot \quad \frac{1}{\epsilon - \sum\limits_{i=a,c} \left(\frac{k_\perp^2 + m^2}{k^+} \right)_i} \tag{133}
$$

(times a color factor) to the $q\overline{q} \to q\overline{q}$ Greens function. (The vertices for quarks and gluons of definite helicity have very simple expressions in terms of the momenta of the particles.) The same rules apply for scattering amplitudes, but with propagators omitted for external lines, and with $\epsilon = P^-$ of the initial (and final) states.

Finally, notice that this quantization procedure and perturbation theory (graph by graph) are manifestly invariant under a large class of Lorentz transformations:

1. boosts along the 3-direction—*i.e.* $p^+ \to Kp^+$, $p^- \to K^{-1}p^-$, $p_\perp \to p_\perp$ for each momentum;

2. transverse boosts—*i.e.* $p^+ \to p^+$, $p^- \to p^- + 2p_\perp \cdot Q_\perp + p^+ Q_\perp^2$, $p_\perp \to p_\perp + p^+ Q_\perp$ for each momentum ($Q_\perp$ like K is dimensionless);

3. rotations about the 3-direction.

It is these invariances which lead to the P^+ and $P_\perp$ frame-independence of the light-cone Fock state wave functions.

Acknowledgments

Hwang, Chueng-Ryong Ji, Bo-Qiang Ma, Hans Christian Pauli, Johan Rathsman, Ivan Schmidt, and Prem Srivastava.

References

[1] R. P. Feynman, Phys. Rev. Lett. **23**, 1415 (1969).

[2] S. J. Brodsky and G. P. Lepage, SLAC-PUB-4947. Published in 'Perturbative Quantum Chromodynamics', Ed. by A.H. Mueller, World Scientific Publ. Co. (1989), p. 93-240 (QCD161:M83).

[3] V. L. Chernyak and A. R. Zhitnitsky, Phys. Rept. **112**, 173 (1984).

[4] G. Sterman and P. Stoler, hep-ph/9708370.

[5] P. Jain, B. Kundu, H. Li, J. P. Ralston and J. Samuelsson, Nucl. Phys. **A666-667**, 75 (2000) [hep-ph/9907388].

[6] N. G. Stefanis, Eur. Phys. J. **C7**, 1 (1999) [hep-ph/9911375].

[7] M. Vanderhaeghen, hep-ph/0007232.

[8] M. Gell-Mann and F. E. Low, Phys. Rev. **95**, 1300 (1954).

[9] M. Gell-Mann and F. Low, Phys. Rev. **84**, 350 (1951).

[10] S. J. Brodsky and J. R. Primack, Annals Phys. **52**, 315 (1969).

[11] V. S. Fadin, E. A. Kuraev and L. N. Lipatov, Phys. Lett. **60B**, 50 (1975); L. N. Lipatov, Yad. Fiz. **23**, 642 (1976) [Sov. J. Nucl. Phys. **23**, 338 (1976)]; E. A. Kuraev, L. N. Lipatov and V. S. Fadin, Zh. Eksp. Teor. Fiz. **71**, 840 (1976) [Sov. JETP **44**, 443 (1976)]; *ibid.* **72**, 377 (1977) [**45**, 199 (1977)]; Ya. Ya. Balitskiĭ and L. N. Lipatov, Yad. Fiz. **28**, 1597 (1978) [Sov. J. Nucl. Phys. **28**, 822 (1978)].

[12] H. D. Abarbanel, S. D. Drell and F. J. Gilman, Phys. Rev. **177**, 2458 (1969).

[13] S. J. Brodsky, F. E. Close and J. F. Gunion, Phys. Rev. **D5**, 1384 (1972).

[14] J. Gasser and H. Leutwyler, Annals Phys. **158**, 142 (1984).

[15] M. A. Shifman, A. I. Vainshtein and V. I. Zakharov, Nucl. Phys. **B147**, 385 (1979).

[16] B. L. Ioffe, Nucl. Phys. **B188**, 317 (1981).

[17] S. Larson and S. E. Koonin, K. Hornbostel, S. J. Brodsky, and H. C. Pauli, Phys. Rev. **D41** 3814 (1990).

[18] S. Brodsky and M. Karliner, in preparation.

[19] S. J. Brodsky and G. R. Farrar, Phys. Rev. Lett. **31**, 1153 (1973).

[20] S. J. Brodsky and G. R. Farrar, Phys. Rev. **D11**, 1309 (1975).

[21] V. A. Matveev, R. M. Muradian and A. N. Tavkhelidze, Lett. Nuovo Cim. **7**, 719 (1973).

[22] M. A. Shupe *et al.*, Phys. Rev. Lett. **40**, 271 (1978).

[23] R. Blankenbecler, S.J. Brodsky, J. F. Gunion and R. Savit, Phys. Rev. **D8**, 4117 (1973).

[24] G. P. Lepage and S. J. Brodsky, Phys. Rev. **D22**, 2157 (1980).

[25] X. Ji, Phys. Rev. **D55**, 7114 (1997), hep-ph/9609381.

[26] A. V. Radyushkin, Phys. Rev. **D56**, 5524 (1997) [hep-ph/9704207].

[27] M. Diehl, T. Feldmann, R. Jakob and P. Kroll, Phys. Lett. **B460**, 204 (1999) hep-ph/9903268.

[28] M. Diehl, T. Feldmann, R. Jakob and P. Kroll, Eur. Phys. J. **C8**, 409 (1999), hep-ph/9811253.

[29] S. J. Brodsky, M. Diehl and D. S. Hwang, hep-ph/0009254.

[30] S. J. Brodsky, L. Frankfurt, J. F. Gunion, A. H. Mueller and M. Strikman, Phys. Rev. **D50**, 3134 (1994), hep-ph/9402283.

[31] D. Muller, D. Robaschik, B. Geyer, F. M. Dittes and J. Horejsi, Fortsch. Phys. **42**, 101 (1994) [hep-ph/9812448].

[32] J. C. Collins, L. Frankfurt and M. Strikman, Phys. Rev. **D56**, 2982 (1997) [hep-ph/9611433].

[33] M. Diehl, T. Gousset, and B. Pire, hep-ph/0003233.

[34] G. P. Lepage and S. J. Brodsky, Phys. Rev. Lett. **43**, 545 (1979).

[35] G. P. Lepage and S. J. Brodsky, Phys. Lett. **B 87**, 359 (1979).

[36] C.-R. Ji, A. Pang, and A. Szczepaniak, *Phys. Rev.* **D52**, 4038 (1995).

[37] S. J. Brodsky, Y. Frishman, G. P. Lepage and C. Sachrajda, *Phys. Lett.* **91B**, 239 (1980).

[38] G. Martinelli and C. T. Sachrajda, Phys. Lett. **B190**, 151 (1987).

[39] D. Daniel, R. Gupta and D. G. Richards, Phys. Rev. **D43**, 3715 (1991).

[40] L. Del Debbio, M. Di Pierro, A. Dougall and C. Sachrajda [UKQCD collaboration], Nucl. Phys. Proc. Suppl. **83-84**, 235 (2000) [hep-lat/9909147].

[41] J. Gronberg *et al.* [CLEO Collaboration], Phys. Rev. **D57**, 33 (1998), hep-ex/9707031.

[42] P. Kroll and M. Raulfs, *Phys. Lett.* **387B**, 848 (1996).

[43] A. V. Radyushkin, *Acta Phys. Polon.* **B26**, 2067 (1995).

[44] S. J. Brodsky, C. Ji, A. Pang and D. G. Robertson, hep-ph/9705221.

[45] A. Schmedding and O. Yakovlev, hep-ph/9905392.

[46] S. J. Brodsky and G. P. Lepage, SLAC-PUB-2294 *Presented at Workshop on Current Topics in High Energy Physics*, Cal Tech., Pasadena, Calif., Feb 13-17, 1979.

[47] A. V. Efremov and A. V. Radyushkin, Theor. Math. Phys. **42** (1980) 97;

[48] V. L. Chernyak, A. R. Zhitnitsky and V. G. Serbo, JETP Lett. **26**, 594 (1977).

[49] V. L. Chernyak, V. G. Serbo and A. R. Zhitnitsky, Sov. J. Nucl. Phys. **31**, 552 (1980).

[50] G. R. Farrar and D. R. Jackson, Phys. Rev. Lett. **43**, 246 (1979).

[51] A. Duncan and A. H. Mueller, Phys. Rev. **D21**, 1636 (1980).

[52] S. Klein, e-Print, nucl-th/9707008.

[53] S. J. Brodsky and P. M. Zerwas, *Nucl. Instrum. Meth.* **A355** 19, (1995), e-Print hep-ph/9407362, and references therein.

[54] S. J. Brodsky and G. P. Lepage, *Phys. Rev.* **D24**, 1808 (1981).

[55] H. Paar *et al.*, CLEO collaboration (to be published).

[56] J. Boyer *et al.*, Phys. Rev. Lett. **56**, 207 (1980); TPC/Two Gamma Collaboration (H. Aihara *et al.*), Phys. Rev. Lett. **57**, 404 (1986).

[57] S. J. Brodsky and G. P. Lepage, Phys. Rev. **D24**, 2848 (1981).

[58] S. J. Brodsky and C. Ji, Phys. Rev. **D33**, 1951 (1986).

[59] V. M. Braun, S. E. Derkachov, G. P. Korchemsky and A. N. Manashov, Nucl. Phys. **B553**, 355 (1999) hep-ph/9902375.

[60] C. E. Carlson, Phys. Rev. **D34**, 2704 (1986).

[61] P. Stoler, Phys. Rept. **226**, 103 (1993).

[62] M. E. Peskin, Phys. Lett. **B88**, 128 (1979).

[63] S. J. Brodsky, G. P. Lepage and S. A. Zaidi, Phys. Rev. **D23**, 1152 (1981).

[64] B. L. Ioffe, Nucl. Phys. **B 188**, 317 (1981); V. M. Belyaev and B. L. Ioffe, Sov. Phys. JETP **56**, 497 (1982).

[65] V. L. Chernyak and I. R. Zhitnitsky, Nucl. Phys. **B246**, 52 (1984).

[66] V. L. Chernyak, A. A. Ogloblin and I. R. Zhitnitsky, Z. Phys. **C42**, 583 (1989).

[67] S. J. Brodsky, J. Ellis, J. S. Hagelin and C. Sachrajda, Nucl. Phys. **B238**, 561 (1984).

[68] B. L. Ioffe and A. V. Smilga, Phys. Lett. **B114**, 353 (1982). V. M. Braun, A. Khodjamirian and M. Maul, Phys. Rev. **D61**, 073004 (2000) [hep-ph/9907495].

[69] V. M. Braun, A. Khodjamirian and M. Maul, Phys. Rev. **D61**, 073004 (2000) [hep-ph/9907495].

[70] S. Brodsky and D. Kharzeev, in preparation.

[71] H. Fujii and D. Kharzeev, Phys. Rev. **D60**, 114039 (1999) [hep-ph/9903495].

[72] C-R Ji, A. F. Sill and R. M. Lombard-Nelsen, Phys. Rev. **D36**, 165 (1987).

[73] I. D. King and C. T. Sachrajda, Nucl. Phys. **B279**, 785 (1987).

[74] M. Gari and N. Stefanis, Phys. Lett. **B175**, 462 (1986), M. Gari and N. Stefanis, Phys. Lett. **187B**, 401 (1987).

[75] P. V. Landshoff, Phys. Rev. **D10**, 1024 (1974).

[76] A. Duncan and A. H. Mueller, Phys. Lett. **B90**, 159 (1980).

[77] A. H. Mueller, CU-TP-219 *Presented at 10th Int. Symp. on Lepton and Photon Interactions at High Energy, Bonn, West Germany, Aug 24-29, 1981.*

[78] S. J. Brodsky and A. H. Mueller, Phys. Lett. **B206**, 685 (1988).

[79] L. L. Frankfurt and M. I. Strikman, Phys. Rept. **160**, 235 (1988).

[80] P. Jain, B. Pire and J. P. Ralston, Phys. Rept. **271**, 67 (1996) [hep-ph/9511333].

[81] D. Ashery [E791 Collaboration], hep-ex/9910024.

[82] A. S. Carroll *et al.*, Phys. Rev. Lett. **61**, 1698 (1988).

[83] Y. Mardor *et al.*, Phys. Lett. **B437**, 257 (1998) [nucl-ex/9710002].

[84] A. Leksanov *et al.* [E850 Collaboration], nucl-ex/0009008.

[85] G. R. Court *et al.*, Phys. Rev. Lett. **57**, 507 (1986).

[86] S. J. Brodsky and G. F. de Teramond, *Phys. Rev. Lett.* **60**, 1924 (1988).

[87] G. F. de Teramond, R. Espinoza and M. Ortega-Rodriguez, Phys. Rev. **D58**, 034012 (1998) [hep-ph/9708202].

[88] J. P. Ralston and B. Pire, Phys. Rev. Lett. **57**, 2330 (1986).

[89] P. Jain, B. Kundu and J. P. Ralston, hep-ph/0005126.

[90] S. J. Brodsky, C. E. Carlson and H. J. Lipkin, Phys. Rev. **D20**, 2278 (1979).

[91] R. L. Anderson *et al.*, Phys. Rev. Lett. **30**, 627 (1973).

[92] S. J. Brodsky and B. T. Chertok, *Phys. Rev.* **D14**, 3003 (1976).

[93] J. F. Gunion, S. J. Brodsky and R. Blankenbecler, Phys. Rev. **D8**, 287 (1973).

[94] D. Sivers, S. J. Brodsky and R. Blankenbecler, Phys. Rept. **23**, 1 (1976).

[95] S. J. Brodsky, C. Ji and G. P. Lepage, Phys. Rev. Lett. **51**, 83 (1983).

[96] G. R. Farrar, K. Huleihel and H. Zhang, Phys. Rev. Lett. **74**, 650 (1995).

[97] S. J. Brodsky and J. R. Hiller, Phys. Rev. **C28**, 475 (1983).

[98] R. J. Holt, Phys. Rev. **C41**, 2400 (1990).

[99] C. Bochna *et al.* [E89-012 Collaboration], Phys. Rev. Lett. **81**, 4576 (1998) [nucl-ex/9808001].

[100] J. E. Belz *et al.*, Phys. Rev. Lett. **74**, 646 (1995).

[101] T. S. Lee, CONF-8805140-10.

[102] A. D. Krisch, *Nucl. Phys. B (Proc. Suppl.)* **25**, 285 (1992).

[103] C. F. Perdrisat [Jefferson Lab Hall A Collaboration], Nucl. Phys. **A663-664**, 38 (2000).

[104] S. J. Brodsky and M. Karliner, *Phys. Rev. Lett.* **78**, 4682 (1997), hep-ph/9704379.

[105] G. P. Lepage, S. J. Brodsky, T. Huang and P. B. Mackenzie, CLNS-82/522, published in Banff Summer Inst.1981:0083 (QCD161:B23:1981); S. J. Brodsky, T. Huang and G. P. Lepage, *In *Banff 1981, Proceedings, Particles and Fields 2*, 143-199.*

[106] E. D. Bloom and F. J. Gilman, Phys. Rev. **D4**, 2901 (1971).

[107] E. D. Bloom and F. J. Gilman, Phys. Rev. Lett. **25**, 1140 (1970).

[108] S. D. Drell and T. Yan, Phys. Rev. Lett. **24**, 181 (1970).

[109] G. B. West, Phys. Rev. Lett. **24**, 1206 (1970).

[110] R. P. Feynman, *Photon-Hadron Interactions*, Benjamin, (1972).

[111] H. Li and G. Sterman, Nucl. Phys. **B381**, 129 (1992).

[112] P. Kroll, Nucl. Phys. **A666-667**, 3 (2000) [hep-ph/9907301].

[113] N. G. Stefanis, W. Schroers and H. C. Kim, hep-ph/0005218.

[114] S. J. Brodsky and P. Huet, Phys. Lett. **B417**, 145 (1998) hep-ph/9707543.

[115] T. Brooks and L. Dixon, hep-ph/0004143.

[116] G. R. Farrar and H. Zhang, Phys. Rev. Lett. **65**, 1721 (1990).

[117] A. S. Kronfeld and B. Nizic, Phys. Rev. **D44**, 3445 (1991).

[118] P. A. Guichon and M. Vanderhaeghen, Prog. Part. Nucl. Phys. **41**, 125 (1998) [hep-ph/9806305].

[119] S. J. Brodsky, F. E. Close and J. F. Gunion, *Phys. Rev.* **D6**, 177 (1972).

[120] N. Isgur and C. H. Llewellyn Smith, *Phys. Lett.* **B217**, 535 (1989).

[121] A. V. Radyushkin, *Phys. Rev.* **D58**, 114008 (1998) hep-ph/9803316.

[122] J. Bolz and P. Kroll, *Z. Phys.* **A356**, 327 (1996) hep-ph/9603289.

[123] S. J. Brodsky, Y. Frishman and G. P. Lepage, Phys. Lett. **B167**, 347 (1986).

[124] S. J. Brodsky, P. Damgaard, Y. Frishman and G. P. Lepage, Phys. Rev. **D33**, 1881 (1986).

[125] D. Müller, *Phys. Rev.* **D49**, 2525 (1994).

[126] P. A. Dirac, Rev. Mod. Phys. **21**, 392 (1949).

[127] For an extensive review and further references see S. J. Brodsky, H. Pauli and S. S. Pinsky, Phys. Rept. **301**, 299 (1998), hep-ph/9705477.

[128] S.J. Brodsky, *Light-Cone Quantized QCD and Novel Hadron Phenomenology*, SLAC-PUB-7645 (1997); S.J. Brodsky and H.C. Pauli, *Light-Cone Quantization and QCD*, Lecture Notes in Physics, vol. 396, eds., H. Mitter *et al.*, Springer-Verlag, Berlin, 1991, Phys. Rept. **301**, 299 (1998).

[129] P. P. Srivastava and S. J. Brodsky, Phys. Rev. **D61**, 025013 (2000), hep-ph/9906423, and in preparation.

[130] S.J. Brodsky, D. S. Hwang, B. Ma and I. Schmidt, hep-th/0003082.

[131] R. L. Jaffe and A. Manohar, Nucl. Phys. **B321**, 343 (1989).

[132] X.-S. Chen, D. Qing, and F. Wang, Chin. Phys. Lett. **16** (1999) 403, hep-ph/9802347; D. Qing, X.-S. Chen, and F. Wang, Phys. Rev. **D 58** (1998) 114032.

[133] S.J. Brodsky and F. Schlumpf, Phys. Lett. **B 329** (1994) 111.

[134] L. Okun and I. Yu. Kobzarev, ZhETF, **43** 1904 (1962) (English translation : JETP **16** 1343 (1963)); L. Okun, in proceedings of the International Conference on Elementary Particles, 4th, Heidelberg, Germany (1967). Edited by H. Filthuth. North-Holland, (1968).

[135] X. Ji, hep-ph/9610369.

[136] X. Ji, Phys. Rev. Lett. **78**, 610 (1997), hep-ph/9603249. 9603249;

[137] O. V. Teryaev, hep-ph/9904376.

[138] S. J. Brodsky and D. S. Hwang, Nucl. Phys. **B543**, 239 (1999), hep-ph/9806358.

[139] C. R. Ji and H. M. Choi, Fizika **B8**, 321 (1999).

[140] S. J. Brodsky and S. D. Drell, Phys. Rev. **D22**, 2236 (1980).

[141] A. Harindranath and R. Kundu, Phys. Rev. **D59**, 116013 (1999), hep-ph/9802406.

[142] S. J. Brodsky, F. E. Close, and J. F. Gunion, Phys. Rev. **D 5** (1972) 1384; Phys. Rev. **D 6** (1972) 177; Phys. Rev. **D 8** (1973) 3678.

[143] X. Ji, Talk presented at 12th Int. Symp. on High-Energy Spin Physics (SPIN96), Amsterdam, Sep. 1996, hep-ph/9610369; Phys. Rev. Lett. **78** (1997) 610; Phys. Rev. **D 55** (1997) 7114.

[144] X. Ji, J. Phys. **G 24**, 1181 (1998), hep-ph/9807358.

[145] A. V. Radyushkin, Phys. Lett. **B 380** (1996) 417, hep-ph/960431.

[146] X. Ji and J. Osborne, Phys. Rev. **D 58** (1998) 094018, hep-ph/9801260.

[147] M. Vanderhaeghen, P. A. Guichon, and M. Guidal, Phys. Rev. Lett. **80** (1998) 5064.

[148] A. V. Radyushkin, Phys. Rev. **D 59** (1999) 014030, hep-ph/9805342.

[149] J. C. Collins and A. Freund, Phys. Rev. **D 59** (1999) 074009, hep-ph/9801262.

[150] J. Blumlein and D. Robaschik, hep-ph/0002071.

[151] M. Penttinen, M. V. Polyakov, A. G. Shuvaev and M. Strikman, hep-ph/0006321.

[152] M. Diehl, T. Feldmann, R. Jakob and P. Kroll, hep-ph/0009255.

[153] X. Ji, *Phys. Rev.* **D55**, 7114 (1997), hep-ph/9609381; X. Ji and J. Osborne, *Phys. Rev.***D58**, 094018 (1998), hep-ph/9801260.

[154] S. J. Brodsky, L. Frankfurt, J. F. Gunion, A. H. Mueller, and M. Strikman, *Phys. Rev.* **D50**, 3134 (1994), hep-ph/9402283.

[155] S. J. Chang, R. G. Root and T. M. Yan, Phys. Rev. **D 7** (1973) 1133.

[156] M. Burkardt, Nucl. Phys. **A 504** (1989) 762; Nucl. Phys. **B 373** (1992) 613; Phys. Rev. **D 52** (1995) 3841.

[157] H.-M. Choi and C.-R. Ji, Phys. Rev. **D 58** (1998) 071901.

[158] K. Hornbostel, S. J. Brodsky, and H. C. Pauli, *Phys. Rev.* **D41** 3814 (1990).

[159] F. Antonuccio and S. Dalley, *Phys. Lett.* **B348**, 55 (1995); *Phys. Lett.* **B376**, 154 (1996); *Nucl. Phys.* **B461**, 275 (1996).

[160] S. D. Bass, S. J. Brodsky and I. Schmidt, Phys. Rev. **D60**, 034010 (1999), hep-ph/9901244.

[161] A. Szczepaniak, E. M. Henley and S. J. Brodsky, *Phys. Lett.* **B243**, 287 (1990).

[162] A. Szczepaniak, *Phys. Rev.* **D54**, 1167 (1996).

[163] P. Ball and V. M. Braun, *Phys. Rev.* **D58**, 094016 (1998) hep-ph/9805422.

[164] M. Beneke, G. Buchalla, M. Neubert and C. T. Sachrajda, hep-ph/9905312.

[165] Y. Keum, H. Li and A. I. Sanda, hep-ph/0004004.

[166] Y. Y. Keum, H. Li and A. I. Sanda, hep-ph/0004173.

[167] H. C. Pauli and S. J. Brodsky, Phys. Rev. **D32**, 2001 (1985).

[168] S. Dalley and I. R. Klebanov, Phys. Rev. **D47**, 2517 (1993) hep-th/9209049.

[169] S. J. Brodsky, J. R. Hiller and G. McCartor, quantization," Phys. Rev. **D58**, 025005 (1998), hep-th/9802120.

[170] S. J. Brodsky, J. R. Hiller and G. McCartor, Phys. Rev. **D60**, 054506 (1999), hep-ph/9903388.

[171] S. Dalley and B. van de Sande, hep-lat/9911035, and S. Dalley (to be published).

[172] J. R. Hiller and S. J. Brodsky, Phys. Rev. **D59**, 016006 (1999), hep-ph/9806541.

[173] F. Antonuccio, I. Filippov, P. Haney, O. Lunin, S. Pinsky, U. Trittmann and J. Hiller [SDLCQ Collaboration], hep-th/9910012.

[174] O. Lunin and S. Pinsky, hep-th/9910222.

[175] P. Haney, J. R. Hiller, O. Lunin, S. Pinsky and U. Trittmann, hep-th/9911243.

[176] A. Bassetto, L. Griguolo and F. Vian, hep-th/9911036.

[177] K. Yamawaki, hep-th/9802037.

[178] S. S. Pinsky and B. van de Sande, Phys. Rev. **D49**, 2001 (1994), hep-ph/9310330.

[179] W. A. Bardeen and R. B. Pearson, Phys. Rev. **D14** (1976) 547.

[180] M. Burkardt, Phys. Rev. **D54** (1996) 2913.

[181] H.-C. Pauli and S. J. Brodsky, Phys. Rev. **D32** (1985) 1993 and 2001.

[182] S. Dalley, hep-ph/0007081.

[183] S. Dalley and B. van de Sande, Nucl. Phys. **B53** (Proc. Suppl.) (1997) 827; Phys. Rev. **D56** (1997) 7917; Phys. Rev. **D59** (1999) 065008; Phys. Rev. Lett. **82** (1999) 1088; Phys. Rev. **D62** 014507 (2000).

[184] S. Dalley, in *New Directions in Quantum Chromodynamics*, C-R. Ji and D-P. Min eds., (AIP, 1999), hep-lat/9911035.

[185] G. P. Lepage and S. J. Brodsky, Phys. Lett. **B87** (1979) 359; Phys. Rev. **D22** (1980) 2157.

[186] A. V. Efremov and A. V. Radyushkin, Phys. Lett. **94B** (1980) 245; Theor. Math. Phys. **42** (1980) 97.

[187] CLEO Collab., J. Gronberg *et al.*, Phys. Rev. **D57** (1998) 33.

[188] S. J. Brodsky, G. P. Lepage and P. B. Mackenzie, Phys. Rev. **D28**, 228 (1983).

[189] A. H. Mueller, *Nucl. Phys.* **B250**, 327 (1985).

[190] P. Ball, M. Beneke and V. M. Braun, *Phys. Rev.* **D52**, 3929 (1995).

[191] G. P. Lepage and P. B. Mackenzie, *Phys. Rev.* **D48**, 2250 (1993).

[192] M. Neubert, *Phys. Rev.* **D51**, 5924 (1995); *Phys. Rev. Lett.* **76**, 3061 (1996).

[193] S. J. Brodsky, C.-R. Ji, A. Peng and D. G. Robertson, Phys. Rev. **D57**, 345 (1998).

[194] C.-R. Ji, A. Sill and R. Lombard-Nelsen, *Phys. Rev.* **D36**, 165 (1987).

[195] C.-R. Ji and F. Amiri, *Phys. Rev.* **D42**, 3764 (1990).

[196] M. Peter, *Phys. Rev. Lett.* **78**, 602 (1997); preprint `hep-ph/9702245`.

[197] S. J. Brodsky, M. S. Gill, M. Melles, and J. Rathsman, Phys. Rev. **D58**, 116006 (1998).

[198] S. J. Brodsky, E. Gardi, G. Grunberg and J. Rathsman, hep-ph/0002065.

[199] S. J. Brodsky, hep-ph/9912340.

[200] S. J. Brodsky and J. Rathsman, hep-ph/9906339.

[201] S.J. Brodsky and H. J. Lu, *Phys. Rev.* **D51**, 3652 (1995) hep-ph/9405218.

[202] S. J. Brodsky, J. R. Pelaez and N. Toumbas, Phys. Rev. **D60**, 037501 (1999) hep-ph/9810424.

[203] S. J. Brodsky, G. T. Gabadadze, A. L. Kataev and H. J. Lu, *Phys. Lett.* **B372**, 133 (1996); hep-ph/9512367.

[204] F. M. Dittes and A. V. Radyushkin, *Sov. J. Nucl. Phys.* **34**, 293 (1981); *Phys. Lett.* **134B**, 359 (1984).

[205] R. D. Field, R. Gupta, S. Otto and L. Chang, *Nucl. Phys.* **B186**, 429 (1981).

[206] E. Braaten and S.-M. Tse, *Phys. Rev.* **D35**, 2255 (1987).

[207] G. Parisi and R. Petronzio, *Phys. Lett.* **95B**, 51 (1980).

[208] G. Curci, M. Greco and Y. Srivastava, *Phys. Rev. Lett.* **43**, 834 (1979); *Nucl. Phys.* **B159**, 451 (1979).

[209] A.C. Mattingly and P. M. Stevenson, *Phys. Rev.* **D49**, 437 (1994).

[210] V. N. Gribov, Lund Report No. LU-TP 91-7, 1991 (unpublished).

[211] K. D. Born, E. Laermann, R. Sommer, P. M. Zerwas, and T. F. Walsh, *Phys. Lett.* **329B**, 325 (1994).

[212] J. M. Cornwall, *Phys. Rev.* **D26**, 1453 (1982).

[213] A. Donnachie and P. V. Landshoff, *Nucl. Phys.* **B311**, 509 (1989).

[214] M. Gay Ducati, F. Halzen and A. A. Natale, *Phys. Rev.* **D48**, 2324 (1993).

[215] C.T.H. Davies *et. al.*, *Phys. Rev.* **D52**, 6519 (1995).

[216] A. X. El-Khadra, G. Hockney, A. Kronfeld and P. B. Mackenzie, *Phys. Rev. Lett.* **69**, 729 (1992).

[217] D.V. Shirkov and S. V. Mikhailov, *Z. Phys.* **C63**, 463 (1994).

[218] S.J. Brodsky, A. H. Hoang, J. H. Kuhn and T. Teubner, *Phys. Lett.* **359B**, 355 (1995).

[219] V. M. Braun, `hep-ph/9505317`.

[220] N. Isgur and C. H. Lewellyn-Smith, *Phys. Rev. Lett.* **52**, 1080 (1984); *Nucl. Phys.* **B317**, 526 (1989).

[221] I. V. Musatov and A. V. Radyushkin, Phys. Rev. **D56**, 2713 (1997) [hep-ph/9702443].

[222] S. Ong, *Phys. Rev.* **D52**, 3111 (1995).

[223] J. Bebek *et al.*, *Phys. Rev.* **D17**, 1693 (1978).

[224] S. R. Amendolia *et al.*, *Nucl. Phys.* **B277**, 168 (1986).

[225] B. Melic, B. Nizic and K. Passek, hep-ph/9903426.

[226] A. Szczepaniak, A. Radyushkin and C. Ji, *Phys. Rev.* **D57**, 2813 (1998) [hep-ph/9708237].

[227] C. J. Bebek *et al.*, *Phys. Rev.* **D13**, 25 (1976).

[228] C. Carlson and J. Milana, *Phys. Rev. Lett.* **65**, 1717 (1990).

[229] J. Volmer, NIKEF Thesis, *The Pion Form Factor via Pion Electroproduction*, (2000), http://www.jlab.org/ volmer/pion.html.

[230] D. V. Shirkov and I. L. Solovtsov, Phys. Rev. Lett. **79**, 1209 (1997) [hep-ph/9704333].

[231] I. L. Solovtsov and D. V. Shirkov, Phys. Lett. **B442**, 344 (1998) [hep-ph/9711251].

[232] D. Bollini, *et. al.*, *Lett. Nuovo Cim.* **14**, 418 (1975).

[233] J. F. Gunion, S. J. Brodsky and R. Blankenbecler, *Phys. Rev.* **D6**, 2652 (1972); R. Blankenbecler and S. J. Brodsky, *Phys. Rev.* **D10**, 2973 (1974).

[234] C. E. Carlson and A. B. Wakely, Phys. Rev. **D48**, 2000 (1993).

[235] S. J. Brodsky, M. Diehl, P. Hoyer and S. Peigne, Phys. Lett. **B449**, 306 (1999) [hep-ph/9812277].

[236] T. Hyer, Phys. Rev. **D48**, 147 (1993).

[237] G. P. Lepage and S. J. Brodsky, *Phys. Rev.* **D22**, 2157 (1980); *Phys. Lett.* **B87**, 359 (1979); *Phys. Rev. Lett.* **43**, 545, 1625(E) (1979).

[238] G. Bertsch, S. J. Brodsky, A. S. Goldhaber, and J. F. Gunion, Phys. Rev. Lett. **47**, 297 (1981).

[239] L. Frankfurt, G. A. Miller, and M. Strikman, Phys. Lett. **B304**, 1 (1993), hep-ph/9305228.

[240] L. Frankfurt, G. A. Miller and M. Strikman, hep-ph/9907214.

[241] S. Brodsky, M. Diehl, P. Hoyer, and S. Peigne, in preparation.

[242] P. Stoler, Few Body Syst. Suppl. **11**, 124 (1999).

[243] G. A. Miller, nucl-th/9910053.

[244] G. A. Miller, S. J. Brodsky and M. Karliner, hep-ph/0002156.

[245] M. Franz, M. V. Polyakov and K. Goeke, hep-ph/0002240.

[246] S. J. Brodsky, C. Peterson and N. Sakai, Phys. Rev. **D23**, 2745 (1981).

[247] S. J. Brodsky, P. Hoyer, C. Peterson and N. Sakai, Phys. Lett. **B93**, 4682 (1980).

[248] B. W. Harris, J. Smith and R. Vogt, Nucl. Phys. **B461**, 181 (1996), hep-ph/9508403.

[249] S. J. Brodsky, G. P. Lepage and S. F. Tuan, Phys. Rev. Lett. **59**, 621 (1987).

[250] V. N. Gribov and L. N. Lipatov, Yad. Fiz. **15**, 781 (1972).

[251] S. J. Brodsky and G. P. Lepage, SLAC-PUB-2447, *Presented at the Summer Institute on Particle Physics, SLAC, Stanford, Calif., July 9-20, 1979.*

[252] D. Muller, hep-ph/9406260.

[253] V. Y. Petrov, M. V. Polyakov, R. Ruskov, C. Weiss and K. Goeke, Phys. Rev. **D59**, 114018 (1999) [hep-ph/9807229].

[254] D. Diakonov and V. Y. Petrov, hep-ph/0009006.

[255] M. B. Hecht, C. D. Roberts and S. M. Schmidt, nucl-th/0008049.

[256] P. P. Srivastava and S. J. Brodsky, hep-ph/9906423.